Aus dem Institut für Neuropathologie
der Medizinischen Fakultät Charité – Universitätsmedizin Berlin

DISSERTATION

Investigating vacuolar features reveals distinct autophagy pathway as a key feature in the pathophysiology of Immune-mediated necrotizing myopathy

zur Erlangung des akademischen Grades
Doctor medicinae (Dr. med.)

vorgelegt der Medizinischen Fakultät
Charité – Universitätsmedizin Berlin

von

Norina Fischer
aus Berlin

Datum der Promotion: 04.03.2022

Vorwort

Teilergebnisse der vorliegenden Arbeit wurden in dem Artikel *Sequestosome-1 (p62) expression reveals chaperone-assisted selective autophagy in immune-mediated necrotizing myopathies.* am 03.08.2019 in dem Journal „**Brain Pathology“** von **N Fischer**, C Preuße, J Radke, D Pehl, Y Allenbach, U Schneider, E Feist, V von Casteleyn, K Hahn, T Ruck, SG Meuth, HH Goebel, R Graf, A Mammen, O Benveniste und W Stenzel (DOI 10.1111/bpa.12772) veröffentlicht.

Table of contents

Abbreviations

AABs	Autoantibodies
AChE	Acetylcholinesterase
AOPD	Adult-onset Pompe disease
ASS	Anti-synthetase syndrome
APP	Amyloid precursor protein
ATF6	Activating transcription factor 6
ATG	Autophagy-related (Human)
Atg	Autophagy-related (Drosophila)
AVM	Autophagic vacuolar myopathy
AVSM	Autophagic vacuoles with sarcolemmal features
BAG3	Bcl2-associated athanogene 3
C5b-9	Terminal complement complex/ membrane attack complex
CASA	Chaperone-assisted selective autophagy
CD8	Cluster of differentiation molecule 8
cDNA	Complementary DNA
CHIP	Carboxyl terminus of HSC70-interacting protein
CK	Creatine kinase
CRYAB	Alpha-B-crystalline
Ct	Cycle threshold
DNA	Desoxy-ribonucleic acid
DM	Dermatomyositis
EDEM1	ER degradation enhancing alpha-mannosidase like protein 1
EIF2α	Eukaryotic translation initiator factor 2α
ENMC	European Neuromuscular Centre
ER	Endoplasmic reticulum
ERAD	ER-associated protein degradation

ERN1	Endoplasmic reticulum to nucleus signaling 1
FUS	Fused in sarcoma protein
GAA	Acid-α-glucosidase
GRP78	Heat shock protein family A (Hsp70) member 5 = HSPA5 = BIP
GSDII	Glycogen storage disease Type II
H&E	Hematoxylin and eosin
HLA	Human leucocyte antigen
HMGCR	3-Hydroxy-3-Methylglutaryl-CoA Reductase
HPF	High power field
HSPA8	Heat shock protein family A (Hsp70) member 8 = Hsc70
HSPB8	Heat shock protein family B (small) member 8
HSC70	Heat shock cognate protein 70 = HSPA8
IFNγ	Interferon gamma
IIM	Idiopathic inflammatory myopathies
IL-1β	Interleukin 1 beta
IMNM	Immune-mediated necrotizing myopathy
IRE-1α	Inositol-requiring 1α = ERN1
LAMP2	Lysosomal-associated membrane protein 2
MAP1LC3A/B	Microtubule-associated protein 1A/1B light chain (gene)
LC3A/B	Microtubule-associated protein 1A/1B light chain (protein)
LIMP1	Lysosomal integral membrane protein 1
LMP7	Proteasome 20S subunit beta 8
LMP10	Proteasome 20S subunit beta 10
MHC	Multihistocompatibility complex
MAPK8	Mitogen-activated protein kinase 8
mTORC1	Mechanistic target of rapamycin kinase 1
mRNA	Messenger ribonucleic acid
MyHC neo	Neonatal myosin heavy chain
NDC	Non-diseased control patients

NSE	Non-specific esterase
p62	Sequestosome-1 (protein)
PAS	Periodic acid Schiff
PE	Phosphatidylethanolamine
PERK	Eukaryotic translation initiation factor 2 alpha kinase 3
PI3K	Class III-phosphatidylinositol 3-kinase
PM	Polymyositis
qPCR	Qualitative polymerase chain reaction
RIDD	Regulated IRE-1 dependent decay
sRNP	Small ribonucleoprotein
SRP	Signal recognition particle
sIBM	Sporadic inclusion body myositis
SQSTM1	Sequestosome-1/p62 (gene)
STAT6	Signal transducer and activator of transcription factor 6
TDP43	TAR-DNA binding protein 43
TGFβ	Transforming growth factor beta
Th1/2 cells	T-helper cells Type 1/2
TNFα	Tumor necrosis factor alpha
TRAF2	TNF receptor associated factor 2
tRNA	Transfer ribonucleic acid
Ub	Ubiquitin
ULK1	Unc-51 like autophagy activating kinase 1
UPR	Unfolded protein response
UPS	Ubiquitin-proteasome-system
V+/V-	IMNM patients with/without detected vacuoles in their muscle biopsies
V-ATPase	Vacuolar proton adenosine triphosphatase
VMA21	Vacuolar ATPase assembly factor
XBP1	X-box-binding protein 1
XMEA	X-linked myopathy with excessive autophagy

Table of figures

Table Directory

Abstract

Background: Immune-mediated necrotizing myopathy (IMNM) is an idiopathic inflammatory myopathy that is characterised by distinct clinical, serological and histopathological features. The exact pathophysiology of this disabling disease is unknown, although a direct myofiber-damaging effect of disease specific autoantibodies against signal-recognition-particle (SRP) and 3-hydroxy-3-methylglutaryl-coenzyme A reductase (HMGCR) and complement activation is emerging as a central process. Immunosuppressant therapy is not always efficient and seronegative patients are common, thus additional processes leading to myofiber impairment must be present.

Objective: In this context, the appearance of vacuolar structures within myofibers of IMNM patients, which have been mentioned but never analysed in more detail, was investigated. Vacuolar structures in muscle disease are often associated with specific pathophysiologic processes. In this regard, the relation of vacuole formation with immunologic events and cellular proteostasis mechanisms were to be illuminated.

Methods: Skeletal muscle biopsies of 56 patients with immune-mediated necrotizing myopathy were analysed retrospectively by histochemical, immunohistochemical and gene expression methods. For comparison, skeletal muscle biopsies of eight sporadic inclusion body myositis and eight non-diseased control patients were analysed accordingly.

Results: The majority of IMNM patients´ skeletal muscle biopsies show a variable number of vacuole-containing myofibers. Histopathological hallmarks of muscle affection of immune-mediated necrotizing myopathy (necrosis, myophagocytosis and immune cell infiltration) were significantly more pronounced in biopsies containing vacuoles (V+) than in biopsies without vacuoles (V-). Investigation of differential immune response, complement involvement, protein aggregation and different degradation pathways showed no significant differences between V+ and V- IMNM patients. Analysing pathways that can be associated with vacuole formation in muscle, a peculiar immunoreactivity pattern of the autophagy-adaptor protein p62 was revealed. Moreover, the specific p62 pattern uncovered the involvement of BAG3-mediated selective autophagy in immune-mediated necrotizing myopathy. Significantly differing *BAG3* mRNA expression levels exposed its particular involvement in immune-mediated necrotizing myopathy versus sporadic inclusion body myositis.

Conclusion: Vacuole formation seems to be collateral myofiber damage in immune-mediated necrotizing myopathy rather than the result of a specific disease mechanism and possibly represents stronger disease affection. BAG3-mediated selective autophagy is altered in IMNM and leads to a distinct histological pattern of p62. The difference in the p62 expression pattern, as well as *BAG3* transcript expression variance between sporadic inclusion body myositis and immune-mediated necrotizing myopathy, can not only be used diagnostically, but also gives insight in the different disease pathomechanisms.

Zusammenfassung

Hintergrund: Die immunvermittelte nekrotisierende Myopathie (IMNM) gehört zu der Gruppe der idiopathischen inflammatorischen Myopathien und ist charakterisiert durch spezifische klinische, serologische und histopathologische Befunde. Die Pathophysiologie dieser Erkrankung ist nicht bekannt, obwohl jüngste Studien eine direkte Muskelfaserschädigung durch spezifische Autoantikörper gegen das Signal Recognition Particle (SRP) und die 3-Hydroxy-3-Methylglutaryl-Coenzym-A-Reduktase (HMGCR) und damit verbundene Komplementsystem-Aktivierung als zentralen Mechanismus aufdeckten. Eine immunsupprimierende Therapie führt nicht immer zu Symptomverbesserung und neben den seropositiven Patienten zeigt ein Großteil der Patienten keine typische Autoantikörperbildung. Das Vorliegen zusätzlicher Krankheitsmechanismen, die zu Muskelschädigung führen, ist demnach wahrscheinlich.

Zielsetzung: In diesem Zusammenhang wurde das Auftreten von vakuolären Strukturen innerhalb von Muskelfasern von Patienten mit IMNM untersucht. Vakuolenbildung ist bei verschiedenen Muskelerkrankungen mit spezifischen pathophysiologischen Prozessen assoziiert. Das Ziel der vorliegenden Arbeit ist so die Untersuchung der vakuolären Strukturen in Hinsicht auf Charakter und Pathogenese; dabei soll insbesondere der Zusammenhang zu immunologischen Prozessen und zu Mechanismen der zellulären Proteinhomöostase aufgeklärt werden.

Methoden: Skelettmuskelbiopsien von 56 Patienten mit immunvermittelter nekrotisierender Myopathie wurden mittels histochemischer, immunhistochemischer und molekularbiologischer Methoden untersucht. Analog wurden die Untersuchungen mit Skelettmuskelproben von acht gesunden Kontrollpersonen und acht Patienten mit sporadischer Einschlusskörpermyositis als Vergleichsgruppen durchgeführt.

Ergebnisse: In Skelettmuskelbiopsien der Mehrheit der Patienten mit IMNM fanden sich vakuoläre Strukturen in variabler Ausprägung. Histopathologische Zeichen für eine Muskelschädigung, wie sie bei der IMNM auftreten, waren bei Patienten, deren Biopsien Vakuolen aufwiesen (V+) signifikant stärker ausgeprägt als bei IMNM Patienten ohne Nachweis von Vakuolen (V-). Die Untersuchung verschiedener immunologischer Phänomene, des Komplementsystems, Proteinaggregation und – abbaumechanismen zeigte keine Unterschiede zwischen den beiden Patientengruppen. Bei der Analyse verschiedener Stoffwechselwege, welche zu Vakuolenbildung im Muskel führen können, zeigte sich ein auffälliges Färbemuster des Autophagie-Adapter-Proteins p62. Dieses Ergebnis führte zu der Entdeckung von Veränderungen der BAG3-vermittelten selektiven Autophagie in Muskelfasern von Patienten mit IMNM. Weiterhin wurden signifikante Unterschiede in der mRNA Expression von *BAG3* zwischen Patienten mit immunvermittelter nekrotisierender Myopathie und Patienten mit sporadischer Einschlusskörpermyositis aufgedeckt.

Schlussfolgerung: Das Entstehen von vakuolären Strukturen im Muskel von IMNM Patienten scheint als kollaterale Muskelschädigung, möglichweise als Zeichen besonders starker Krankheitsaktivität im Rahmen der Erkrankung aufzutreten und ist nicht mit einem spezifischen Mechanismus assoziiert. Es liegt eine Veränderung im Stoffwechselweg der BAG3-vermittelten selektiven Autophagie vor, was zu einem spezifischen histologischen Muster von p62 führt. Die Unterschiede der p62 Morphologie als auch die unterschiedliche *BAG3* mRNA Quantität bei Patienten mit IMNM bzw. sIBM könnten nicht nur diagnostisch genutzt werden, sondern geben zusätzlich Aufschluss über die jeweiligen pathophysiologischen Vorgänge.

1. Introduction

1.1. Idiopathic Inflammatory Myopathies: Historical considerations

Immune-Mediated Necrotizing Myopathy (IMNM) is recognized as an entity within the group of idiopathic inflammatory myopathies (IIM), consisting of the entities sporadic inclusion body myositis (sIBM), Dermatomyositis (DM), Polymyositis (PM), Immune-mediate necrotizing myopathy (IMNM) and non-specific myositis (1).

The written history of the idiopathic inflammatory myopathies goes back about 150 years to the pathologists Ernst Leberecht Wagner and Heinrich Unverricht who in 1887 both independently published case reports of a patient with acute muscle weakness, edematous upper limbs and histopathological signs of muscle inflammation and degeneration (2). The authors each independently chose the title "Polymyositis" for their reported cases and in succession agreed on the name of "Polymyositis acuta" for this "new" disease entity, a name that coined the group of inflammatory myopathies for most of the time to come. The name "Dermatomyositis" also originates in that decade and is owed to the fact that Unverricht considered skin pathologies as an essential component of the disease, thus deeming this term in 1891 as more fitting (2, 3).

The first systematic assessment of inflammatory myopathies was accomplished by Bohan and Peter in 1975, in which they recognized two forms of inflammatory myopathies, Polymyositis (PM) and Dermatomyositis (DM) (4, 5). Whereas Caspary *et al*. in 1964 and Stern *et al*. in 1967 questioned the autoimmune origin of polymyositis due to their findings that autoantibodies (antinuclear factor or anti-muscle antibodies) were not significantly more frequent in Polymyositis than in "non-immunological muscle wasting disease" (6, 7), several groups in the following years did indeed find evidence for anti-myoglobin- and antinuclear- antibodies in polymyositis (8-10). The first polymyositis specific antibody against the histidyl-tRNA synthetase "Jo1" was discovered in 1983 (11, 12), and shortly after anti-Mi2 was proposed as a Dermatomyositis-specific antibody against a nuclear helicase protein (13).

Against the backdrop of increasing interest in immunological pathomechanisms of autoimmune diseases, antibodies against small ribonucleoproteins (sRNPs) were described (14-17). In this context the cytoplasmic signal recognition particle (SRP), one of the antibodies which still holds immense importance for IMNM today, came into focus as a potential antigen. The first description of SRP as a target for specific autoantibodies in polymyositis was introduced by Reeves *et al*. in

1986 (18). Moreover, a number of additional antibodies against different cellular structures in the group of inflammatory myopathies and overlap syndromes emerged in the following years (17, 19-23).

In 1991, based on different myositis-specific antibodies instead of just their pathology, Love and colleagues first proposed a systematic distinction of the inflammatory myopathies recognized to that date. The study of 212 patients indicated that serological and immunogenic features pose a more accurate marker for distinguishing certain myositis subgroups than solely the clinical manifestation. Even though each "autoantibody disease subtype" does show distinct clinical features that had been discussed before, this paper was the first systematic review (24). Up to this point the group of idiopathic inflammatory myopathies as considered e.g. by Love *et al*. comprised the group of PM, DM, connective-tissue-disease-associated myositis, cancer-associated myositis and sIBM. It wasn´t until 2002 that another subgroup with specific clinical and histopathological features was introduced by Miller *et al*., termed "anti-SRP-antibody-syndrome" or "myopathy with anti-SRP-antibodies (25). Anti-SRP-antibodies were so far ruled as a serological feature of PM but were now proposed as a distinct form of immune-mediated myositis – one that would in succession be called immune-mediated necrotizing myopathy.

The first "official" and international recognition of this new subgroup now called Immune-Mediated Necrotizing Myopathy (IMNM, or Necrotizing Autoimmune Myopathy, NAM) occurred during the 119th European Neuromuscular Center (ENMC) international workshop on idiopathic inflammatory myopathies in 2003. It was here that a number of specialists agreed on classification criteria for the different IIM subgroups, including officially naming IMNM with some distinct but not entirely specific criteria. (26)

1.2. Immune-mediated necrotizing myopathy as a distinct clinicopathological entity

Throughout the years, more and more knowledge accumulated about the immune-mediated necrotizing myopathy that helped delineate IMNM from other forms of IIMs. The distinct clinical and histopathological features of IMNM were consented on at the 224th European Neuromuscular Center (ENMC) international workshop in October 2016 (27).

On the histopathological level, IMNM is first and foremost defined and delineated from other IIMs by the presence of a variable number of diffusely distributed necrotic myofibers which are at different stages of necrosis, myophagocytosis or myofiber regeneration. In contrast to other IIMs lymphocytes are rare, but nevertheless continuously present. The most prevalent infiltrate in

IMNM muscle tissue consists of macrophages. Further typical histopathological features are the expression of MHC class I on non-necrotic or non-regenerating fibers, sarcolemmal complement deposition, and proliferation of the endomysium and enlarged capillaries. (27) The common clinical characteristics of IMNM are the subacute onset of moderate to severe proximal muscle weakness and an elevated serum creatinine – kinase (CK). Treatment options, always including immune suppressive agents, are mostly efficient, but the escalation of medication schemes is frequently necessary. Independent of these obligate clinical features and the histopathological criteria, the international group of experts agreed that IMNM can be subdivided into three different groups, according to the presence of autoantibodies: "anti-SRP-myopathy", "anti-HMGCR-myopathy" and an "antibody-negative myopathy" with no or unknown myositis-specific antibodies. (27-29)

Which pathways on an inter- or intracellular level play a role in myofiber damage are unknown to date. A few authors mention the existence of (rimmed) vacuoles in muscle sections of IMNM (30-34), which led to the present investigation of this phenomenon.

1.3. Autophagic vacuolar myopathies (AVMs)

The pathologic presence of vacuoles within myofibers is frequent in different kinds of myopathies and is in fact responsible for the umbrella term "Autophagic vacuolar myopathies" (AVM) (35). The term "AVM" for a group of diseases is firstly a descriptive name based on histopathological and ultrastructural features that imply their autophagic/lysosomal nature. The possible underlying causes for this histopathological "symptom" are numerous: from clearly defined genetic myopathies over idiopathic inflammatory myopathies to drug-induced/toxic myopathies. Yet, which one could be considered the causative reason in IMNM is still unclear. On plain hematoxylin and eosin (H&E) staining, the vacuoles of all AVMs appear similar, although in histochemical and immunohistochemical stainings differences in their characteristics can be observed and used to draw conclusions to their origin and possible development. The most prominent forms are described in the following.

1.3.1. Hereditary autophagic vacuolar myopathies

Glycogen storage disease Type II: Pompe disease

One of the earliest recognized myopathies with autophagic vacuoles and the first discovered "lysosomal storage disorders" is glycogen storage disease Type II (GSDII), or Pompe disease (36). Pompe disease is an autosomal recessive disease with a number of different mutations within the

acid-α-glucosidase (*GAA*)-gene and subsequent limited activity or complete deficiency of acid-α-glucosidase (GAA) (36, 37). The extent of the residual enzyme activity correlates with the degree of clinical affection: the infantile form of Pompe disease with enzyme activity less than 1% is marked by the onset of symptoms in the newborn period and a mostly lethal course of disease within the first year of life. The less severe forms of GSDII, the adult-onset Pompe disease (AOPD) with onset between adolescence and late adulthood show, amongst other symptoms, only mild to moderate skeletal muscle impairment corresponding to enzyme activity levels ranging from 15 to 40%. The most lifespan limiting complication in these groups is the impairment of respiratory muscles, which is common. (36, 38)

Acid-α-glucosidase (or acid maltase) is an enzyme almost exclusively located in the lysosomal compartment of the cells where it catalyses the hydrolysation of glycogen polymers to glucose (36, 39-41). The GAA deficiency leads to the formation of large intracytoplasmic vacuoles filled with nondescript materials that stain positively for periodic acid schiff (PAS) and acid phosphatase, designating the contents as glycogen and lysosome-originating (35, 39). It is possibly not only the accumulation of glycogen within lysosomes and cytoplasm but also the excessive formation of autophagic vacuoles that disturb myofiber integrity and therefore disturb normal muscle function (39).

Danon disease

Danon disease is one of the most typical hereditary autophagic vacuolar myopathies. It is classified, like Pompe disease, as a primary lysosomal storage disorder, even though the genetic context and thus likely the pathophysiological mechanisms differ. Danon disease is an X-linked hereditary myopathy with different mutations on the lysosomal-associated membrane protein 2 (*LAMP2*) gene which leads to complete LAMP2 deficiency in affected patients. (42)

As a transmembrane protein, LAMP2 plays a role in maintaining the integrity of assembling lysosomes and therefore preventing the release of proteolytic enzymes from the lysosome into the cytoplasm (35). Additionally, it is essential for a process called “autophagosome maturation” during which autophagosomes fuse with endosomes. The exact mechanism by which the lack of LAMP2 eventually leads to muscular weakness, myofiber pathology with myofiber size variations and vacuole formation is unclear, although it is hypothesized that impairment of lysosome and endosomes impedes autophagosome maturation and consequently leads to autophagosome accumulation (43).

On an ultrastructural level, the autophagic features of the vacuoles in Danon disease are evident: the content is made up of cellular degradation products ("cytoplasmic debris"), electron-dense material and myeloid bodies. More specifically, the autophagic vacuoles can be described as autolysosomal vacuoles in accordance with the presence of lysosomal integral membrane protein-1 (LIMP-1)-positive aggregates and basophilic granules in H&E stainings corresponding to the LIMP-1 aggregates. (44) Some of these autolysosome accumulations are surrounded by dystrophin-positive structures and have thus been termed "autophagic vacuoles with sarcolemmal features" (AVSFs). The sarcolemmal nature of these specific vacuoles was corroborated by the fact that in addition to dystrophin, the membranes of AVSFs contain all of the typical proteins of the sarcolemma: α-sarcoglycan, dystrobrevin, α- and β-dystroglycan, utrophin, dysferlin, caveolin-3 and collagen IV. (44)

X-linked myopathy with excessive autophagy (XMEA)

XMEA is also considered an autophagic vacuolar myopathy and even ranged under the AVSF-myopathies (44). The genetic background of XMEA are different single-nucleotide mutations in the *VMA21* gene (45). *VMA21* encodes for a chaperone protein that is essential for the correct assembly of the vacuolar ATPase (V-ATPase), a membrane-bound proton pump (46, 47). V-ATPase is a ubiquitously expressed enzyme that, amongst other functions, helps maintaining the acidic environment inside of lysosomes (47). Ramachandran *et al*. postulate that lacking, respectively malfunctioning V-ATPase, with subsequently less acidic lysosomal environment and a decline in lysosomal enzymatic activity leads to hindrance of the last steps of autophagy, and therefore to accumulation of autophagolysosomes with indigestible content (45). This process is spurred by an additional upregulation of autophagy by inhibition of the gene for mechanistic target of rapamycin kinase 1 *(mTORC1)* due to lack of free amino acids and as a "feedback mechanism" to the missing completion of the autophagy process and accumulation of autophagolysosomes (45). Histopathologically, muscle sections of patients with XMEA show a large number of cytoplasmic vacuoles, complement and MHC class I deposition in the sarcolemma and duplicated basement membranes. (48) Vacuoles also show deposits of complement membrane attack complex C5b-9 and stain positively for the sarcolemmal proteins dystrophin, dysferlin, caveolin-3 and spectrin (44), as well as acetylcholinesterase (AchE) (48). Electron microscopic studies support the autophagic nature of the vacuoles as they are filled with cellular debris and occasionally fuse with the sarcolemma in an exocytotic manner. These studies also show the multi-layered basal lamina in detail (48).

Nishino and colleagues differentiate myopathies with autophagic vacuoles with sarcolemmal features (AVSF) from other AVMs. AVSF-containing myopathies are Danon disease, XMEA, infantile onset AVM and adult onset AVM. They are characterised by autophagic vacuoles surrounded by membranes with sarcolemmal features and acetylcholinesterase-activity in the vacuolar membranes. (35) Autophagic vacuolar myopathies that do not contain AVSFs (e.g. Pompe disease, hereditary inclusion body myositis (hIBM) and sporadic inclusion body myositis (sIBM)) are delineated by the presence of only very few vacuoles with inconsistent staining for dystrophin or other sarcolemmal membrane proteins and the complete absence of acetylcholinesterase or non-specific esterase (NSE) staining of the vacuoles. (44)

1.3.2. Toxic myopathies with vacuolar features

Different drugs, especially those with amphiphilic features are prone to intercalate in biological membranes and can cause myopathies with autophagic lysosomal vacuoles (49).

Chloroquine-induced myopathy

Examples for drugs causing these myopathies are chloroquine and hydroxychloroquine. These anti-malaria and anti-rheumatic drugs may, after intake of 200-500mg/d of chloroquine for one year or more, lead to moderate generalized muscle weakness with focus on proximal muscles (50, 51). Morphological examination reveals (sometimes rimmed) vacuoles inside the cytoplasm that stain positively for acid phosphatase, indicating the lysosomal origin of the vacuoles (50-52). Vacuolar staining for microtubule-associated protein 1 light chain (MAP1LC3 or LC3) and the autophagy adaptor protein sequestosome-1/p62 also strongly suggest their autophago-lysosomal nature and can be used diagnostically (53). Ultrastructural analysis confirm the autophagic-lysosomal origin by observation of myeloid bodies and cellular degradation products inside the vacuoles (50-52). The presence of curvilinear, membranous structures in electron microscopy images is noted throughout the literature about hydroxychloroquine-induced myopathies (50, 53, 54) and has even been considered as pathognomonic for this drug-induced myopathy (50).

Colchicine- induced myopathy

Colchicine-induced myopathy is another myopathy that presents, among other symptoms, vacuole formation inside myofibers (55, 56). Positive vacuolar staining for acid phosphatase and the presence of electron-dense cell “debris” and lysosomal degradation products on an ultrastructural level also allow the classification of colchicine-induced myopathy as a vacuolar autophagic myopathy (55-59). The accumulation of autophagic vacuoles and lysosomes is thought to be the

consequence of colchicine-induced impairment of microtubules and therefore disruption of intracellular transport namely that of autophagosomes and lysosomes (60, 61).

Amiodarone-induced myopathy

Amiodarone has also been reported to cause a myopathy featuring rimmed as well as non-rimmed vacuoles. Ultrastructural studies show intracytoplasmic vacuoles filled with lysosomal debris. (62) Due to its amphiphilic and cationic features amiodarone is very susceptible to becoming encased in lysosomal membranes and to form complexes with phospholipids inside lysosomes that cannot be degraded. These amiodarone-phospholipid complexes can accumulate in a number of cells and lead to the well-known side effects of amiodarone: interstitial lung fibrosis, cornea opacity and neurotoxicity. (63) These side effects are also classified under the term "drug-induced phospholipidosis" (64). It can be speculated that the vacuoles observed within myofibers in amiodarone treated patients are thus also accumulated lysosomes containing amiodarone-phospholipid conglomerates failing to be processed or degraded (49, 62).

1.3.3. Inflammatory myopathy with vacuolar features

Sporadic Inclusion Body Myositis (sIBM)

Sporadic inclusion body myositis is the only inflammatory myopathy in which rimmed vacuoles are obligatory and part of the histopathological diagnostic criteria, denominating it an interesting comparison partner for IMNM.

SIBM is an idiopathic inflammatory myopathy affecting mainly patients above 50 years of age. Clinically and pathologically, it is characterised by a chronical progressive weakness of especially finger flexors and knee extensors, combined with swallowing difficulties, and the presence of a considerable inflammatory infiltrate, protein aggregates within myofibers and, notably, of rimmed vacuoles. (65) Concerning the pathophysiology of sIBM, it is currently postulated that degenerative as well as inflammatory processes play a major role in disease development, although it is disputed which process stands at the beginning and which is secondary (66-69). Benveniste *et al.* propose that an inflammatory reaction within the muscle with invading $CD8^+$ T cells and secretion of different cytokines might pose the first trigger for an intracellular stress response and myofiber damage. The subsequent upregulation of different proteins like MHC class I leads to an overstrain of protein-processing and -degradation systems. In combination with genetic predisposing factors, environmental factors and aging processes' insufficient protein degradation systems (autophagy as well as the ubiquitin-proteasome-system) fail and eventually lead to the accumulation of abnormally folded protein, namely amyloid, TDP-43, phosphorylated Tau (p-

Tau) and p62 (69). Supporting this hypothesis is the fact that intracellular amyloid deposits due to *APP* mRNA upregulation can be induced by exposure to the pro-inflammatory cytokine IL-1β (66). The study of Nogalska *et al.* found aggregates of paired helical filaments encased by p62 on an ultrastructural level as well as the co-localization of p62 and p-Tau in sIBM. This prompted their hypothesis of p62 with its attached cargo p-Tau to be hindered by the lumps of paired helical filaments; suggesting p62 accumulation as a secondary pathomechanism in sIBM. (70)

That autoimmunity is a key player in the primary disease pathophysiology of sIBM is underpinned by the significantly increased presence of HLA-I (HLA-B8) and HLA-II (HLA-DR3, -DR52, -DQ2) antigens, corresponding to a higher frequency of mainly *HLA-DRB1*03:01* allele in sIBM patients (71-75). At a closer look, the correlation of *HLA-DRB1* alleles with sIBM was found within the amino acid sequence of the peptide binding part (76), possibly suggesting pathological antigen binding or an altered antigen presentation mode. The abundant and consistent presence of sarcolemmal MHC class I expression in sIBM myofibers and the possible existence of sIBM specific autoantibodies also point towards an autoimmune cause (69). Recent work has highlighted a putative role of $KLRG1^+$ T cells in the pathomechanism of sIBM as well (77, 78).

1.4. Cellular degradation pathways (leading to vacuole formation)

1.4.1. Autophagy

Autophagy is a ubiquitously present cellular degradation process that allows the turnover of cellular components. The turnover of cellular parts is essential for maintaining the homeostasis of cell metabolism but is also an integral part of pathophysiologic states. Under conditions of nutrient depletion, increased autophagy may replenish energy sources via increased disassembly of macromolecules into its basic components. (79, 80) On the other side of the spectrum, autophagy facilitates the degradation of misfolded proteins or defective organelles in order to maintain normal cell function. The important role of autophagy for intact cell metabolism is underlined by the growing knowledge about autophagy in a number of conditions including aging, cancer, infections and several neurodegenerative diseases. Vacuole formation and pathologic protein aggregation are present in a number of diseases where autophagy is involved or has even been shown to be impaired (81).

Autophagy comprises three main types of degradation mechanisms that are distinguished: macroautophagy, microautophagy and chaperone-mediated autophagy. The “classical” form of autophagy, macroautophagy, hereafter referred to as autophagy, starts with the formation of an isolation membrane or phagophore upon a trigger, for example starvation. (82, 83) Two main

protein complexes are responsible for the induction and growth of the phagophore: the Unc-51 like autophagy activating kinase 1 (ULK1) complex (corresponding to autophagy-related 1 complex (Atg1) in yeast) and the class III-phosphatidylinositol 3-kinase (PI3K) complex (79). The ULK1 complex, consisting of the serine-threonine kinase ULK1, ATG13, ATG101 and FIP200, is thought to be the first effector in the cascade of autophagy: upon dissociation of mTORC1, the main inhibitor of autophagy under nutrient-rich conditions, it may be activated and subsequently activate other autophagy-related (ATG) proteins (80, 84). Class III-PI3K, the other main initiation complex, is comprised of VPS34, VPS15, Beclin1 and ATG14. Via the production of phosphatidylinositol-3-phosphate, this complex facilitates the formation of a curved membrane which allows the binding and recruitment of additional ATG proteins (79, 80). With the help of several other ATG protein complexes the conjugation of Atg8 to phosphatidylethanolamine (PE) is achieved, which then allows elongation of the isolation membrane and eventually autophagosome closing (79, 85). The mammalian equivalent of Atg8, LC3 or MAP1LC3 (microtubule-associated protein 1A/1B light chain) undergoes two modification steps from the cytosolic LC3-I to the membrane-bound PE-containing LC3-II, which is integrated in the developing phagophore (86). The protein complex of ATG5 and ATG12 is thought to form a coat of the growing phagophore and thereby being another key player of facilitating the membrane expansion (82, 86). The macromolecules or parts of the cytoplasm to be degraded by the autophagosome are selected by two different mechanisms: first, the so far suspected unselective enclosure of parts of the cytoplasm via the expansion and sealing of the phagophore ("bulk autophagy"), and secondly the elimination of specifically targeted proteins or protein aggregates. In the process termed "selective autophagy" the labelling of proteins to be delivered to the autophagosome is similar to the ubiquitin-proteasome system. The protein sequestosome 1, or p62, harbours binding structures for ubiquitin as well as LC3-II and thereby acts as a connecting element between ubiquitinated proteins and the autophagosome. (87) P62 has been shown to provide an intracellular scaffold for shuttling decomposition-prone proteins, protein aggregates or even entire organelles to the autophagosome (88). After the sequestration of its target substrates and completion of the autophagosome fusion with late endosomes or lysosomes occurs, the necessary enzymes for the breakdown of the contents and "building blocks" of the autophagosome are yielded (89, 90).

1.4.2. Chaperone-assisted selective autophagy (CASA)

Up until recently, three different autophagy pathways were thought to exist: the above illustrated macroautophagy, microautophagy and chaperone-mediated autophagy. In microautophagy, direct

endocytosis of small parts of the cytoplasm by lysosomes instead of de-novo formation of autophagosomes takes place (91). Chaperone-mediated autophagy is a more selective kind of autophagy in which a chaperone complex recognizes a specific amino acid sequence motif, exposed for instance due to misfolding. The chaperone complex shuttles the recognized protein to the lysosome, where via binding and interaction with the transmembrane protein LAMP2A the defective protein is transported across the lysosomal membrane and degraded within. (92) However, in addition to these processes another type of autophagy has been discovered that promises to play an important role for muscle function (93). This chaperone-assisted selective autophagy (CASA) appears to be another cascade supplying selective autophagy or it resembles the more detailed disclosure of the underlying mechanisms. CASA is characterized by the interaction of the chaperone complex of BAG3/CHIP/HSPB8/HSC70 with p62. The ubiquitin ligase CHIP (Carboxyl terminus of HSC70-interacting protein), known for its interacting with the chaperones Hsp70 and Hsp90 and being the main supplier of the ubiquitin-proteasome-system (UPS) with degradation prone substrates (94), here recognizes and facilitates ubiquitination of BAG3/HSC70/HSPB8-held proteins (93). Consecutively, BAG3/CHIP recruit p62, which acts as a connecting element between the CASA complex plus its ubiquitinated protein and the forming of autophagosome. Bcl2-associated athanogene 3 (BAG3) and p62 are ubiquitinated themselves and therefore efficiently recycled with the autophagosome contents (90, 93).

Arndt *et al*. first described these mechanisms and coined the term "CASA" in starvin-deficient (functional homologue of BAG3) Drosophila that presented severe muscle weakness. It was shown that CASA assumes an essential task in maintaining myofiber integrity and function by degrading "used" Z-disc structures under physiological conditions. (93) This role in physiological muscle function was confirmed by Ulbricht *et al.* for humans, showing an upregulation of CASA associated genes and proteins after Z-disc disintegration following physical exercise (95). The importance of CASA for normal muscle function in mammals is emphasized by BAG3-associated pathologic conditions: BAG3-deficient mice present with a severe myopathy and early death (96) and patients carrying a heterozygote *BAG3* mutation suffer from a severe type of genetic myofibrillar myopathy with muscle weakness, cardiomyopathy and neuropathy (97). In all of these BAG3-associated physiological or pathological conditions, the resulting Z-disc defects can been observed on an ultrastructural level (93, 95, 97). However, an impairment of CASA or involvement of BAG3 in inflammatory myopathies has not been shown before.

1.4.3. Ubiquitin-proteasome system (UPS)

The ubiquitin-proteasome system (UPS) is a lysosome-independent machinery mainly for degrading cytoplasmic or nuclear proteins with a short live span (87, 98). The degrading component of the UPS is the 26S proteasome which consists of a 20S proteolytic centre and a 19S "lid" that regulates substrate uptake. The 20S core of the proteasome has a hollow cylindrical shape, formed by α- and β-subunit rings, which bear their hydrolytic sites directed at the centre of the cylinder (99). Through this channel the proteins to be dismantled are shuttled. The 19S regulatory cap recognizes and binds ubiquitinated proteins, facilitates their unfolding in order to enter the proteasome and recycles the ubiquitin tags (87, 100). The ubiquitination is essential for proteins to become degraded via this pathway, whereby it doesn´t matter if the substrate is mono- or polyubiquitinated (87). The decomposition of short-lived proteins and misfolded or aggregated proteins in the "classic" UPS also functions to the end of antigen peptide production (101). This production of antigen peptides being presented at the cellular surface via MHC class I is enhanced further by another type of proteasome complex, the immune proteasome. The immune proteasome comprised the subunits β1i/LMP2, β51/LMP7 and β2i/LMP10 (MECL1) which are expressed at higher levels under inflammatory conditions and substitute three constitutively expressed subunits of the 26S proteasome. These immune proteasome subunits hydrolyse presented proteins at different sites than the "classic" proteasome, generating more peptides that can be presented via MHC class I. (102)

The upregulation of immune proteasome subunits has been shown in muscle tissue and peripheral immune cells of the inflammatory myopathies sIBM, dermatomyositis and polymyositis and is purported to be induced by IFNγ production, subsequently leading to pathologic T cell activation and expansion in skeletal muscle (103).

1.4.4. Endoplasmic reticulum stress and the Unfolded Protein Response (UPR)

Endoplasmic reticulum (ER) stress is described as an overload of the ER with un- or misfolded proteins caused by the disproportion of an increase in protein synthesis (*e.g.* due to higher demand under certain conditions) that exceeds ER processing capacities. As a consequence, the nascent, unfolded proteins aggregate within the ER and disrupt normal ER functioning. (104) The cellular answer to this kind of ER stress is the unfolded protein response (UPR), a conjunction of different ER-originating pathways that deal with the amassing processing load via adaptation of transcription and protein synthesis (104, 105).

The “first-line response” to ER stress is a reduction of the number of proteins being transported to the ER in order to quickly attenuate the processing load. This is achieved by the protein kinase (PKR)-like ER kinase (PERK), which phosphorylates the eukaryotic translation initiator factor 2α (eIF2α) and thereby stops 80S ribosome composition, and thus effective translation (106). Other mechanisms, including the regulated IRE-1 dependent decay (RIDD) decrease the further transport of nascent proteins towards the ER (107). Important for both of these pathways is the ER chaperone HSPA5 or GRP78: GRP78 is bound to PERK and IRE-1 in the ER, but dissociates under ER stress conditions, enabling the transduction of a stress response via the mentioned pathways (108). In addition to PERK, two other main signaling pathways are initiated upon ER stress conditions, the ATF6 (activating transcription factor 6) and the IRE1α (inositol-requiring 1α) pathway. These ER-membrane spanning proteins initiate cascades that both culminate in the upregulation of a number of genes involved in ER function and maintenance. IRE1α leads via its RNAse activity to the splicing of X-box-binding protein 1 (XBP1) mRNA, which then induces transcription ER chaperone genes, ER-associated protein degradation (ERAD) genes and genes enabling ER membrane expansion. The downstream effects of ATF6 include direct upregulation of XBP1 and ERAD effector genes. (104, 107, 109) All in all, via different effector mechanisms the UPR decreases the oncoming number of proteins on the one hand, and on the other increases the protein processing ability of the ER to maintain its regular functioning under ER stress conditions. Closely connected to the UPR is the ER-associated protein degradation (ERAD), which is upregulated as part of the UPR. If unfolded proteins remain in the ER for too long or repair mechanisms fail, terminally defective proteins are modified in variable ways and eventually “retro-translocated” through the ER into the cytoplasm where they are degraded by selective autophagy or the UPR. An important function within this process, termed ERAD, is held by EDEM1 (ER degradation enhancing alpha mannosidase-like protein 1), a soluble ER protein that facilitates modification and retro-translocation of misfolded proteins. Upon ER stress, EDEM1 is upregulated to help attenuate the accumulating burden of defective proteins. (110, 111)

ER stress has been shown to play a role in some inflammatory myopathies, while the deregulation of ER stress response mechanisms, analyzed in mouse models of sIBM and IIM, has been proposed as important non-immune pathways in the pathophysiology of IIMs (112, 113). Despite the increasing evidence of ER stress-related processes as possible contributors to muscle impairment in IIMs, little is known about ER stress in the context of IMNM.

1.4.5. Interconnection of cellular degradation pathways

As elaborated above, mammalian cells hold a multitude of different protein degrading systems enabling them to deal with a number of physiological and pathological conditions under which fine-tuned homeostasis of the intracellular protein metabolism is challenged. In order to perform this task and meet the ever-present need for effective and adequate protein disposal under variable provocations, a crosstalk between the different degradation cascades is crucial. Hence, it is not surprising that several suspected or proven connections between the cells' degradation systems exist. The most obvious connection of pathways is the fusion of the autophagosome with early lysosomes, leaving the process of autophagosome formation without purpose if its contents were not decomposed by lysosomal hydrolases.

A connecting element between the UPS and autophagy are the ubiquitin chains, dedicating proteins to a fate of degradation via the UPS or autophagy when conjugated to lysine tails of the particular proteins. Though specificity differences in this ubiquitination system exists (e.g. the ubiquitin molecules binding to slightly different conformations, UPS ubiquitin chains binding exclusively soluble proteins and p62 as an adaptor of ubiquitinated proteins for autophagy), an overlap of the two degradation systems proteasome and autophagy due to the ubiquitination is possible and results in the possibility of ubiquitinated proteins being degraded by either process if necessary. In line with this, it has been shown that autophagy is activated under conditions of proteasome inhibition, suggesting that autophagy may compensate an impaired proteasome system via decreasing accumulating protein burden. This kind of compensatory mechanism does not seem to function the other way around; in contrast, impaired autophagy seems to result in the decrease of proteasome function as well. (87, 114) Due to the differences in the substrate characteristics of the two pathways (UPS accepting only soluble proteins whereas macroautophagy being able to degrade protein aggregates and entire organelles), it may not seem surprising that a compensation of the proteasome for the autophagy processes is not possible. Upon defects of the autophagic machinery the accumulation of p62 has been hypothesized as being responsible for impaired proteasome activity via competitive removal of proteins needed for ubiquitin processing (87, 115). As a link between the activation of autophagy and proteasome impairment, the ER and its unfolded protein response (UPR) are widely accepted, though the exact mechanisms are disputed (87, 116). Drug-induced ER stress in yeast has been shown to upregulate autophagy related genes (116) and in murine embryonic fibroblasts, ER stress-induced apoptosis due to aggregating polyglutamine could be prevented via induction of autophagy (116, 117). Two of the UPR pathways have been purported to be involved in autophagy activation; the IRE1/TRAF2/MAPK8 pathway and the

PERK/eIF2α cascade via de-inhibition of ATG12. In addition, calcium- signalling could lead to an increase in autophagic processes via inhibition of mTOR, the most potent autophagy inhibitor. (116) The association between the ER and its intrinsic degradation system, ERAD with the UPS, is clearer. Proteins processed through ERAD are relocated into the cytoplasm where ubiquitination and degradation through the proteasome takes place (118). To summarize, crosstalk between the different degradation pathways exist and involves the physiological transport of substrates from one to another degradation machinery (like feeding of ERAD substrates into the UPS) as well as compensatory mechanisms in the case of increased need of protein removal or loss of one of the degradation systems.

1.5. Current state of research

Vacuole formation and autophagy as well as other cellular degradation and turnover processes play an important role in different kinds of myopathies. Common variables are mostly progressive muscular weakness of different muscle groups and the formation of intracytoplasmic vacuoles or aggregates with mostly distinct features. The underlying mechanisms leading to myofiber damage and successive muscular weakness are not well understood. As a recognized idiopathic inflammatory myopathy, immune-mediated necrotizing myopathy with the two notable components of myofiber necrosis and the presence of specific autoantibodies, is fairly new. Although these hallmarks have been described in some detail, the role of the autoantibodies and the mechanisms leading to myofiber necrosis remain unexplored. This is of concern since the clinical course of IMNM can be severe: in three-quarters of the patients, muscular weakness persists during the first year of treatment and can even lead to patients being bedridden or wheelchair-bound (119, 120). Moreover, in half of the affected patients, muscle strength does not fully recover after four years despite extensive treatment (31), and therapeutic schemes need to be escalated frequently with disease-modifying antirheumatic drugs (32). Due to frequent relapses, tapering medication is seldom possible (31, 32, 119). The persisting muscle weakness is especially concerning because disease manifestation in childhood and adolescence is possible and younger age at onset is associated with even less muscle strength (31, 32), making IMNM a possible long-term disabling condition with great repercussions on both private and professional life. Equally alarming is the mostly very rapidly disabling course of disease, leading to disabling muscle weakness within six months (119). Owing to these facts, advancement in pathophysiological understanding of the disease in order to specify treatment options is urgently needed. Little research has been conducted about the underlying pathomechanisms of IMNM so far. It has been found that serum containing the IMNM-specific antibodies anti-SRP and anti-HMGCR leads to

atrophy of mature myotubes and is associated with increased production of reactive oxygen species and pro-inflammatory cytokines (TNFα and IL-6) (121). The atrophy is conceivably caused by IL-6 mediated upregulation of so-called "atrogenes". Furthermore, in the presence of anti-SRP and anti-HMGCR autoantibodies (aAbs), the amount of anti-inflammatory myokines IL-4 and IL-23 is significantly decreased and myoblast fusion processes inhibited, rendering impaired muscle regeneration another possible antibody-induced effect and reason for chronic muscular weakness (121). That humoral autoimmunity is part of the disease pathogenesis seems indisputable, which is further supported by studies showing that anti-HMGCR as well as anti-SRP autoantibody levels correspond positively to CK levels and, in the case of anti-HMGCR-aAbs inversely correspond to muscular strength (31, 121, 122). Nevertheless, the question has persisted as to how interaction between immune cell receptors and autoantigens occurs, given the fact that both HMGCR and SRP are localized inside the cell and not known to be expressed at its surface (123), although recent studies suggest an ectopic expression of the corresponding antigens on the sarcolemma (124). Another possible mechanism causing myofiber damage is the complement-mediated cell lysis triggered by SRP/immune complex formation. This hypothesis has been prompted by a study showing a topological association of activated complement (C3c) and SRP in myoblast cultures incubated with anti-SRP^{+} serum. (125) Recently, Allenbach *et al.* found evidence for antibody-mediated activation of the classical complement pathway (124) and Bergua *et al.* were able to demonstrate a complement-mediated myofiber damage by applying IMNM patient derived anti-SRP- and anti-HMGCR-IgG in a mouse model (126). It has been speculated that due to the special histopathology observed in anti-SRP-myopathy, localised ischemic processes could be involved in disease pathology (25), although no further studies in that regard have been conducted. Although a direct pathogenic role of anti-SRP- and anti-HMGCR-aAbs seems very likely in the light of recent results obtained in studies with mice and humans (126), other pathways are likely to be involved in IMNM pathogenesis, since immunosuppressant therapy is not always successful and a proportion of seronegative IMNM patients exists. Thus, the investigation of other contributing pathogenic pathways is crucial.

2. Objectives

In the routine medical diagnostic as well as in scientific contexts the presence of vacuolar structures in IMNM muscle biopsies can be found. Vacuoles, albeit not commonly noticed or commented features of IMNM, are mentioned in the literature. (32, 122, 127) As described above, vacuole formation is a histopathological element of a number of different myopathies. It is almost always associated with cellular degradation processes, especially autophagy, the lysosomal compartment or the ubiquitin-proteasome system. The aim of this study was to investigate the role of vacuoles in INMN. In order to achieve this, the following hypotheses were pursued:

I. Vacuole formation is a specific phenomenon of IMNM

Vacuole formation in muscle cells can be observed in a number of different pathologies and can often be related to specific intracellular pathways, as in the case of Danon disease or glycogen storage disease Type II. Likewise, it can be hypothesized that vacuole formation in IMNM is a disease specific aspect that stands in affiliation with distinct intracellular processes. This raises the following question:

II. What is the nature and content of the vacuoles in IMNM?

Since vacuole formation in myopathies is often associated with impairment of the autophagic/lysosomal system, one or several steps in these related processes could lead to vacuole formation in IMNM. If vacuole formation takes places in the context of irregular autophagy this would not only bring new insight in the pathophysiology of the disease but also give way to new treatment possibilities.

III. Vacuole formation is associated with immunological phenomena

IMNM belongs to the group of idiopathic inflammatory myopathies that are characterised by the occurring inflammation. Thus, a predominance of specific inflammatory/ immunologic pathways could be involved in vacuole formation.

IV. Vacuole formation is related to degenerative protein aggregation

Autophagy is one of the main cellular machineries able to degrade aggregating proteins, and protein aggregates are common pathologic features that can be related to autophagic dysfunction in several diseases. Accordingly, vacuole formation in IMNM could also be

associated with abnormal protein aggregation. If this hypothesis cannot be confirmed, the following question needs to be considered:

V. Other intracellular degradation systems are involved in the pathophysiology of IMNM and lead to vacuole formation

In all types of IIMs, IMNM being one of them, muscle cells are exposed to cell stress ranging from inflammatory stimuli over ischemic conditions to pathologic protein accumulation. As a response to different cell stresses one of the cells compensation mechanisms is increased protein synthesis, and at the same time upregulation of protein turnover processes. In several myopathies, including sIBM, dysfunction of additional intracellular degradation cascades have been associated with myofiber damage (113, 128). Therefore, these processes, namely the immune proteasome and the ER stress response could be altered in IMNM as well and might be related to vacuole formation.

VI. Vacuoles are an expression of clinical and morphological disease severity

Keeping in mind the most often very severe course of disease and the positive correlation of CK with disease severity, decreasing muscle strength and autoantibody levels in IMNM patients, overall muscle affection including the histopathological features of IMNM could be associated with vacuole formation and reflected by an advanced clinical course of the disease.

3. Materials

Table 1: Reagents and general material

Product	Company
Chloroform	Roth, Germany
Ethanol	Baker, Germany
Isopropanol	Merck, Germany
Nuclease-Free Water	Quiagen, USA
Dulbecco's Phosphate buffered saline (PBS)	Biochrom, Germany
Acetone	Merck, Germany
Normal serum goat	Vektor Laboratories, USA
ROTI-HISTOKITT II	Roth, Germany
Mayers Hematoxylin Solution	Merck, Germany
Eosin-Y	Brunschwig Chemie, Netherlands
Xylol	Baker, Germany
Eppendorf tubes	
Object slides	
MicroAmp Fast 96-Well Reaction Plate	Life Technologies / ThermoFisher, Germany
MicroAmp Optical Adhesive Film	Life Technologies / ThermoFisher, Germany
VECTASHIELD® Mounting Medium with DAPI	Vektor Laboratories, USA
Fettstift DakoPen	Agilent Technologies, USA

Table 2: Commercial kits and enzymes

Product	Company
peqGOLD TriFast™	PEQLAB Biotechnologie, Germany
Glycogen	Invitrogen, Germany
DNA-*free*™ DNA Removal Kit	Invitrogen, Germany
High-Capacity cDNA Archive Kit	Applied Biosystems, USA
TaqMan® Fast Universal PCR Master Mix	Life Technologies, Germany

Table 3: Laboratory equipment

Product	Company
PCR UnoCycler	VWR, Germany
Cryo-Star Microm HM560	Fisher Scientific, Germany
Microplate Reader TECAN Infinite 200	Tecan, Germany
7900 HT Fast Real-Time PCR System	Applied Biosystems, USA
Heraeus Fresco 17 Centrifuge	Thermo Scientific
Heraeus Multifuge 35R+ Centrifuge	Thermo Scientific
Vortex-Genie 2	Scientific Industries

Table 4: Antibodies

Specificity	Host	Clone	Dilution	Company
β-Amyloid	Mouse	4G8	1:3000	Covance, USA
α-B-Crystallin	Mouse	1B6.1-3G4	1:2500	Abcam, UK
αLaminin-5	Mouse	4C7	1:30,000	Chemicon, Germany
BAG3	Rabbit	polyclonal	1:500	Abcam, UK
β-Spectrin	Mouse	RBC2/3D5	1:100	Novocastra Laboratories, UK
C5b-9	Mouse	aE11	1:200	DAKO, Germany
CD8	Mouse	C8/144B	1:50	DAKO, Germany
CD31	Mouse	7C70A	1:25	DAKO, Germany
CD45	Mouse	2B11	1:400	DAKO, Germany
CD56 (N-CAM)	Mouse	ERIC-1	1:200	Bio-Rad, USA
CD68	Mouse	EMB11	1:100	DAKO, Germany
CD138	Mouse	polyclonal	1:30	DAKO, Germany
FUS	Rabbit	polyclonal	1:500	Sigma-Aldrich, Germany
HSP70	Mouse	polyclonal	1:100	Abcam, UK
LC3-B (I and II)	Mouse	2G6	1:50	nanoTools, Germany
LAMP2	Mouse	5H2	1:500	Santa Cruz Biotechnology, USA
MHC class I	Mouse	W6/32	1:1000	DAKO, Germany
MHC class II	Mouse	C3R/43	1:100	DAKO; Germany
Neonatal myosin heavy chain	Mouse	NB-MyHCn	1:20	Novocastra Laboratories, UK

Neonatal myosin heavy chain	Mouse	NB-MyHCn	1:20	Novocastra Laboratories, UK
Phospho-Tau	Mouse	AT8	1:40	Thermo Fisher Scientific, USA
SQSTM1/p62	Rabbit	polyclonal	1:100	Abcam, UK
SQSTM1/p62	Mouse	3/p62	1:100	BD Transduction Laboratories, USA
Ubiquitin	Rabbit	polyclonal	1:1000	DAKO, Germany
Utrophin	Mouse	DRP3/20C5	1:10	Novocastra, UK
TDP43	Rabbit	polyclonal	1:250	Protein Tech Group (PTG), USA

Secondary antibody	**Host**	**Target species**	**Dilution**	**Company**
Cy3	Goat	Rabbit	1:100	Dianova, Germany
Cy3	Goat	Mouse	1:100	Dianova, Germany
Alexa Fluor® 488	Goat	Rabbit	1:100	Invitrogen, Germany
Alexa Fluor® 488	Goat	Mouse	1:100	Invitrogen, Germany

Table 5: Quantitative Real-Time PCR Assays

TaqMan Gene Expression Assay (Life Technologies/ThermoFisher)	**Reference number**
TaqMan® Gene Exp Assay *BAG3*	Hs00188713_m1
TaqMan® Gene Exp Assay Beclin (*BECN1*)	Hs00186838_m1
TaqMan® Gene Exp Assay CD206 (*MRC1*)	Hs00267207_m1
TaqMan® Gene Exp Assay Calreticulin (*CALR3*)	Hs00376764_m1
TaqMan® Gene Exp Assay *CCL17*	Hs00171074_m1
TaqMan® Gene Exp Assay CHOP (*DDIT3*)	Hs00358796_g1
TaqMan® Gene Exp Assay *CXCL13*	Hs00757930_m1
TaqMan® Gene Exp Assay *EDEM1*	Hs00976004_m1
TaqMan® Gene Exp Assay *HSPA5* (Grp78)	Hs00976004_m1
TaqMan® Gene Exp Assay *IFNG*	Hs00989291_m1
TaqMan® Gene Exp Assay *IL1B*	Hs01555410_m1
TaqMan® Gene Exp Assay *IL12A*	Hs01011518_m1
TaqMan® Gene Exp Assay *IL4*	Hs00929862_m1
TaqMan® Gene Exp Assay *IL4R*	Hs00166237_m1
TaqMan® Gene Exp Assay *IL6*	Hs00985639_m1
TaqMan® Gene Exp Assay LC3 (*MAP1LC3A*)	Hs01076567_g1
TaqMan® Gene Exp Assay LMP2 (*PSMB9*)	Hs00160610_m1
TaqMan® Gene Exp Assay LMP7 (*PSMB8*)	Hs00544760_g1
TaqMan® Gene Exp Assay p62 (*SQSTM1*)	Hs01061917_g1
TaqMan® Gene Exp Assay *STAT1*	Hs01013989_m1
TaqMan® Gene Exp Assay *PGK1*	Hs99999906_m1
TaqMan® Gene Exp Assay *STAT2*	Hs01013123_m1
TaqMan® Gene Exp Assay *STAT6*	Hs00598625_m1
TaqMan® Gene Exp Assay *TGFB1*	Hs00998133_m1
TaqMan® Gene Exp Assay TNFa (*TNF*)	Hs00174128_m1
TaqMan® Gene Exp Assay *ULK1*	Hs00186838_m1

Methods

3.1. Patients

Retrospective analysis was conducted on skeletal muscle biopsies of 56 IMNM patients. Skeletal muscle biopsies of eight sIBM patients and six non-diseased controls (NDC) were used as a comparison or, control group, respectively. All biopsies were taken for diagnostic reasons at Charité University Hospital in Berlin or Pitié-Salpêtrière University Hospital in Paris and immediately cryoconserved in liquid nitrogen. The Charité ethics committee approved the study (EA1/204/11), and informed consent was obtained for all patients locally. Muscle specimens were stored at -80°C until further processing. Inclusion criteria for IMNM patients were based on the histopathological criteria for immune-mediated necrotizing myopathy, defined at the 224th ENMC Workshop in October 2016 ("Clinicopathological classification of Immune-mediated necrotizing myopathies", (27)) and the presence of anti-SRP or anti-HMGCR-autoantibodies in patient serum. SIBM patients were included based on the diagnosis issued by the Department of Neuropathology at the Charité. Biopsies of non-diseased control patients (NDC) were performed for diagnostic reasons on muscle pain or weakness but no myofiber damage or changes were observed. Additionally, these patients showed normal inflammatory laboratory markers and normal CK values.

3.2. Histology

The preparation of 8 µm thick muscle sections was carried out with the cryostat Cryo-Star Microm HM560 (Fisher Scientific, Germany). Cutting was executed at -20°C, sections mounted on object slides and dried for 24 hours at 4°C. The storing of mounted sections was realized at -20°C until staining. In addition to the sections, 1 mg of muscle tissue was cut and stored at -80°C for further molecular biological analysis.

3.2.1. Histochemistry and immunohistochemical stainings

Histochemical stainings were performed with hematoxylin & eosin (H&E), modified Gömöri trichrome, non-specific esterase (NSE), acid phosphatase and acetylcholine esterase. A histochemical staining protocol is listed below, exemplarily for H&E staining. Immunohistochemial stainings were performed using standard diagnostic procedures with antibodies against the molecules listed in Table 5.

3.2.2. Hematoxylin & eosin staining

With the hematoxylin and eosin staining, an illustration of the nucleus and the cytoplasm of cells is achieved. Staining of strongly basophilic structures like DNA and histones inside the nucleus was done by installing the sections into a hemalum bath for three minutes. Consecutive washing of the sections under tap water for two minutes led to the violet-blue coloration of the hemalum by means of an increase in the pH. Next, the sections were inserted into eosin for 30 seconds. After another washing step, the tissue was dehydrated by using an ascending alcohol series (70%, 80%, 96%, 100% alcohol for one minute each), after which the tissue was cleared by administration to Xylol I and II for one minute each. The sections were mounted with cover slips using ROTI-HISTOKITT II (Roth, Germany) and dried afterwards.

3.2.3. Quantification

The following semi-quantitative scores were defined to assess the histological stainings (exemplary score shown in Figure 1):

Score	H&E and NSE
0	No myophagocytosis
1	Single myophagocytosis
2	Diffusely scattered myophagocytosis
3	Ample amount of diffusely distributed myophagocytosis

Score	MHC class I
0	No sarcolemmal staining
1	Focal sarcolemmal staining (< 30% of myofibers)
2	30% - 60% of myofibers with sarcolemmal staining (and/or focal accumulation)
3	> 60% of myofibers with sarcolemmal staining

Score	CD56 and MHC neonatal
0	No sarcolemmal staining
1	Focal sarcolemmal staining (< 15% of myofibers)
2	15% - 30% of myofibers with sarcolemmal staining (and/or focal accumulation)
3	> 30% of myofibers with sarcolemmal staining

Score	CD68
0	No macrophages
1	Few macrophages focally
2	Moderate number of macrophages
3	Ample number of macrophages, diffusely distributed

Score	CD45
0	No leucocytes
1	Singular leucocytes
2	Several leucocytes focally
3	Several leucocytes in diffuse distribution

Score	C5b-9
0	No sarcolemmal staining
1	Single fibers with sarcolemmal staining
2	Focally several fibers with sarcolemmal staining
3	Diffuse distribution of an ample number of fibers with strong sarcolemmal staining

Score	CD8
0	No $CD8^+$ cells
1	Singular $CD8^+$ cells
2	Some $CD8^+$ cells focally
3	Some $CD8^+$ cells in diffuse distribution

Score	LAMP2
0	Physiological staining of lysosomes
1	Some fibers with few enlarged lysosomes
2	Many diffusely distributed fibers with few enlarged lysosomes
3	Many diffusely distributed fibers with considerably enlarged lysosomes

Score	Laminin-α5
0	No sarcolemmal staining
1	Focal sarcolemmal staining (< 30% of myofibers)
2	30% - 60% of myofibers with sarcolemmal staining (and/or focal accumulation)
3	> 60% of myofibers with sarcolemmal staining, diffuse distribution

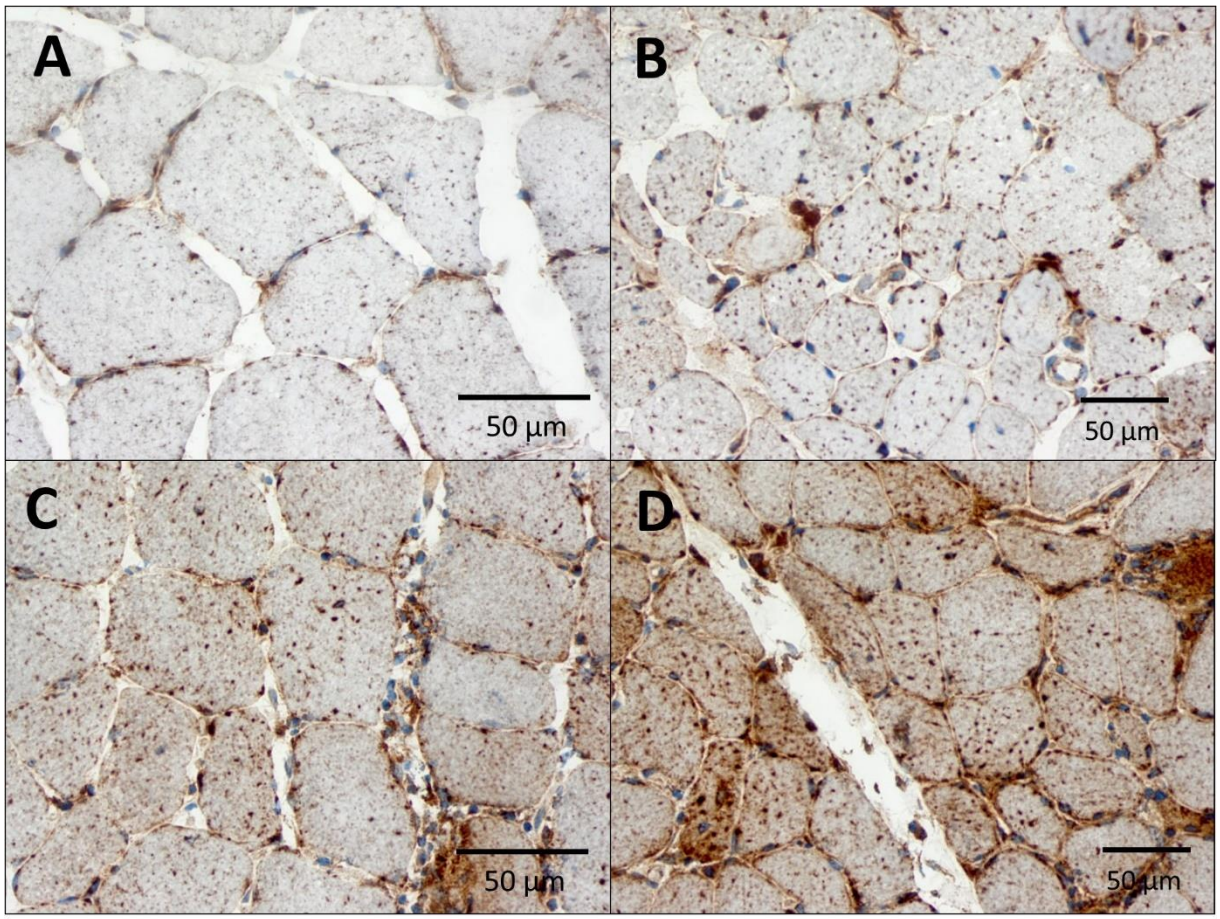

Figure 1 Semiquantitative score of LAMP2 staining of IMNM skeletal muscle biopsies

A: *Score 0: Physiological staining of lysosomes* ***B:*** *Score 1: Some fibers with few enlarged lysosomes* ***C****: Score 2: Many diffusely distributed fibers with few enlarged lysosomes* ***D****: Score 3: Many diffusely distributed fibers with considerably enlarged lysosomes*

3.2.4. Cell counts

For the quantification of $CD138^+$ cells (plasma cells) and $CD8^+$ cells (cytotoxic T cells) cell counts per 10 high power fields (HPF, one high-power field is defined as 0.16 mm^2) were carried out. Also, cell counts/10 HPFs of myofibers staining positive for p62 and LC3, respectively, were conducted.

3.2.5. Double immunofluorescence stainings

Muscle sections stored at -20°C were adapted to room temperature (RT) for 20 minutes. As a first step, specimen sections were fixed in acetone for ten minutes. Afterwards, the sections were blocked with serum, followed by the administration of the first primary antibody. After incubation for 12 hours at 4°C (or 1h at RT) and a washing step, the secondary antibody was applied. After another washing step, the second primary antibody was applied for one hour at room temperature. Another washing step in PBS was followed by the application of the second secondary antibody. After incubation and a final washing step, the sections were mounted with DAPI medium and left

to dry and stored at 4°C without exposure to light. The analysis of the immunofluorescence stains and caption of images was carried out with the Olympus BX53F immunofluorescence microscope (Olympus, Tokyo, Japan).

3.3. Gene expression analysis

3.3.1. RNA-Isolation

RNA isolation from cryopreserved muscle specimens was executed using the Trizol-Chloroform method: muscle tissue is homogenized and dissolved in 1000 µl TRIzol (TriFast™, PEQLAB Biotechnologie, Pennsylvania). This dilution, consisting of phenol and Guanidinium Isothiocyanat causes cell lysis and protein denaturation. The homogenate was incubated at room temperature for five minutes. The addition of 200 µl Chloroform, firm mixing and subsequent centrifugation at 10,000 G for ten minutes leads to phase separation of the homogenate: denatured proteins and cell debris remain on the bottom, organic layer with phenol and chloroform. The DNA stays in the middle interphase and the RNA in the upper, watery layer. After transfer of the upper phase into a new tube, adding of 0.5 µl RNAse-free glycogen and 500 µl Isopropanol causes RNA precipitation. Following ten minutes of incubation at room temperature and ten minutes centrifugation at 12,000 g, the RNA remains as a pellet at the bottom of the tube. The supernatant is discarded, and the pellet washed with 75% ethanol. After another centrifugation step (12,000 g for 10 minutes), the ethanol containing supernatant is discarded and the remaining RNA dried at room temperature for 20 minutes. In a final step, the RNA is resuspended in 30 µl RNAse-free H_20. The RNA concentration was determined photometrically using the Microplate Reader TECAN Infinite 200 (Tecan Trading AG, Switzerland).

3.3.2. Transcription of RNA to cDNA

The transcription of extracted RNA into its complementary cDNA sequence was achieved by polymerase chain reaction (PCR). At first an enzymatic DNA digestion was performed using DNA-*free*™ DNA Removal Kit (Invitrogen, Germany). RNA was prepared with the following components following the manufacturers' instructions:

2,2 µg RNA + 5 µl DNase-Buffer (10x) + 1 µl rDNAse + x µl H2O (total volume 50µl)

The rDNAse eliminates the remaining DNA in the RNA solution. The addition of 5 µl DNAse Inactivation reagent ensures inactivation of the enzyme. After two minutes of centrifugation, the RNA-containing supernatant was transferred into PCR reaction tubes. The synthesis of the complementary single strand DNA was carried out using the High-Capacity cDNA Archive Kit

(Applied Biosystems, Foster City, CA). At first a PCR-Master Mix was prepared, containing the necessary components for the polymerase chain reaction: 10 µl 10x Reverse Transcriptase Buffer, 10µl 10x Reverse Transcriptase Random Primer, 4 µl 25x dNTP Mix, 5 µl Reverse Transcriptase and 21 µl RNAse-free H2O.

The cDNA synthesis was carried out in the PCR-Thermocycler Uno-Cycler (VWR, Germany) under the following conditions: incubation of the RNA at 25°C for ten minutes, followed by cDNA elongation at 75°C for two hours. A heating step up to 85°C for five seconds inactivates the reverse transcriptase; afterwards the cDNA is kept at 4°C. The storing of the cDNA until further processing takes place at 20°C.

3.3.3. Quantitative (real-time) polymerase chain reaction (qPCR)

The quantitative (real-time) polymerase chain reaction (qPCR) differs from the "classical" polymerase chain reaction in the way that during qPCR the amplified gene product is detected and quantified after each PCR cycle. By measuring the increase of the gene product during the exponential phase of the PCR it is possible to draw conclusions about the original amount of the gene transcript in question. The measurement of the transcript quantity is carried out via detection of a fluorescence signal. Prior to the conduction of the qPCR, a Master Mix for every gene to be analysed was prepared. The Master Mix contains the necessary substances for the amplification of the gene transcript:

10 µl PCR Mastermix consisting of heat stable Ampli-Taq-Gold® DNA-Polymerase, Reverse Transcriptase, dNTPs with dUTP, Uracil-DNA Glycosylase, Buffer and Passive Reference Dye (TaqMan® Fast Universal PCR Master Mix, Applied Biosystems, USA).

For each reaction 7 µl RNAse-free water and 1 µl of the respective gene assay (Table 6) were added. 2 µl per well of each cDNA sample were administered onto a 96-well-PCR plate (MicroAmp Fast 96-Well Reaction Plate, Life Technologies). 18 µl of the prepared Master Mix per well were added. Each gene was analysed as a triplet. After each PCR cycle the fluorescence signal of the amplified DNA sequence was detected by a laser. The fluorescence signal was produced by the technique of fluorescence resonance energy transfer (FRET). The qPCR data was analysed using the software SDS 2.3. and RQ Manager 1.2.1 (Applied Biosystems, USA). For each gene a cycle threshold (Ct-value) was determined. The Ct-value equates to the number of PCR cycles, after which the fluorescence signal is detected that is clearly off the background signal. It is measured at the vertex of the exponential phase of the DNA amplification. The gene *PGK1*, which corresponds to the enzyme phosphoglycerate kinase (PGK1) which is expressed in

all myofibers was used as an internal reference. To determine the relative expression of a target gene, first the Ct-value of the genes in one sample was normalized to the mean of the measured Ct-values of PGK: $\Delta Ct_{target\ gene}$= mean Ct $_{target\ gene}$ – (mean Ct $_{PGK1}$).

Next, the $\Delta Ct_{target\ gene}$ was set into relation with the $\Delta Ct_{control}$ of the target gene in non-diseased control patients: $\Delta\Delta Ct = \Delta Ct_{target} - \Delta Ct_{control}$. This allows the relative quantification (RQ) of the target gene in the sample. The RQ-value is calculated by taking the second logarithm of the negative ΔΔCt-value: RQ = 2^-ΔΔCt.

3.4. Statistics

All statistics were performed using GraphPadPrism 5.0 and 8.3.0 software (GraphPad Software, Inc., La Jolla, USA). Non-normalized distribution was assumed for all datasets. Accordingly, the Mann-Whitney U-test was used to assess differences in the histopathology between the V- and the V+ group. Differences in mRNA expression were analysed using the Kruskal-Wallis one-way ANOVA with Dunn´s multiple comparison test. The significance level was set at $p < 0.05$.

4. Results

4.1. Clinical data

Of 56 analysed IMNM patients, 64% (36 patients) were female, 36% (20 patients) were male. The mean age at the time of biopsy was 55.3 years (standard deviation 18.8) with the youngest patient being 16 and the oldest being 92 at the time of biopsy. Female patients were 52 years old on average, whereas male patients showed an average age of 62. Regarding the autoantibody status, 41% (23 patients) of all analysed patients were anti-SRP-positive, 29% (16 patients) anti-HMGCR-positive and for 30% (17 cases) the status for these two autoantibodies was unknown and could not be obtained retrospectively. One patient was reported to be positive for both antibodies.

4.2. General histopathology

Of the 63 originally analyzed IMNM skeletal muscle biopsies seven samples previously classified as IMNM presented for IMNM atypical histological features and were therefore excluded from further investigations. The remaining 56 biopsies presented general signs of muscle pathology such as variations in myofiber size and internalized nuclei, as shown in Figure 2 B. In addition, these biopsies showed the typical histopathological features of IMNM as defined by the 224th

ENMC workshop in different degrees (exemplary image in Figure 2 B) (27). Seven biopsies displayed very poor muscle tissue quality which limited their complete evaluation. 37.5% (21 of 56 patients) showed an ample amount of diffusely distributed myophagocytosis, 36% (20 patients) a moderate amount of diffusely scattered myophagocytosis and 23% (13 patients) only single myophagocytosis. 3.5% (two patients) showed no myophagocytosis in the section analyzed. The same distribution was found for the amount of myofiber necrosis.

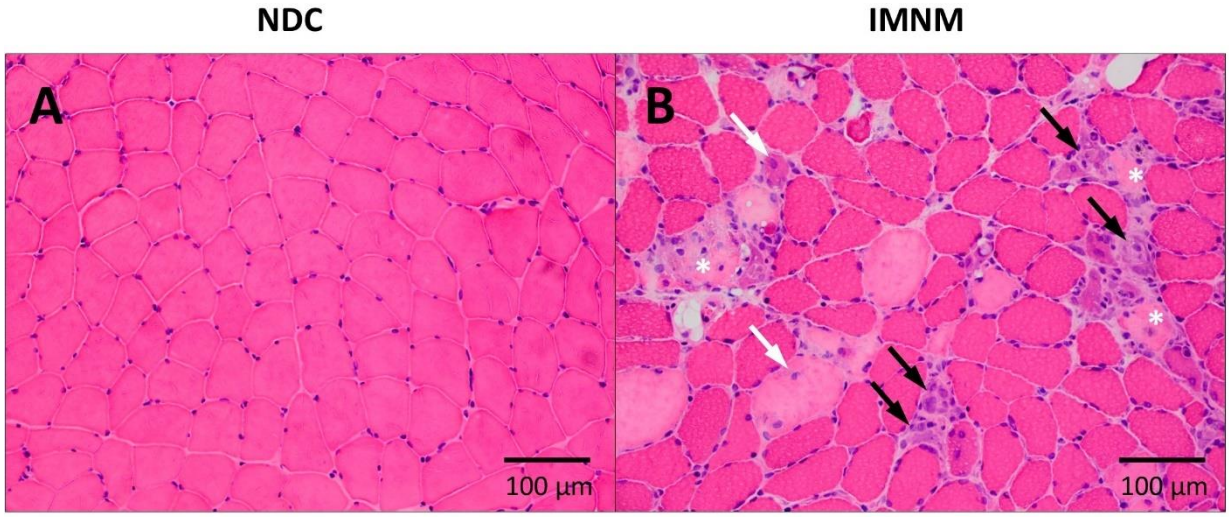

Figure 2 Skeletal muscle biopsies in H&E stain of a non-diseased control and an IMNM patient

A: *H&E stain of a skeletal muscle biopsy of a healthy control patient showing a pattern of evenly sized intact myofibers with small nuclei at their periphery* ***B:*** *H&E stained skeletal muscle section of an IMNM patient showing irregular myofibers of different sizes with partly internalized nuclei (white arrows), necrotic fibers (black arrows) and myophagocytosis (white asterisks).*

Vacuolar structures are frequently found in IMNM

Vacuolar structures, rimmed as well as non-rimmed, have been observed in immune-mediated necrotizing myopathy, but have not been described in more detail (120, 122). The first aim of the current study was therefore the detailed analysis and description of vacuoles in IMNM skeletal muscle biopsies. The number of vacuoles was assessed in Gömöri trichrome staining or, if section quality was too poor for analysis, in standard H&E staining (Figure 3 A-C). Of 56 IMNM patients, 37 showed different numbers of myofibers containing vacuoles, eleven displayed no vacuoles and eight could not be analyzed due to poor muscle quality. This accounts for 77% of IMNM patients showing vacuolar structures and 23% showing no vacuoles within analyzed muscle fibers.

Total number of IMNM patients analyzed	48	100%
N° of IMNM patients **with** vacuoles (V+)	37	77%
N° of IMNM patients **without** vacuoles (V-)	11	23%

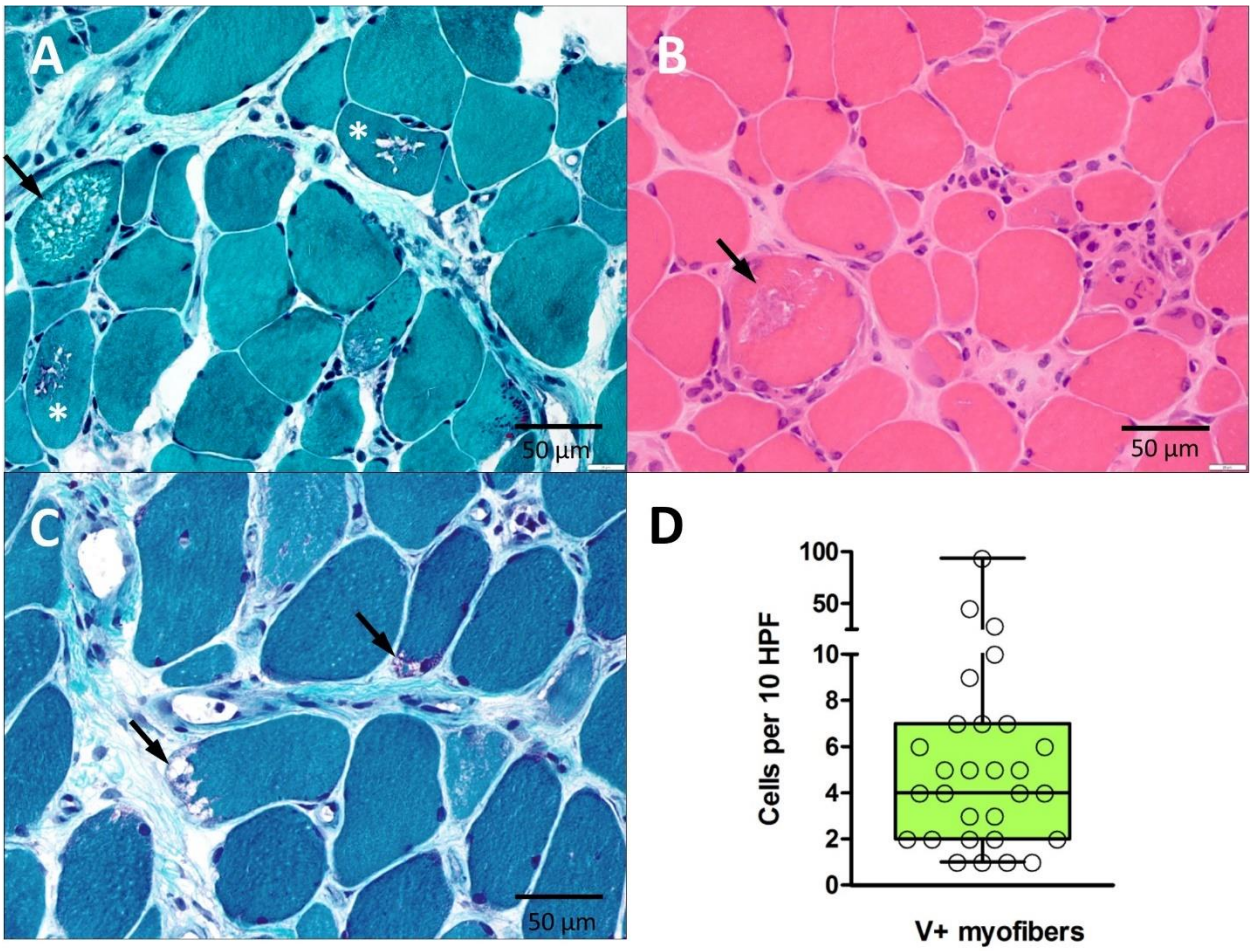

Figure 3 Myofibers contain vacuoles in IMNM patients skeletal muscle biopsies

A: *One HPF of an IMNM patient in Gömöri trichrome stain with three myofibers containing vacuoles (arrow and white asterisks). The vacuoles appear in fibers of normal size and shape.* ***B-C:*** *Vacuoles appear in different configurations as shown in two more HPF with vacuole-containing myofibers. Stains are H&E in B and Gömöri trichrome in C.* ***D****: The observed number of myofibers containing vacuoles in IMNM skeletal muscle biopsies ranged from only one fiber up to 94 fibers with vacuoles/10 HPF. Most patients showed between one and ten myofibers with vacuoles/10 HPF. One high-power field is defined as 0.16 mm^2.*

Primarily, the vacuole-positive group (V+) was subdivided into two subgroups according to the number of vacuoles (Group 1: 1-4 fibers with vacuoles/ten high power fields (HPF), Group 2: five and more fibers with vacuoles/ten HPF). In the course of the investigation it became obvious that these two groups did not significantly differ, neither in expression or distribution of various proteins nor in expression of cytokines and chemokines. Hence, merely the differentiation between a “vacuole positive” (V+) and a “vacuole negative” (V-) group was made. Nevertheless, it is of interest to point out that a considerable variation in the number of myofibers with vacuoles exists, ranging from only one fiber with vacuoles up to 94 myofibers with vacuoles per ten HPF (Figure 3 D). The majority of patients (70%, 26 of 37 biopsies with vacuoles), however, displayed one to ten fibers with vacuoles per ten HPF.

The mean age of disease onset (age at time of biopsy) in the V- group was 59, and 54 years in the V+ group, albeit with no significant difference. The gender distribution in the two groups is also balanced: Of ten patients without vacuoles, five were male and six female. In the V+ group, 23 patients were female and eleven patients male.

4.3. Comparison of the general histopathology of V+ versus V- patients

The hallmarks of IMNM muscle pathology, myophagocytosis, myofiber necrosis and regeneration have been reported to be present in a very varying amount between patients (32, 122). For a more detailed general description of the two groups in question and in order to assess the phenomenon of vacuole formation in the context of these myopathic processes, these main features in the two groups V- and V+ were evaluated.

The amount of myophagocytosis, as shown by stain with nonspecific esterase, is significantly higher in the V+ group than in the V- group (Figure 4 E). In addition, the group with vacuoles also shows a significant higher amount of necrosis, indicated by small myofibers with a pale or hyperconcentrated cytoplasm, disruption of the sarcolemma or complete fiber disintegration in late stages when compared to the group without vacuoles (Figure 4 A, B, E). Regarding markers of myofiber regeneration, neonatal myosin heavy chain (MyHC neonatal) and CD56, no significant difference was found between the V+ and the V- group, even though a tendency of more fibers being stained with neonatal myosin as well as CD56 could be observed in the vacuole-positive group (Figure 4 E).

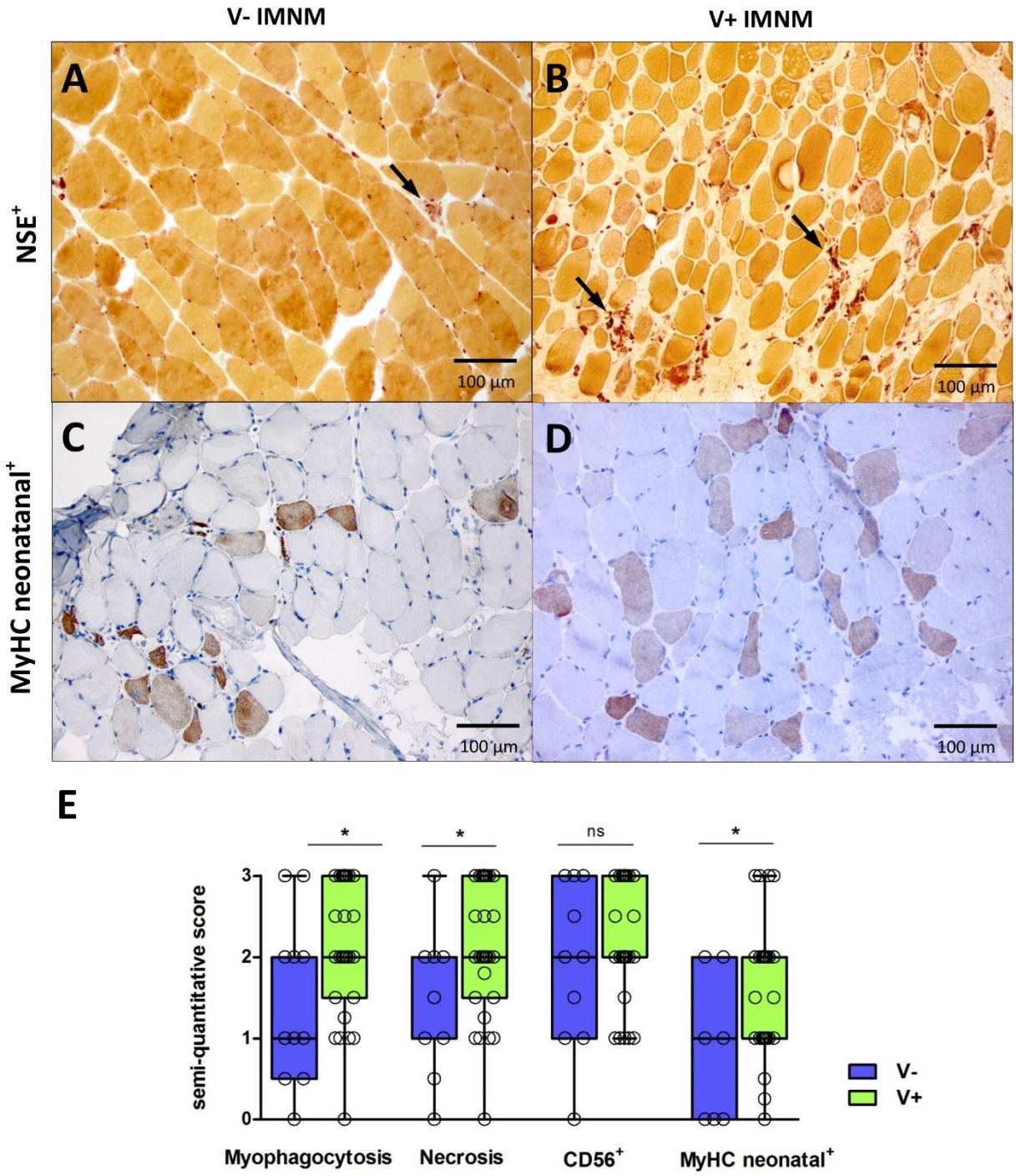

Figure 4 General histopathological features of IMNM are more pronounced in V+ patients

Comparing the amount of myophagocytosis and necrosis in NSE stain, V- patients show only few necrotic myofibers (arrow in A), whereas V+ patients display an ample number of necrotic fibers (exemplary arrows in B). ***C-D:*** *Both groups display a number of regenerating fibers, indicated by positive staining for neonatal myosin heavy chain (MyHC neonatal).* ***E****: Semi-quantitative score of necrosis and myophagocytosis in IMNM biopsies, assessed by stain for non-specific esterase show a significant higher number of myophagocytosis (p=0.0379) and necrosis (p=0.0114) in the V+ group when compared with the V- group. Regeneration processes, analyzed by stain with CD56 and MyHC neonatal tend to be increased in V+ patients, though this difference is only significant for stain with neonatal myosin heavy chain. The Mann-Whitney U-test was used for statistical analysis.*

4.4. Effect of infiltrating immune cells and other immunological phenomena in IMNM

Based on different studies and indicators, like the remission under glucocorticoid therapy, presence of inflammatory infiltrate and autoantibodies, it is evident, that immunological processes play an essential part in the pathogenesis of IMNM. For a more detailed description of the immune reaction and differentiation between the two IMNM groups, the existence of various immune cells was evaluated. It has been demonstrated repeatedly, and recently international consensus was reached on the fact, that the most prominent cellular infiltrate in IMNM consists of $CD68^+$ macrophages and that lymphocytes are rather rare in the majority of skeletal muscle biopsies (129). However, the role of the infiltrating cells for disease development has not been investigated. Thus, an evaluation of the amount and composition of the cellular infiltrate between V- and V+ IMNM patients was relevant and an implication for their pathophysiological effect.

The presence of $CD68^+$ cells in the endomysium is a pronounced feature in both groups, displaying few macrophages up to an ample amount in a diffuse distribution. In only 3% of the V+ group (1 patient, n=34) and 9% of the V- group (1 patient, n=11) no macrophages were found. No significant difference in the number of macrophages between the V+ and V- group was seen, but a trend towards a higher number of macrophages in the V+ group can be detected, as shown in Figure 5 E (left boxplot). As assessed by staining with CD45, there was a significant higher number of leucocytes in V+ patients when compared with V- patient muscle biopsies (Figure 5 E, right boxplot).

Furthermore, $CD8^+$ cytotoxic T cells have been observed as part of the cellular infiltrate in IMNM (129), which led me to investigate whether their presence might be involved in vacuole formation. $CD8^+$ cells are present in 93% of IMNM skeletal muscle biopsies (41 biopsies, n=44), while 7% (3 biopsies) contained no $CD8^+$ cells. There was no significant difference in the number of $CD8^+$ cells regarding the existence of vacuoles, even though biopsies with vacuoles tend to show a higher number of $CD8^+$ cells (Figure 5 E, middle boxplot).

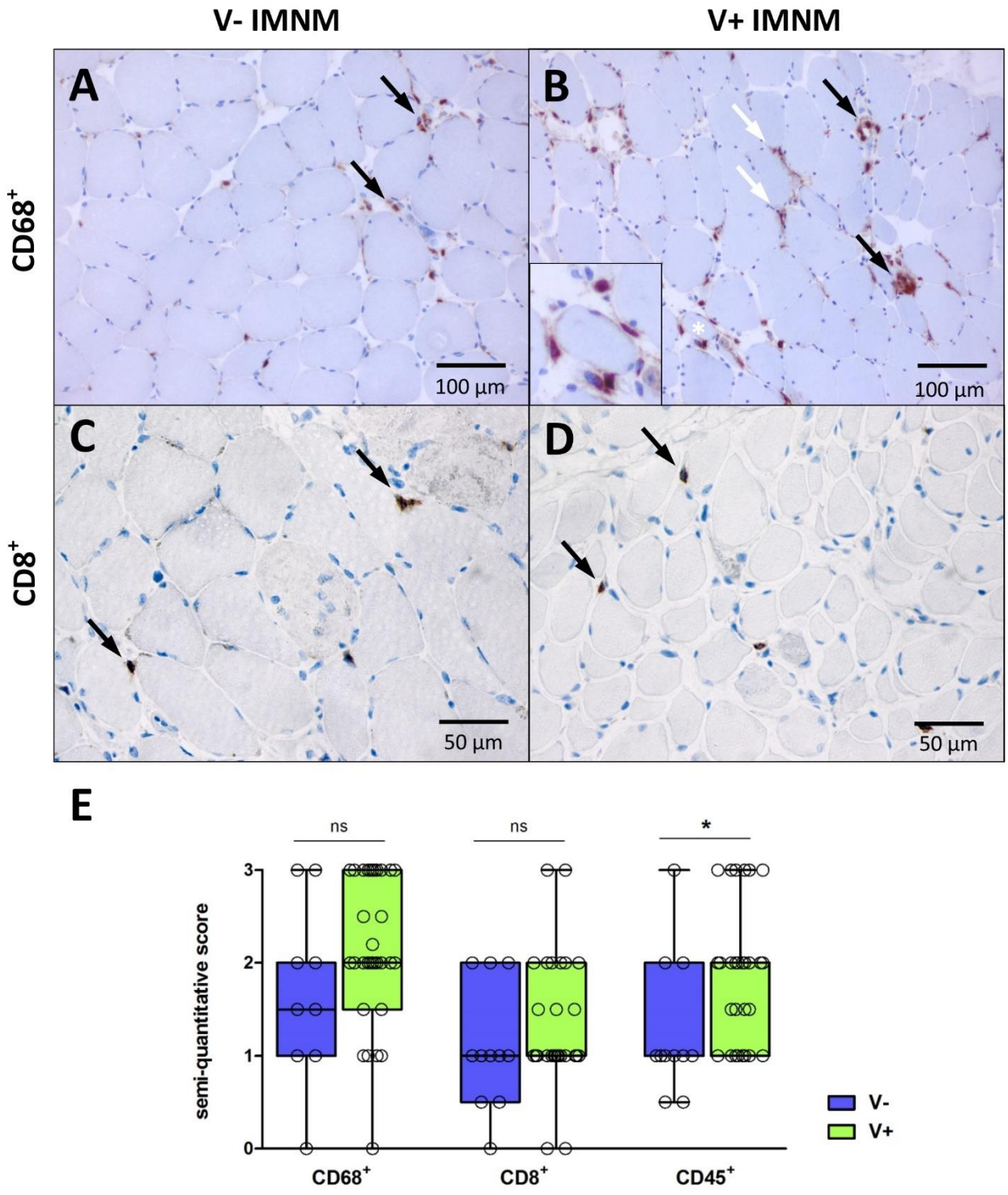

Figure 5 Similar distribution of immune cell infiltrate in V- and V+ skeletal muscle biopsies

***A-D**: Histopathology of CD68 and CD8 stain in V- and V+ IMNM patient biopsies. Black arrows in A and B point at $CD68^+$ macrophages invading necrotic fibers. **B:** White asterisk indicates necrotic myofiber surrounded by macrophages. White arrows point at macrophages close to normal appearing fibers (detail amplified in the box). **C-D**: Black arrows indicate $CD8^+$ T cells in V- (C) and V+ (D) IMNM patient muscle biopsies. The number of $CD8^+$ T cells appears to be similar in both groups. **E:** A significantly higher number of $CD45^+$ cells (p=0.0173) is present in the V+ group (histology not shown). More skeletal muscle biopsies with a high number of macrophages are found in the V+ group, as visible in A versus B, though no significance in this difference could be observed. Scoring of $CD8^+$ T cells in V- versus V+ confirms that there is no significant difference between the groups. Statistical analyses in E) were performed using the Mann-Whitney U-test.*

Sarcolemmal MHC class I expression on non-regenerating and non-necrotic myofibers has been described as a histopathological feature of IMNM in several studies. Needham *et al.* found a "diffuse" or "multifocal" pattern of MHC class I in IMNM skeletal muscle biopsies and MHC class I deposition can be used for the diagnosis "idiopathic inflammatory myopathy" (130). Hence, an investigation of MHC class I in the context of vacuole formation promised to be illuminating. Skeletal muscle fibers of healthy controls showed no sarcolemmal or sarcoplasmic MHC class I deposition, as shown exemplarily in Figure 6 C. In contrast, almost all of the analyzed IMNM patients (n=48, 92% (44 IMNM patients)) showed some degree of sarcolemmal or sarcoplasmic MHC class I expression (Figure 6 D). By applying the semi-quantitative scoring system for myofibers displaying MHC class I on the sarcolemma or within the sarcoplasm it could be revealed that both V+ and V- IMNM skeletal muscle biopsies showed comparable numbers of non-necrotic and non-regenerating myofibers with MHC class I deposition (Figure 6 A, B, D).

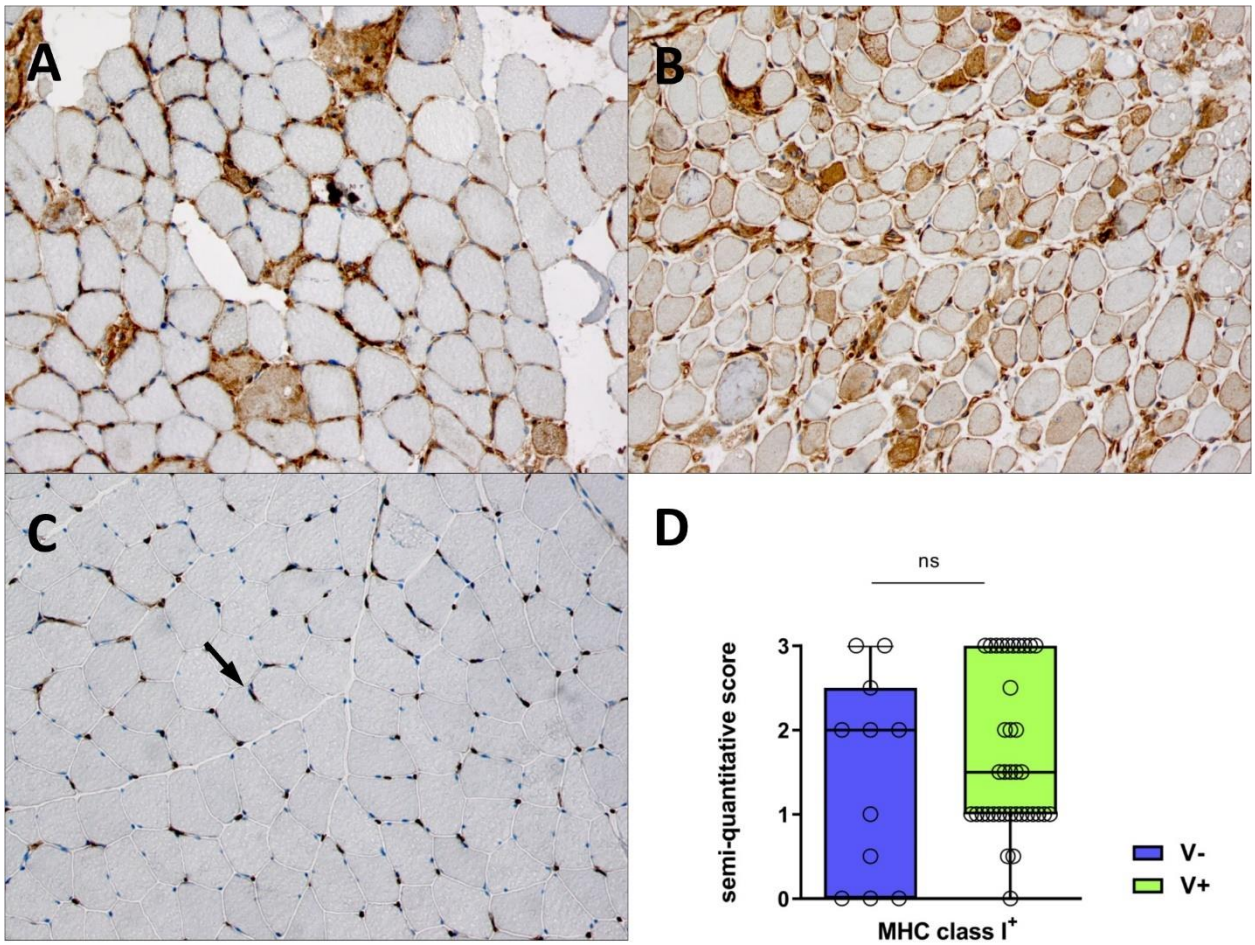

Figure 6 MHC class I expression on myofibers is present and the degree comparable in both V- and V+ IMNM patients

A-C: *Staining for MHC class I on V-, V+ and NDC patients muscle biopsies. Both V- (A) and V+ (B) biopsies display diffuse sarcolemmal and sarcoplasmic staining for MHC class I that does not appear in non-disease controls (C).* ***A:*** *A moderate number of myofibers (score 2) with sarcoplasmic MHC class I deposition in a V- IMNM patient.* ***B****: A V+ IMNM biopsy with an ample amount of sarcolemmal and sarcoplasmic MHC class I deposition (score 3).* ***C:*** *In NDC muscle, no MHC class I deposition is found of myofibers (arrow indicates the physiological MHC class I staining of capillaries).* ***D:*** *Both IMNM groups show a comparable amount of sarcolemmal or sarcoplasmic MHC class I deposition ranging from zero MHC class I positive fibers (score 0) over single positive fibers (score 1) up to an ample amount of MHC class I staining (score 3, shown in B).*

Preuße and colleagues have shown that the immune reaction in IMNM skeletal muscle tissue is most prominently driven by T helper cells Type I (Th1)/ classically activated macrophages (M1) and this finding can even be used diagnostically for differentiating IMNM and non-IMNM (129). As this immune reaction appears to be essential in IMNM, further exploration of the relation between the Th1/M1 response and vacuole formation in muscle tissue IMNM patients was conducted. For a more comprehensive analysis, the T helper cell Type 2/alternatively activated macrophage (M2) response was also assessed, which is widely accepted as a rather humoral-related immune response, in the context of V- and V+ IMNM skeletal muscle biopsies. As shown in Figure 7 A, mRNA of all important players of the Th1/M1 immune response, *IFNG*, *TNFA* and the transcription factor *STAT1* and *STAT2* are expressed at significantly higher levels in V+ IMNM patients than in NDC. *IFNG* levels are significantly elevated in the V- IMNM group as well, when

compared with NDC. Between the V- and V+ IMNM patients, no significant difference in the expression of markers of a Th1/M1 response was found. Interestingly, when looking at T helper cell Type 2-related markers, significantly higher levels of CD206 (*MRC1*) and *IL4-receptor* in the V+ group compared with the V- group could be found.

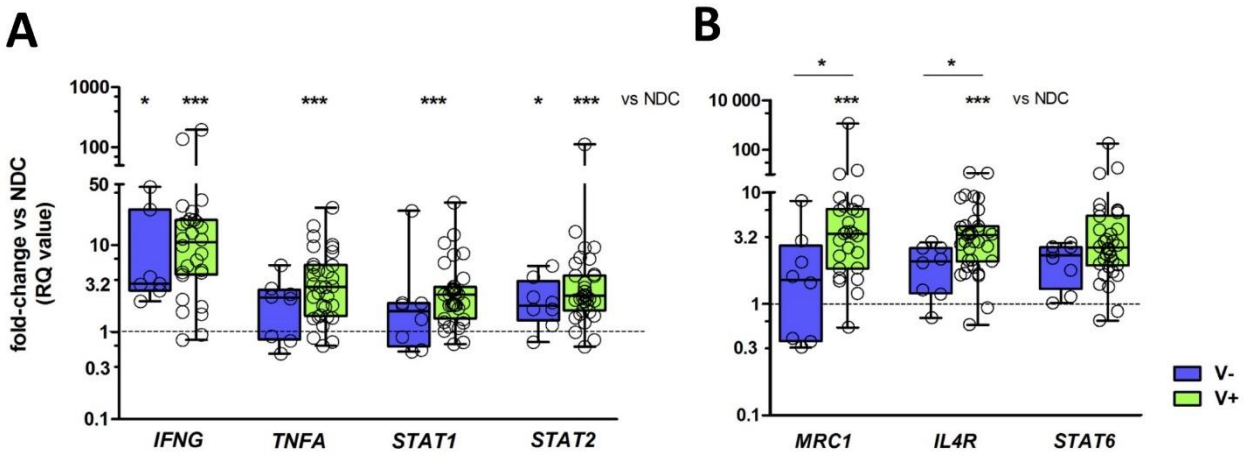

Figure 7 MRNA transcript levels of Th1/M1 and Th2/M2 immune response markers in V- and V+ skeletal muscle biopsies

***A**: mRNA expression of Th1/M1-related cytokines IFNy and TNFα and the transcription factors STAT1 and STAT2 is significantly increased in V+ IMNM patients when compared with NDC (asterisks, $p < 0.0005$). IFNG and STAT2 are also expressed at significantly higher levels in V- when compared with NDC (asterisks, $p < 0.05$). **B:** The mRNA levels of all Th2/M2- associated markers are significantly higher in V+ patients than in NDC (asterisks, $p < 0.0001$). The mRNA levels encoding for the surface proteins CD206 and IL4 receptor are significantly increased in V+ IMNM patients compared to V- IMNM patients ($p < 0.05$). Statistical analysis for comparison of both groups versus NDC was accomplished using the Kruskal-Wallis one-way ANOVA with Dunn´s multiple comparison test; for comparison of fold-change mRNA expression levels of V- vs V+, the Mann-Whitney U-test was performed. The dotted line indicates expression level of respective genes in NDC group (= 1-fold expression).*

TGFβ, an immune modulatory cytokine with various effects on immune response and tissue remodelling shows an increase in mRNA expression levels up to 40-fold in IMNM skeletal muscle tissue compared with NDC. Comparing V- and V+ patients, fold-change of *TGFB* levels in V+ are significantly higher than in V- IMNM patients (Figure 8).

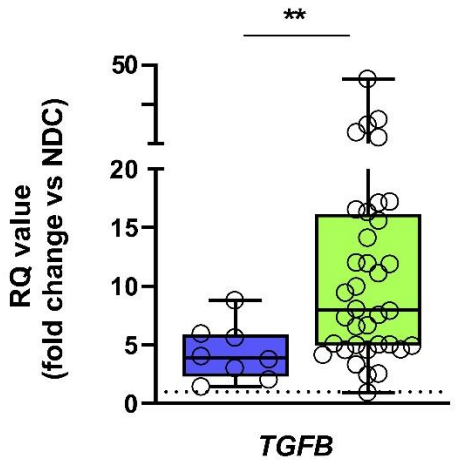

Figure 8 Significant TGFB upregulation in V+ versus V- IMNM patients skeletal muscle biopsies

MRNA expression of TGFB is increased up to 40-fold in V+ IMNM patients skeletal muscle tissue compared with NDC. In V+ IMNM patients, TGFB levels are significantly increased when compared with V- IMNM patients skeletal muscle biopsies. Statistical analysis for comparison of both groups versus NDC was accomplished using the Kruskal-Wallis one-way ANOVA with Dunn´s multiple comparison test; for comparison of fold-change mRNA expression levels of V- vs V+, the Mann-Whitney U-test was performed. The dotted line indicates TGFB expression level in NDC group (= 1-fold expression).

4.5. Influence of humoral immune mechanisms

Since the presence of B cells in IMNM, especially in anti-SRP^{+} patients, has been described before, an evaluation of the relation between B cell presence and the formation of vacuoles was also of interest. To achieve this, staining for the plasma cell marker CD138 (Figure 9 A) was performed which showed that 53% (24 biopsies, n=45) of the IMNM biopsies contained plasma cells, ranging from one to 100 plasma cells per ten HPFs. The great majority (87.5%, 21 biopsies) of these displayed a number of one to ten plasma cells per ten HPF; two biopsies with more than 50 plasma cells per 10 HPF being the exception. 46% (21 biopsies) showed no plasma cells. The number of plasma cells observed was similar when comparing the groups V+ and V-, as shown in Figure 9 B. Of note, the cases with a very high number of plasma cells were found within the V+ group (Figure 9 B).

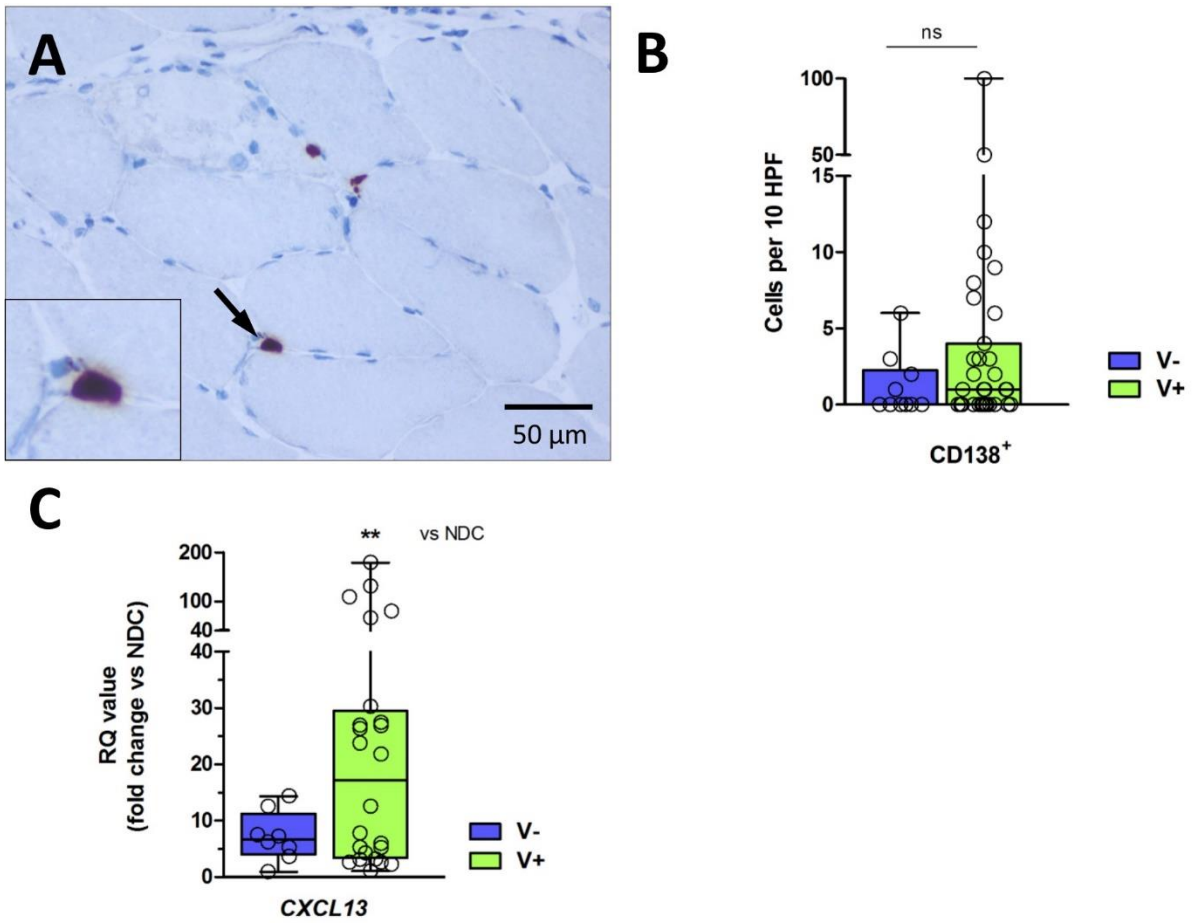

Figure 9 A similar number of plasma cells is present in both IMNM groups

***A**: Image of three plasma cells (exemplarily indicated by arrow) on one high power field (HPF) of a V+ biopsy. **B:** A comparable number of CD138$^+$ plasma cells is present in V- and V+ skeletal muscle biopsies, with a trend towards more plasma cells in V+ biopsies. **C**: mRNA expression of the B cell activator and attractant CXCL13 is significantly increased in V+ versus NDC (asterisk, p = 0.0111) Comparing CXCL13 expression in V- versus V+, CXCL13 appears to be increased in V+ skeletal muscle biopsies, though no statistical significance was found when tested with the Mann-Whitney U-test (p=0.2231).*

In order to determine if the trend towards a higher number of plasma cells in V+ IMNM patients is also represented by an increased expression of the corresponding chemokine *CXCL13*, a B cell attractor and activator (131, 132), its expression was assessed on mRNA level. The V+ group shows a significant increase in *CXCL13* mRNA expression compared with non-diseased control patients, however, the fold change expression of *CXCL13* does not significantly differ between the V+ and V- group (Figure 9 C).

As another arm of the humoral immune response, the presence of the terminal complement complex (C5b-9) on the sarcolemma of IMNM myofibers has been consistently described (1, 129, 130). The present study could confirm these results: sarcolemmal and sarcoplasmic deposition of complement was found to different degrees in most IMNM patients, but not seen in muscle of non-diseased control patients (Figure 10 A-C). On histological examination, a trend towards a higher

number of complement decorated fibers in V+ patients compared with V- patients was observed, though this trend was not statistically significant (Figure 10 D).

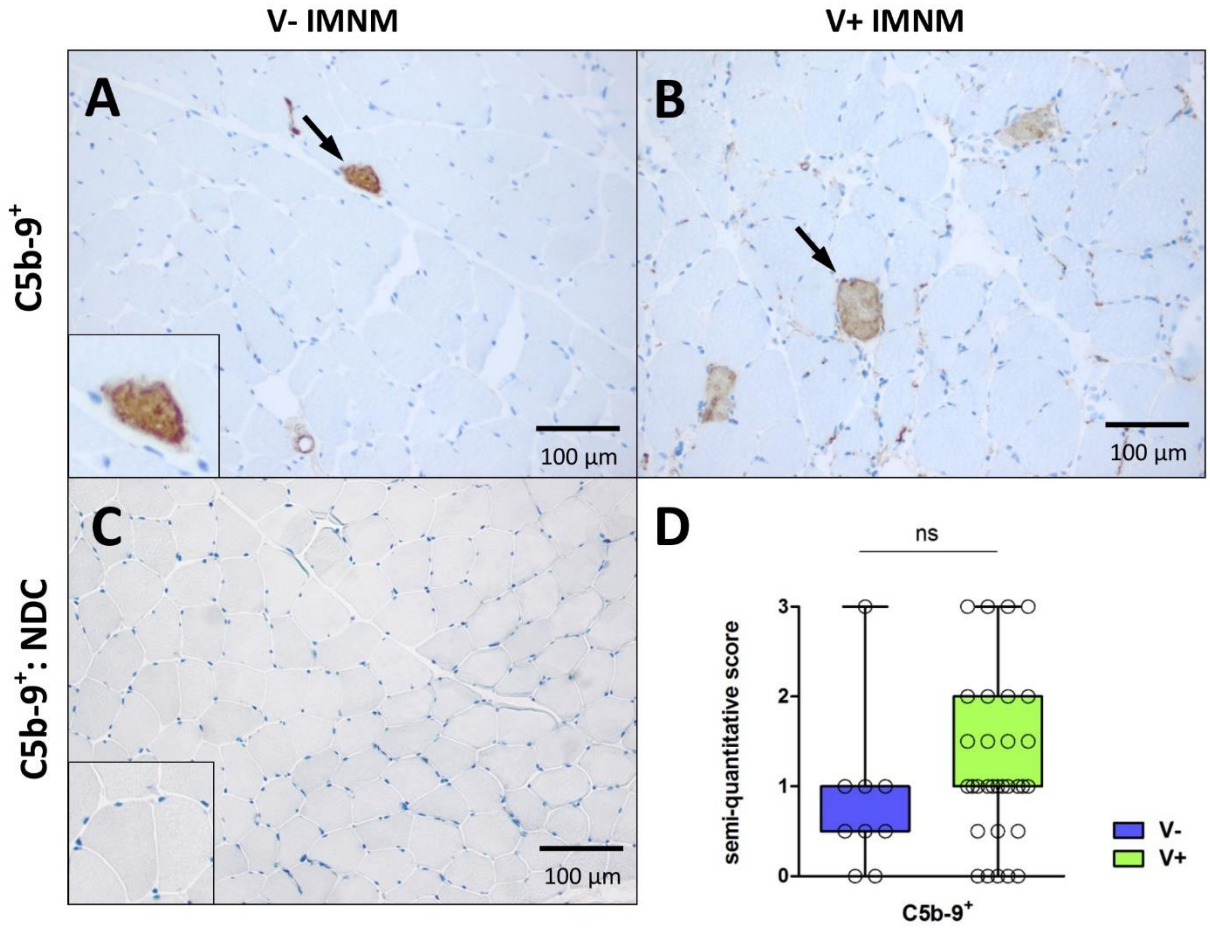

Figure 10 Complement deposition is found to a similar extent in V- and V+ IMNM patients

A-B: Strong sarcoplasmic complement (C5b-9) staining can be found in V- (A) as well as V+ skeletal muscle biopsies (B), exemplary myofiber indicated by arrows. C: Muscle fibers of NDC do not show any staining for C5b-9 (detail shown in box). D: Semi-quantitative scoring confirms that the majority of IMNM skeletal muscle biopsies show different numbers of myofibers with sarcolemmal or sarcoplasmic complement (C5b-9) deposition. No significant difference in the number of C5b-9+ fibers was found between V- and V+ patients. Statistical analysis was conducted using the Mann-Whitney U-test.

4.6. Summary of general and immunological aspects in IMNM subgroups

Vacuole formation is a common feature of IMNM, observed in 77% of the present cohort of 58 retrospectively analysed IMNM patients and not present in 23% of the analysed IMNM skeletal muscle biopsies. The distribution of age and gender is comparable in both groups. Comparing the two groups of IMNM patients with and without vacuoles, evaluation by general enzyme- and histopathological stainings revealed that the V+ group of IMNM patients shows a significantly higher number of necrotic myofibers and fibers undergoing phagocytosis. Regarding the regeneration markers, both groups display a comparable moderate to high amount of neonatal

myosin heavy chain (MyHC neonatal) with a visible trend towards more deposition of MyHC neonatal in the V+ group.

The cellular infiltrate in both groups is comprised of $CD68^+$ macrophages, $CD45^+$ leucocytes and $CD8^+$ T cells, with macrophages (and leucocytes) being most prominent. The number of infiltrating leucocytes is significantly higher in V+ patients, whereas $CD8^+$ T cell infiltrate is similar in V- and V+ IMNM patients. In addition, both groups display a comparable number of myofibers with sarcolemmal and sarcoplasmic MHC class I deposition that is not seen in healthy control muscle. Regarding the cellular immune response on gene expression level, IMNM patients show increased mRNA levels of markers for both the Th1/M1 and the Th2/M2 mediated immune reaction (Figure 6). Interestingly, there was no significant difference between V- and V+ patients in the expression of Th1/M1-related molecules, whereas markers of the Th2/M2 immune response showed significantly higher expression in V+ compared to V- (Figure 6 B). This could also be observed for gene expression of the immune-modulatory cytokine TGFβ, which was significantly increased in V+ IMNM patients (Figure 7). Involvement of B cell mediated immunologic effects also seems to be present in V+ patients, indicated by a significant increase in expression of the B cell chemoattractant *CXCL13* in V+ IMNM skeletal muscle biopsies in comparison with normal controls. Complementing this is also the presence of slightly more $CD138^+$ plasma cells in V+ muscle biopsies, although V- IMNM biopsies contain few plasma cells as well. Pronounced complement deposition, on the other hand, is present in both IMNM groups.

4.7. Description and analysis of vacuolar structures in IMNM

4.7.1. Analysis of protein aggregation

Vacuoles in IMNM are not characterised by sarcolemmal features and no abnormal protein aggregation is found in vacuoles of skeletal muscle biopsies from IMNM patients

Some myopathies that histopathologically show vacuole formation harbour vacuoles with sarcolemmal features like autophagic vacuolar myopathies of adulthood, Vici syndrome, Danon disease and sometimes Pompe disease, indicating their sarcolemmal origin as opposed to vacuoles that do not possess a sarcolemmal membrane. To assess the origin of the vacuoles found in IMNM patient biopsies, stainings for the sarcolemmal protein β-spectrin, and for acetylcholine esterase (AchE) were performed. Of 30 exemplary analysed V+ biopsies, 20 (54%) showed no acetylcholine esterase activity on the vacuoles. Three biopsies showed single vacuoles staining positively for acetylcholine esterase and seven V+ skeletal muscle biopsies showed AchE staining

on the sarcolemma but not on vacuoles, indicating extra-junctional AchE activity as a marker for regeneration (data not shown).

For β-spectrin, only single vacuoles staining positively could be found in five skeletal muscle biopsies of the V+ group, while twelve biopsies of V+ IMNM patients were β-spectrin-negative. In the V- group no positive staining was observed, except for one biopsy with sarcoplasmic β-spectrin and one biopsy with AchE activity on the sarcolemma (data not shown).

Abnormal protein aggregation has been shown to be involved in vacuole formation of sIBM, which led me to investigate whether protein aggregates are also present in IMNM muscle, especially relating to vacuolar structures. The investigation showed no positive staining for Fused in sarcoma (FUS) protein in any of the stained biopsies (9 V- and 31 V+, see exemplary image in Figure 11 B). The same was the case for AT8, an antibody binding phosphorylated tau, and anti-amyloid, for which all 41 IMNM patients skeletal muscle biopsies (7 V-, 34 V+) assessed were negative (exemplary image in Figure 11 C). Equally, the analysis of TDP-43, a nuclear DNA-binding protein that forms pathological aggregates in sIBM, amyotrophic lateral sclerosis and frontotemporal dementia (133, 134) showed no staining in 33 biopsies (6 V- and 27 V+) and only one V+ biopsy showed a very weak staining pattern (data not shown).

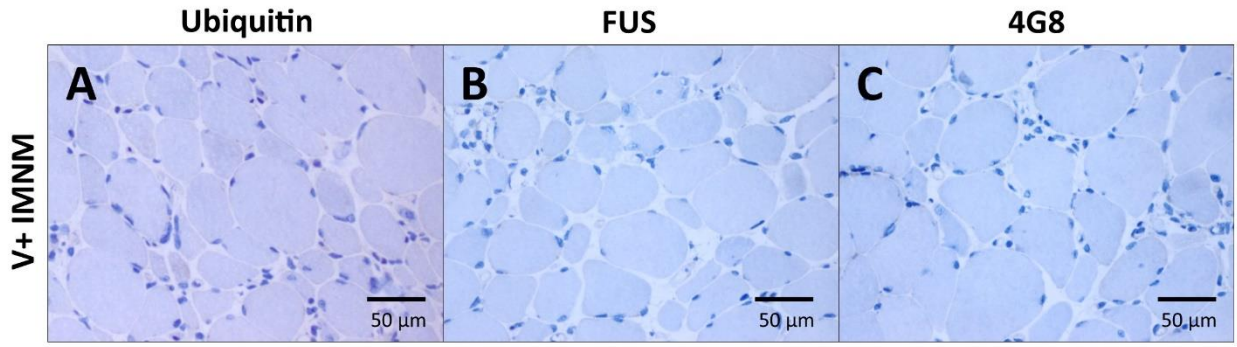

Figure 11 No abnormal protein aggregation in either IMNM subgroups

A-C: *No positive staining of vacuoles or other cytoplasmic structures for ubiquitin, FUS or amyloid was found. Shown are representative skeletal muscle sections of V+ patients; ubiquitin stainings were performed on 27 biopsies (7 V-, 20 V+) FUS stainings were performed on 40 biopsies (9 V-, 31 V+) and analysis for amyloid included 41 biopsies (7 V-, 34 V+) (data not shown).*

4.7.2. The role of protein degradation mechanisms on vacuole formation

Autophagy proteins are deposited throughout the sarcoplasm in IMNM patients, but autophagy-related genes are only partially upregulated.

Autophagy is a cellular degradation pathway that plays a relevant role in different myopathies and, importantly, for myopathies characterized by vacuole formation (35, 39, 43, 48). Hence, it was of importance to explore whether altered autophagic pathways also take part in vacuole formation and muscle pathology of IMNM. Since defective autophagic mechanisms also pose a possible starting point for new therapies, this approach seemed especially promising and valuable.

In order to comprehensively assess the autophagic process, several stainings for proteins involved in autophagosome formation and lysosome composition were performed and the respective gene expression of viable autophagy related genes was evaluated. First of all, a positive staining of myofibers for the autophagy-related protein LC3-B (from here referred to as LC3) was observed, a protein that marks autophagic structures from the forming isolation membrane/phagophore up until fusion of the autophagosome with lysosomes (86, 135) (Figure 12 A-B). Equally, positive staining for p62/sequestosome-1 (from here referred to as p62) was found, a protein that connects poly-ubiquitinated proteins with LC3 in IMNM (Figure 12 C-D). Staining for both proteins did not mark myofibers in the muscle tissue of NDC (Figure 12 E-F). Interestingly, for these histological features significant differences between the vacuole positive and vacuole negative IMNM groups were present. V+ biopsies displayed significantly more myofibers staining positively for p62, and LC3 staining also seemed to be found more often in V+ than in V- biopsies, although not statistically significant (Figure 12 G). Morphologically, LC3 showed a distribution of several single foci to intense and diffuse staining of great parts of the sarcoplasm. There seemed to be a tendency of LC3 deposition on the periphery of the sarcoplasm, close to the sarcolemma. Staining for LC3 was mainly found in smaller appearing myofibers (Figure 12 C, D). The morphology of p62 resembles that of LC3 with a mild to strong diffuse staining of the entire sarcoplasm, even though generally the staining of p62 appeared more pronounced than that of LC3 (Figure 12 A-D).

Analysing gene expression of autophagy-related genes via qPCR, IMNM V+ skeletal muscle biopsies show significantly increased levels of *MAPLC3A* mRNA (from here referred to as *LC3*) compared with non-diseased control patients (NDC) (Figure 12 H). MRNA encoding *SQSTM1*/*p62* (from here referred to as *p62*) however, was not significantly more expressed in either IMNM group compared to healthy control patients. No significant difference was found in

the expression of *LC3* or *p62* when comparing the V- and V+ IMNM groups. In addition, there was no significant increase of *BECLIN* or *ULK1* mRNA levels, both genes related to initiation of autophagy, neither in the IMNM groups among each other nor compared to NDC patients (Figure 12 H).

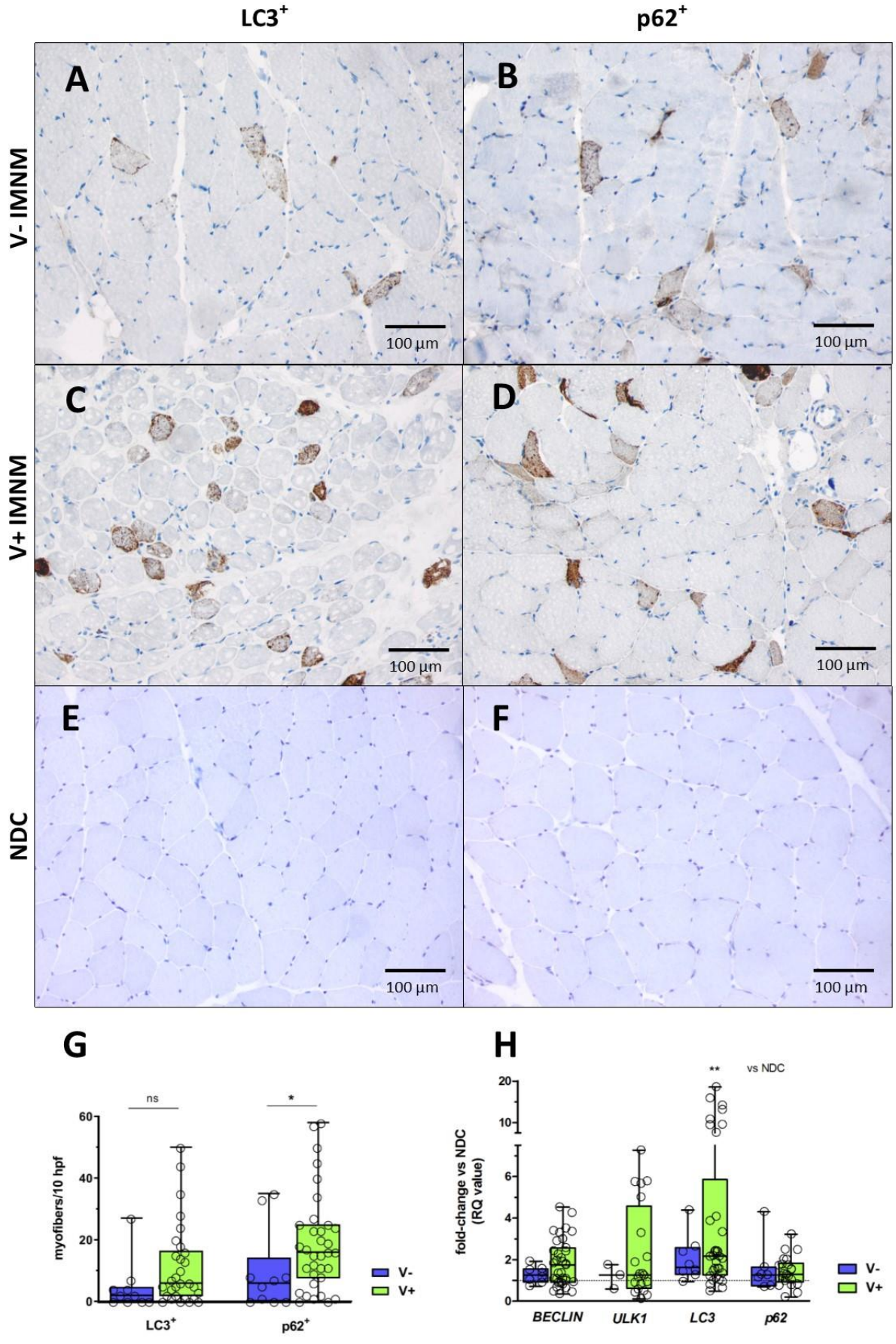

Figure 12 – Legend on next page –

Figure 12 V+ IMNM patients show increased levels of autophagy-related proteins upon histological analysis

***A-D**: Histological stainings for the autophagy-related proteins LC3 and p62 show positive myofibers in both V- (A) and V+ (B) IMNM patients. C and D show the high number of LC3 and p62 positive fibers in V+ IMNM biopsies, while staining for those autophagy markers can be significantly less in V- skeletal muscle (A, B). **E-F**: No staining for LC3 or p62 can be observed in NDC. **G:** Analyzing the histopathology, V+ patients show a significantly higher number of myofibers staining positively for p62. The number of LC3 positive fibers was similar in the V- and V+ group. **H**: mRNA levels of autophagy related gene MAPLC3A is significantly increased in V+ patients compared to NDC, while there is no increase in SQSTM1/p62 mRNA expression neither in comparison with NDC (data not shown) nor between V- and V+ patients. BECLIN and ULK1 mRNA levels were not significantly increased in either IMNM group. Statistical analysis in G was performed using the Mann-Whitney U-test (p=0.0367 for p62) and the Kruskal-Wallis one-way ANOVA with Dunn´s multiple comparison test (p=0.0056 for V+ vs. NDC for MAPLC3) in H. The dotted line in H indicates expression level of respective genes in NDC group (= 1-fold expression).*

On a closer look at p62 morphology, the variable degree of diffuse staining of the entire sarcoplasm of often normal appearing myofibers could be verified (Figure 13 B-D). The observed range comprises the presence of very fine $p62^{+}$ puncta to intense staining of the entire sarcoplasm (Figure 13 A, B, D), also within the same IMNM biopsy (Figure 13 C). Sometimes, a peripheral or perinuclear accentuation for p62 was found (Figure 13 B).

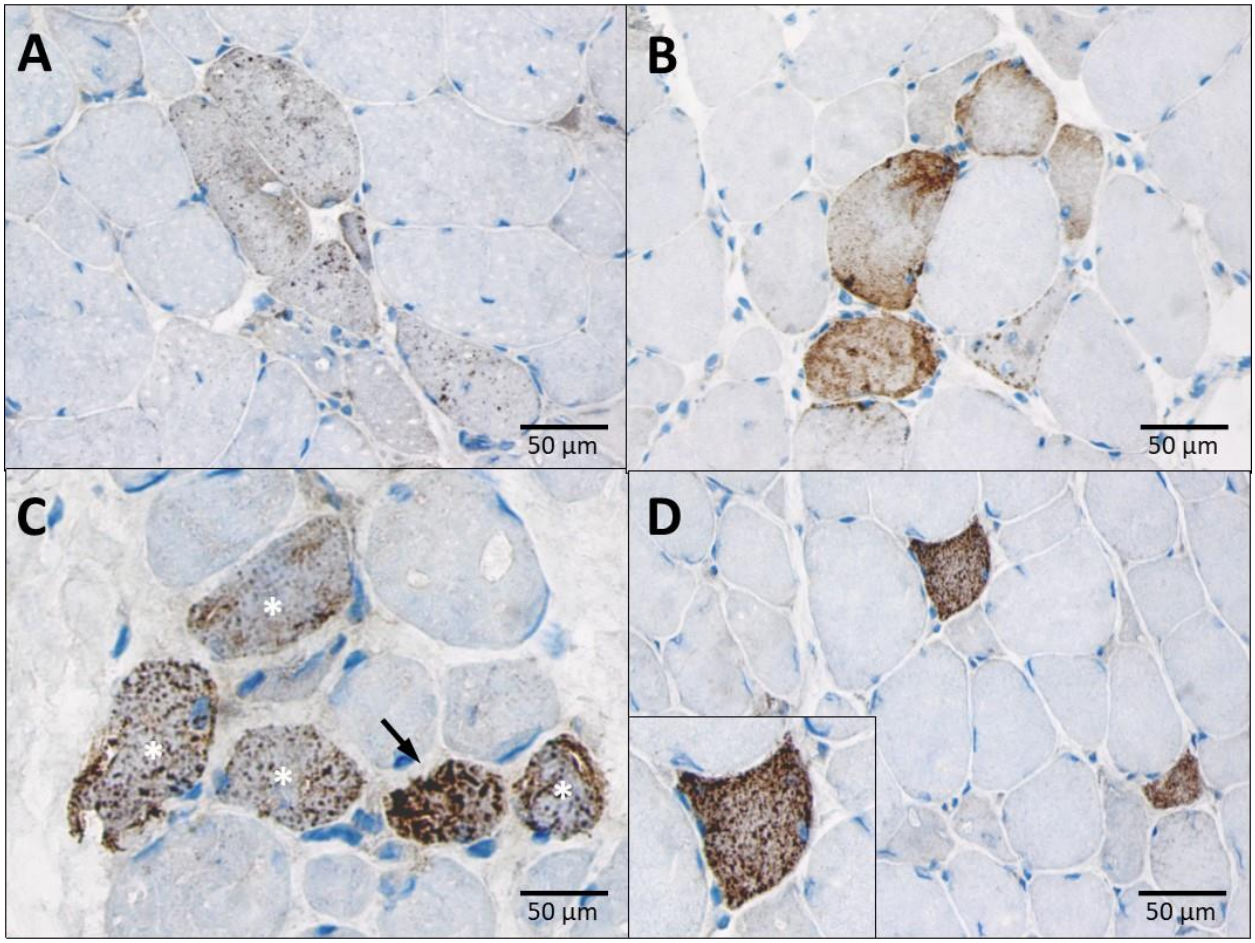

Figure 13 Morphology of p62 staining in IMNM myofibers

***A-D**: p62 stainings in IMNM skeletal muscle biopsies show a diffuse distribution of p62 throughout the entire sarcoplasm with variable intensity ranging from a subtle pattern of small puncta (A) over increasing density of the puncta (B) and marked fibers in C up to a strong staining of the entire myofiber (arrow in C, detail in D).*

Increased expression of immunoproteasome subunits in V+ skeletal muscle biopsies

The upregulation of subunits of the immunoproteasome has been shown and a connection to the pathological MHC class I and MHC class II expression on myofibers of inflammatory myopathies has been proposed (103). The studied group of "inflammatory myopathies" comprised of sIBM, DM as well as PM cases, whereas the role of the immunoproteasome specifically in IMNM has not been addressed to date. Since most IMNM skeletal muscle biopsies show MHC class I upregulation and the proteins presented by MHC class I are processed by the immunoproteasome it would be of great interest to know whether this antigen-processing machinery is also altered in IMNM and if a relation to vacuole formation exists. Indeed, compared with skeletal muscle tissue of healthy control patients, V+ patients showed a significant higher expression of the immunoproteasome subunits *β1i/LMP2* and *β5i/LMP7* mRNA, ranging from 1.3 up to a 30-fold

higher expression (Figure 14). When comparing immunoproteasome expression between the V- and the V+ group, no significant differences were found (Figure 14).

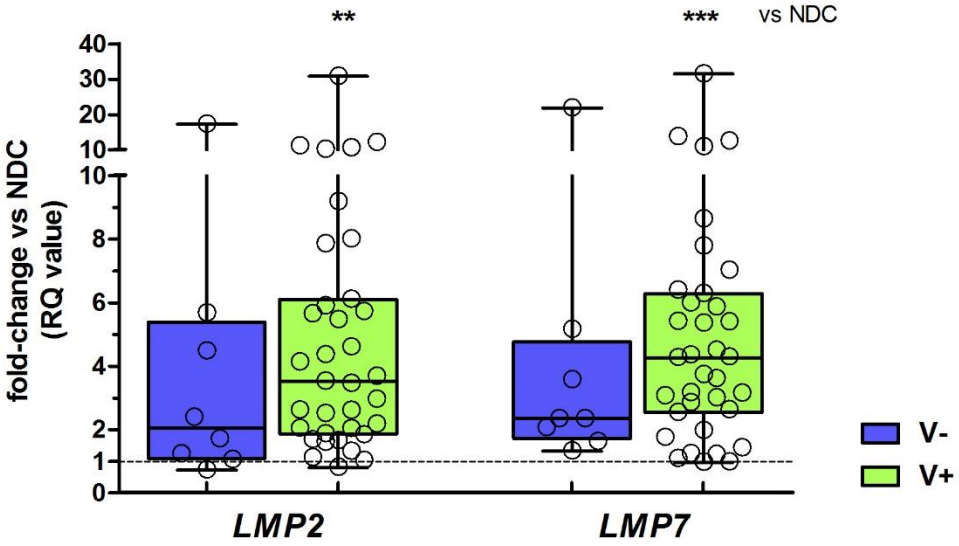

Figure 14 Increased expression of immunoproteasome subunits in IMNM

QPCR analysis revealed significantly increased levels of immunoproteasome subunits β1i/LMP2 (p=0.0016) and β5i/LMP7 (p=0.0005) mRNA in the V+ IMNM group when compared with NDC. Comparing the V- and V+ group with each other, no significant difference in immunoproteasome mRNA expression was found. Statistical analysis was performed using the Kruskal-Wallis one-way ANOVA with Dunn´s multiple comparison test for analysis of V-and V+ vs NDC and the Mann-Whitney U-test for comparing fold-change expression of V- vs V+. The dotted line indicates expression level of respective genes in NDC group (= 1-fold expression).

ER stress and ER-related degradation mechanisms play a role in IMNM

The ER stress response has been shown to be activated in other inflammatory myopathies (DM, PM and sIBM) and been suggested as an essential non-immune mediated pathway adding to myofiber damage (112, 136). Thus, the investigation of the ER response pathway in IMNM was an important step in order to evaluate vacuole origin and gain insight into possible disease pathogenesis.

The present analysis revealed that in V+ IMNM muscle tissue mRNA of the ER stress response induced genes *XBP1* and *EDEM1* are expressed at significantly higher levels than in healthy control muscle tissue, ranging from four to eight times of normal expression (Figure 15). No significant increase in expression of *CHOP*, an ER stress induced mediater of apoptosis, is present for either IMNM group compared with non-diseased control patients. In addition, mRNA levels of *HSPA5/GRP78,* encoding for a constitutive ER chaperone protein that also binds ER stress

sensing molecules in their inactivated state are expressed to a similar degree in NDC as well as V- and V+ patients (Figure 15).

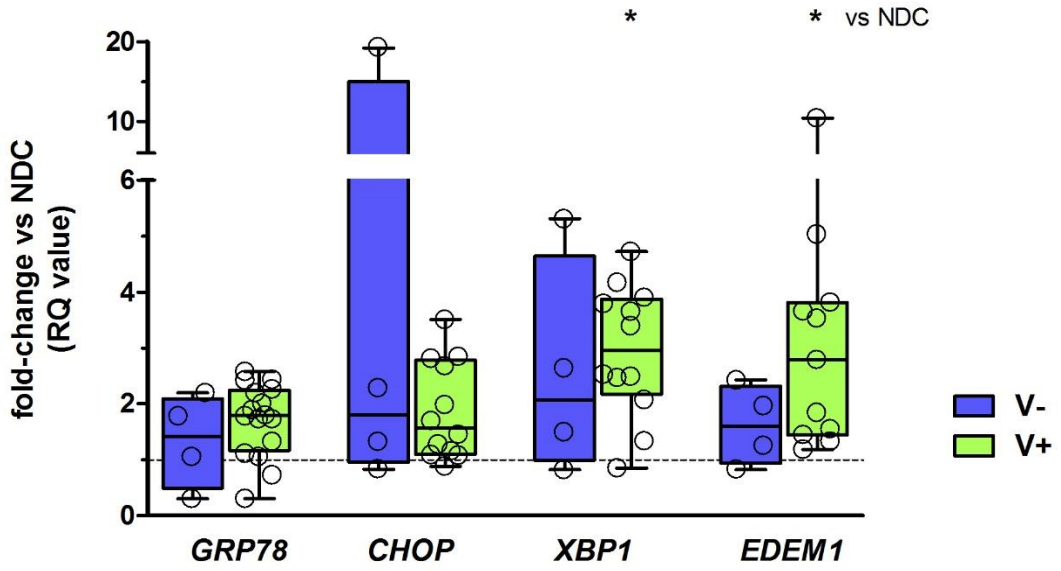

Figure 15 ER stress induced effector genes are upregulated in V+ IMNM patients

V+ skeletal muscle biopsies show significantly increased mRNA levels of ER stress response induced genes EDEM1 (p=0.0116) and XBP1 (p=0.0377) compared with NDC patients. No significant increase in mRNA levels of the ER housekeeping chaperone GRP78 or ER stress response mediated apoptosis inducer CHOP was found comparing the V- or V+ group with each other or with NDC. Statistical analysis for comparison of NDC vs V- and V+ was performed using Kruskal-Wallis one-way ANOVA with Dunn´s multiple comparison test and the Mann-Whitney U-test for comparing fold-change expression of V- vs V+. The dotted line indicates expression level of respective genes in NDC group (= 1-fold expression).

4.8. Summary of alterated protein degradation processes in IMNM

The exploration of the various cellular degradation pathways in V- and V+ IMNM patients revealed intense staining of IMNM muscle fibers with autophagy-related proteins LC3 and p62, which is not seen in healthy control muscle biopsies. Both V- and V+ skeletal muscle biopsies stained positively for the autophagy-essential molecules LC3 and p62, with significant more myofibers in the V+ group staining positively for p62. The observed morphology of p62 staining showed a strikingly distinct pattern of moderate to intense diffuse distribution throughout the entire sarcoplasm. This alteration of autophagy-related proteins is only partly represented on the gene expression level: mRNA levels of *LC3* are significantly increased in V+ skeletal muscle biopsies when compared with muscle tissue of non-diseased control patients but no change in mRNA expression of *p62* was found (Figure 12 H).

MRNA levels of the immunoproteasome subunits β5i/LMP7 and β1i/LMP2 are signficantly increased in V+ patients compared with NDC. Analogous to this, ER stress-induced gene transcripts of *XBP1* and *EDEM1* are expressed at significantly higher levels in V+ patients than in NDC. No significant differences can be observed between the two IMNM groups for both the immunoproteasome and ER stress markers.

All in all, IMNM skeletal muscle biopsies and especially those of V+ patients reveal increased levels of immunoproteasome- and ER stress response-related gene transcripts. MRNA levels of the autophagy related marker p62 is not elevated in IMNM. However, IMNM patients skeletal muscle biopsies show immunoreactivity for LC3 and p62 and significant differences in the number of p62-immunoreactive myofibers are present between the V- and the V+ group. Since differences between V- and V+ IMNM patients appeared not to be present because of specific underlying mechanisms, both subgroups were combined for the comparison with sIBM.

4.9. Comparison of autophagy processes in sIBM versus IMNM

The presented analysis of autophagy related macromolecules in IMNM showed a peculiar staining pattern for LC3 and p62 in the histopathological exploration as well as increased expression of *LC3* on the mRNA expression level. P62 has been shown repeatedly to form aggregates in sIBM and a pathophysiological role is hypothesized (137). Recently, attention has been drawn to an sIBM- specific pattern of p62 staining that can be used diagnostically (138). SIBM is thus the only inflammatory myopathy where a role and specific morphology for p62-positive aggregates has been described. Therefore, sIBM was chosen as comparison partner for IMNM, as the present analysis has shown that IMNM is another IIM where a distinct p62 pathology seems to play a crucial role.

For mRNA expression levels, both IMNM patients and sIBM patients showed significantly increased mRNA levels of *LC3* when compared with non-diseased control patients (up to 20-fold in IMNM and up to 10-fold in sIBM, Figure 16). On comparing IMNM and sIBM, similar levels of *LC3* and *p62* were found, and no increase in *p62* expression compared with NDC was discerned in either group (Figure 16).

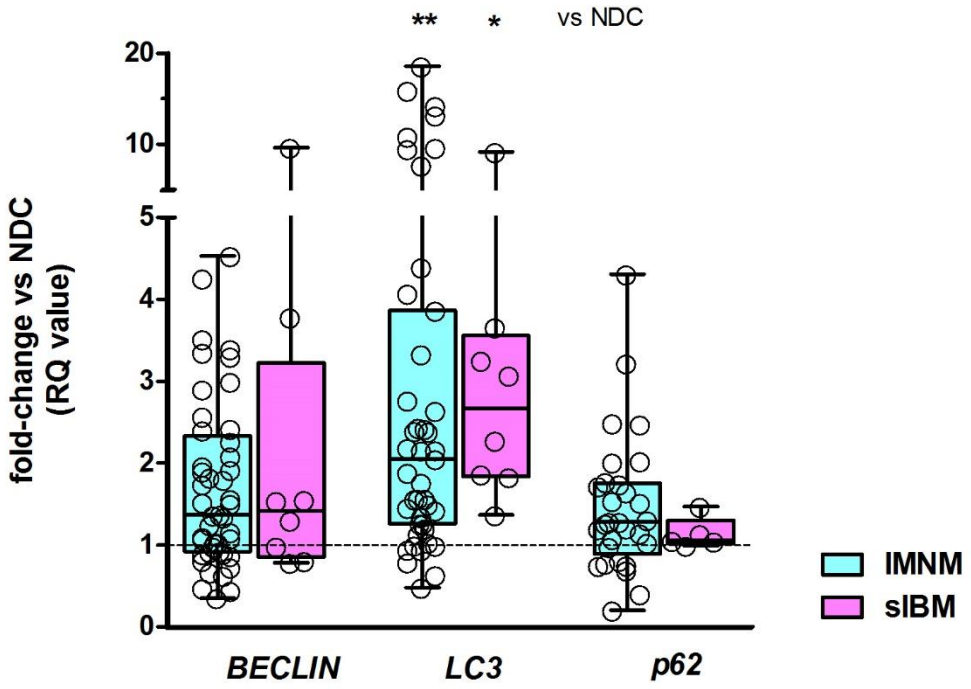

Figure 16 Similar mRNA expression levels of autophagy markers in IMNM and sIBM

No significant differences in mRNA expression levels of autophagy-related genes were found between IMNM and sIBM patients. Compared with NDC, IMNM patients showed significantly increased levels of LC3 (up to 18-fold), indicated by the asterisks. Equally, sIBM patients showed significantly higher mRNA levels of LC3 compared with NDC. Neither IMNM patients nor sIBM patients showed increased expression of p62. Statistical analyses between either of the groups with NDC was performed using the Kruskal-Wallis one-way ANOVA with Dunn´s multiple comparison test, one asterisk represents a $p < 0.05$ and two asterisks a $p < 0.005$. The Mann-Whitney U-test was applied for comparing mRNA fold-change expression of IMNM vs sIBM. The dotted line indicates expression level of respective genes in NDC group (= 1-fold expression).

On the morphological level, however, striking differences were present. As shown in Figure 17 D-F the p62 deposits in sIBM appeared as coarse, thick puncta, localized throughout the cytoplasm, close to the periphery or around the nucleus. In contrast, p62 in IMNM skeletal muscle fibers was distributed in a diffuse manner throughout the entire sarcoplasm as very fine puncta with slight emphasis on the periphery of the myofibers (Figure 17 A-C).

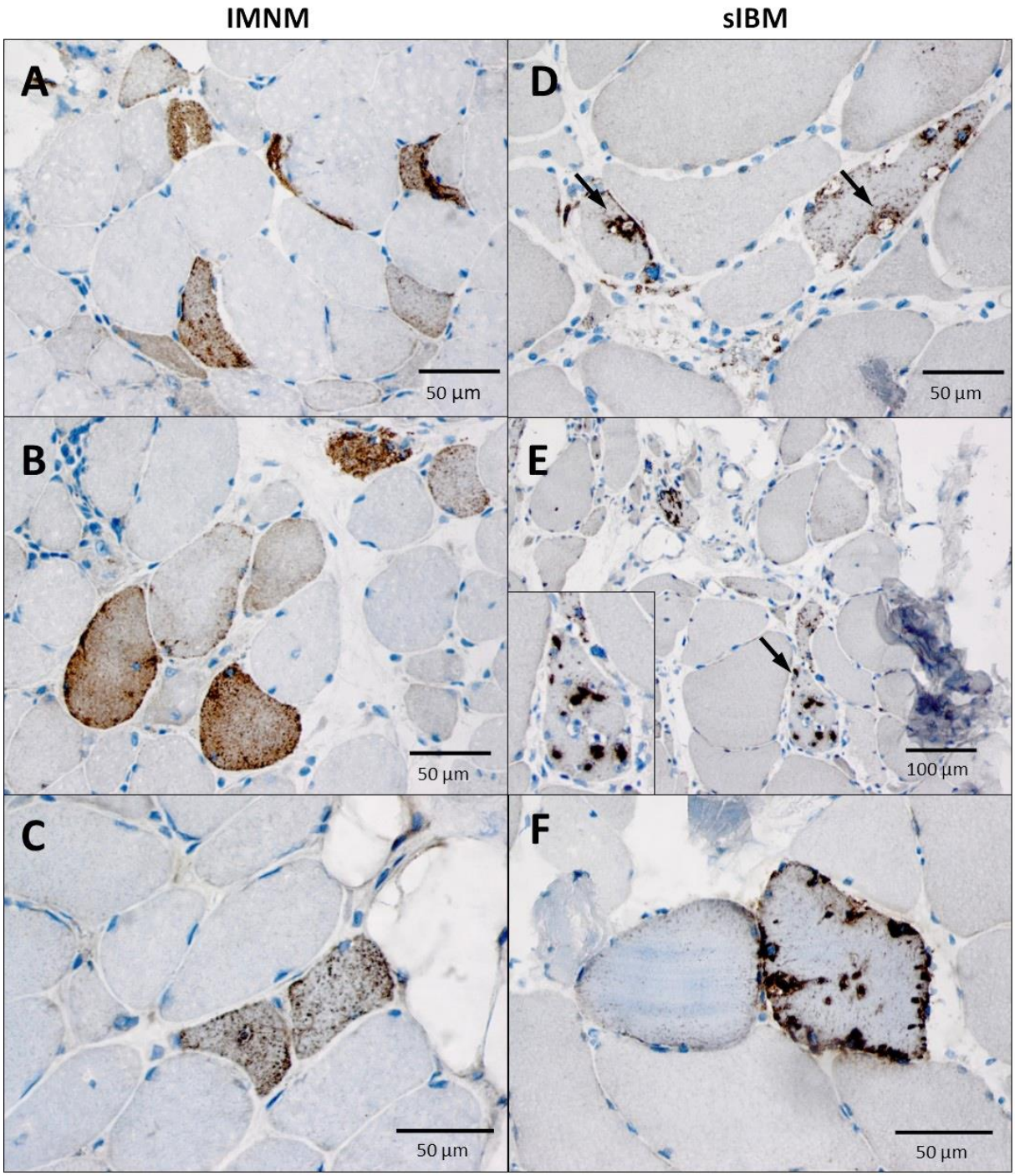

Figure 17 Distinct differences in the morphology of p62 in myofibers of IMNM versus sIBM patients

A-C*: p62 in IMNM muscle biopsies is distributed as very fine puncta evenly throughout the entire sarcoplasm.* ***D-F:*** *p62 in sIBM muscle biopsies appear as coarse circumscribed deposits in the sarcoplasm (arrow in E, myofiber magnified in box; F), surrounding vacuolar structures (arrows in D) close to the sarcolemma (F) or surrounding the nucleus (arrows in F).*

4.10. Chaperone-assisted selective autophagy in IMNM and sIBM

Since p62 is a robust marker for selective autophagy processes and plays an integral role in the chaperone-assisted selective autophagy (CASA) pathway shown to be essential for muscle fiber integrity and function, a more detailed analysis of CASA-related proteins in IMNM skeletal muscle biopsies was conducted.

On the histopathological level, as the main chaperone proteins involved in CASA, BAG3 and HSP70 show a positive staining reaction in IMNM muscle fibers (Figure 18), not seen in NDC patients´ muscle tissue (data not shown). HSP70 appears diffusely distributed throughout the sarcoplasm (Figure 18 A, B) and stained the sarcolemma of vacuolated fibers (Figure 18 C). BAG3 also shows diffuse sarcoplasmic immunoreactivity (Figure 18 D), as well as subsarcolemmal staining (myofibers indicated by arrows in Figure 18 E, F).

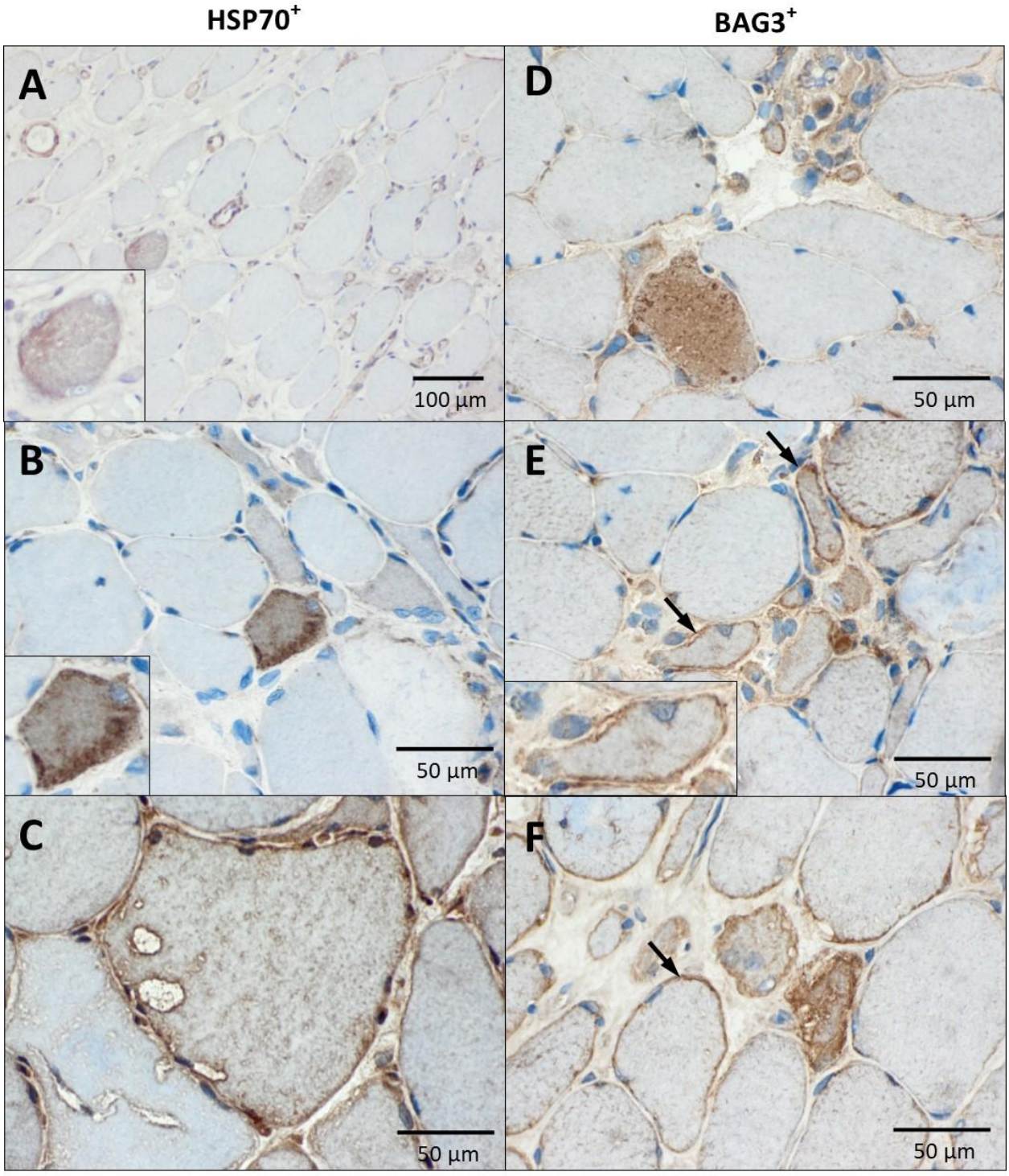

Figure 18 IMNM skeletal muscle biopsies stain positively for CASA key proteins HSP70 and BAG3

*Myofibers of IMNM patients show diffuse sarcoplasmic staining with HSP70 (**A-C**) and diffuse sarcoplasmic (**E-F**) as well as sarcolemmal staining (arrows in **D** and **E**) with BAG3, two of the main proteins involved in chaperone-assisted selective autophagy (CASA).*

Upon analysis of serial sections of the same IMNM skeletal muscle biopsy, the deposition of p62, HSP70, BAG3 and another small heat shock protein, αB-Crystallin in the same myofiber revealed itself, as shown in Figure 19 A-D (the image in the box shows an amplification of the myofiber

pointed at by the arrow). In addition, double immunofluorescence stains showed a co-localization of p62 with HSP70 (Figure 19 E), BAG3 (Figure 19 F) and αB-crystalline (Figure 19 G).

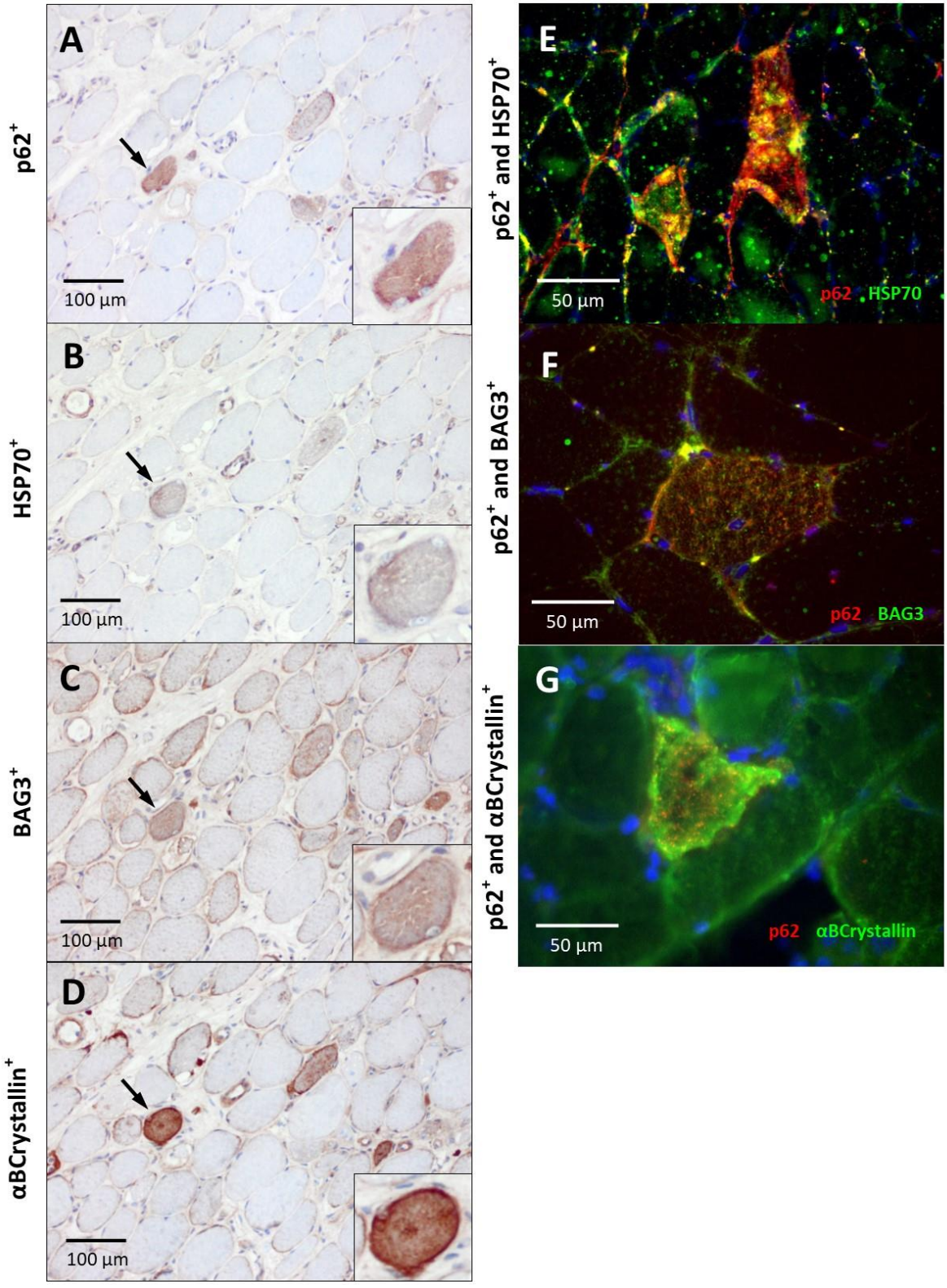

Figure 19 – Legend on next page –

Figure 19 Co-localization of p62 with CASA-related proteins and the chaperone αB-Crystallin in IMNM muscle fibers

***A-D**: Staining of the same myofibers (arrows; magnified in detail) with p62, HSP70, BAG3 and αB-Crystallin in serial sections of an IMNM skeletal muscle biopsy. **E-G:** Immunofluorescence staining reveal co-localization of p62(red) with HSP70 (green) (E), p62 (red) with BAG3 (green) (F) and p62 (red) with αB-Crystallin (green) (G).*

On the mRNA level, *BAG3* expression in IMNM patients is comparable with that in non-diseased control patients. This is also the case for *HSPA8* and *HSPB8*. Interestingly, *CRYAB* levels were increased by up to two- to threefold compared with NDC, although not statistically significant. When comparing gene expression levels of these CASA-related molecules of IMNM with sIBM, no significant differences were present for *CRYAB*, *HSPA8* or *HSPB8*. However, the muscle tissue of sIBM patients showed significantly lower *BAG3* mRNA levels than the skeletal muscle biopsies of IMNM patients (Figure 20).

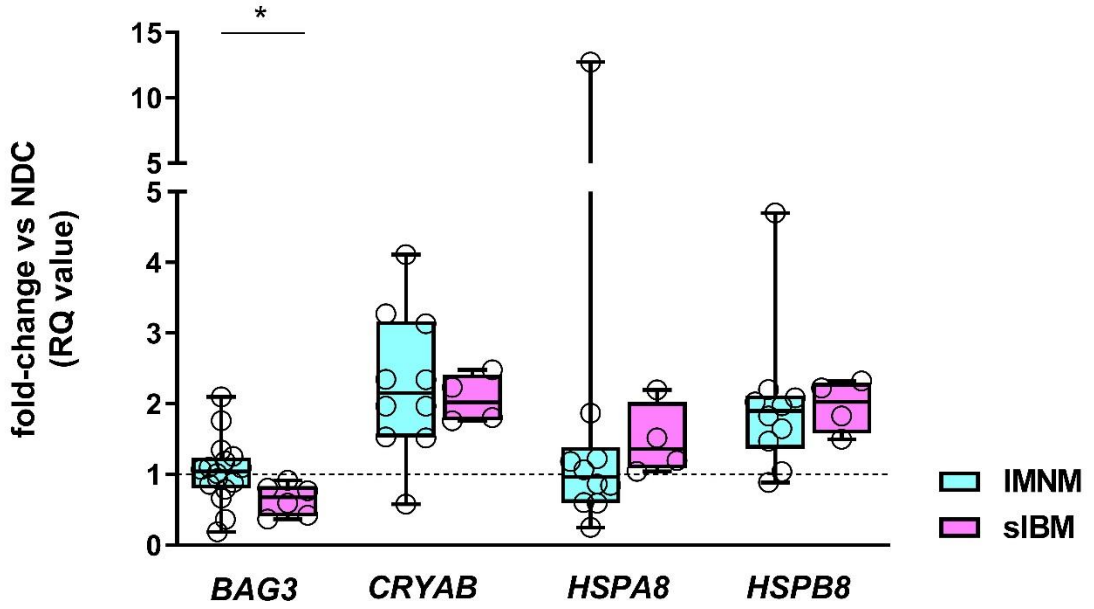

Figure 20 Relative mRNA expression of CASA-related genes in IMNM and sIBM

BAG3 mRNA levels in IMNM skeletal muscle biopsies are comparable with those in NDC. However, BAG3 expression is significantly decreased in sIBM patients when compared with V+ IMNM patients (p = 0.0328). For CASA-related genes CRAYB, HSPA8 and HSPB8 no significant differences between IMNM and sIBM patients were found. The Mann-Whitney U-test was applied for comparing mRNA fold-change expression of IMNM vs sIBM. The dotted line indicates expression level of respective genes in NDC group (= 1-fold expression).

Since ER stress induced genes are upregulated in IMNM, and ER stress related mechanisms have been described in sIBM (136), ER stress gene transcripts of IMNM with sIBM were compared. In that analysis, up to 4 to 6-fold higher levels of *XBP1* and *EDEM1* in sIBM compared with NDC were found. Compared with the equally elevated levels of these transcripts in IMNM, there was no significant difference (Figure 21).

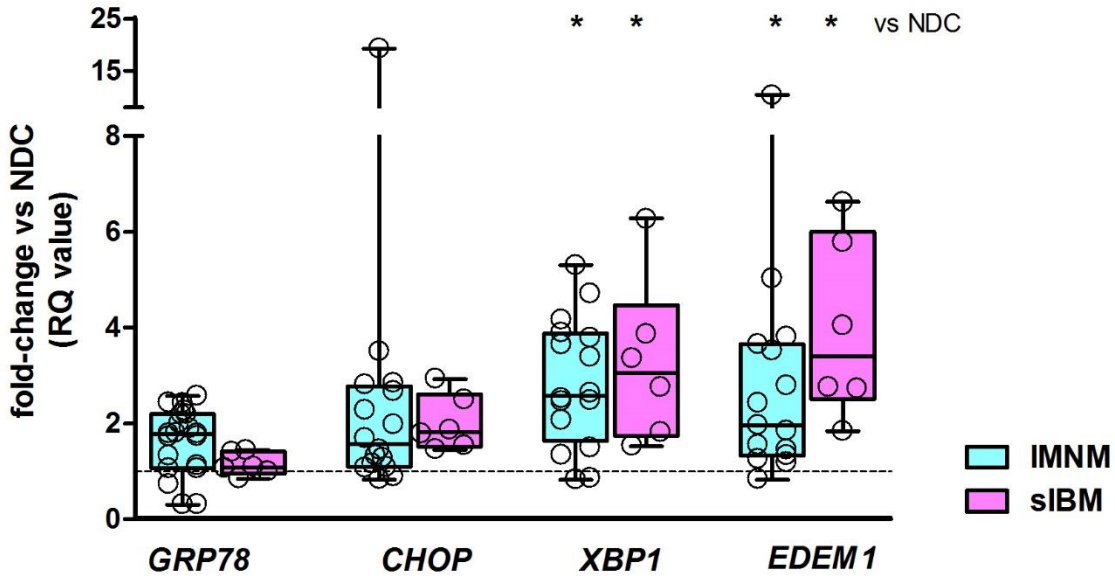

Figure 21 ER stress response genes are equally upregulated in IMNM and sIBM

MRNA transcript levels of ER stress response effector genes XBP1 and EDEM1 are significantly upregulated in IMNM and sIBM patients muscle tissue compared with NDC (asterisks, p <0.05). No significant differences between IMNM and sIBM were present in this analysis. Statistical analyses between either of the groups with NDC was performed using the Kruskal-Wallis one-way ANOVA with Dunn´s multiple comparison test. The Mann-Whitney U-test was applied for comparing mRNA fold-change expression of IMNM vs sIBM. The dotted line indicates expression level of respective genes in NDC group (= 1-fold expression).

4.11. Connection of immunologic processes to CASA

The next question was to gain an understanding of the relationship between Chaperone-assisted selective autophagy and the immunologic processes that take place within the muscle of IMNM. In order to achieve this, double immune fluorescence stainings were performed that showed a co-localization of sarcoplasmic p62 and MHC class I (Figure 22). MHC class I^+ fibers did not always show p62-positivity and vice versa (data not shown).

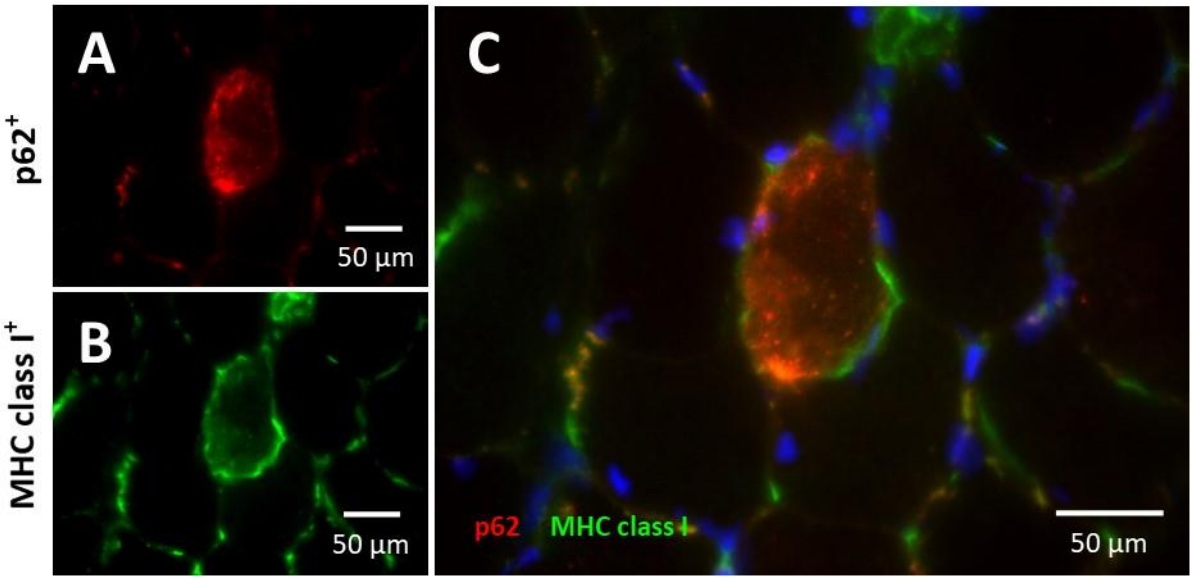

Figure 22 Co-localization of p62 and MHC class I in myofibers of IMNM patients

*Immunofluorescence stainings for p62 (**A**) and MHC class I (**B**) show a clear sarcoplasmic co-localization in myofibers of IMNM patients (**C**).*

5. Discussion

Vacuolar structures of different origin are a common feature in several acquired or hereditary myopathies, and can, upon their analysis, give valuable clues about disease pathophysiology and help in developing targeted therapies. For example, vacuoles form in infantile-onset Pompe disease, due to the lack of acid alpha-glucosidase (GAA) and the subsequent accumulation of glycogen and lysosomal debris (37). By substitution of human recombinant GAA, which is available as a treatment option since 2006, a decrease of intracellular glycogen aggregates can be noted. More importantly however, overall life expectancy, ventilator-free survival as well as motor skill development of affected patients increased significantly in this previously lethal condition. (139, 140) In Danon disease and X-linked myopathy with excessive autophagy (XMEA), the nature of the vacuoles helped in drawing conclusions on the underlying pathology (LAMP2 deficiency in Danon disease and V-ATPase dysfunction in XMEA, respectively) and can therefore be useful in promoting treatment options: a gene therapy phase 1 study for Danon disease is currently recruiting (141) (142). Identifying the cause for vacuole formation is therefore essential and can have a direct impact on therapeutic possibilities.

In IMNM, the presence of vacuoles has been mentioned in the literature and is apparent in a diagnostic context, albeit not yet described or analysed in more detail (30-33). As the present results show, vacuoles are indeed a very common histopathological feature of IMNM, being

present in more than three quarters of the analysed IMNM skeletal muscle biopsies. In order to understand the role of vacuoles and the reason for their formation in the pathophysiology of IMNM, first the differences between vacuole negative (V-) and vacuole positive (V+) patients regarding the histopathological hallmarks of IMNM were investigated. The analysis revealed significantly more necrotic myofibers and fibers undergoing myophagocytosis in V+ skeletal muscle biopsies, whereas the number of regenerating fibers was similar in both subgroups. This could imply that 1) biopsies containing vacuoles are more severely affected by the underlying pathophysiologic processes with increased cellular turnover or that 2) vacuoles are an expression of a longer course of disease. Consequently, regenerating processes are as active as in a shorter disease duration but no longer effective anymore, leading to damaged, vacuolated myofibers through incomplete regeneration. Investigating the inflammatory status in V+ and V- IMNM skeletal muscle biopsies, $CD68^+$ macrophages were found to be the most common infiltrating cells in both IMNM groups with a trend towards higher numbers of macrophages in V+ patients. This trend was confirmed when analysing the presence of all leucocytes via staining for the leucocyte common antigen CD45, which shows significantly higher numbers of leucocytes in V+ compared to V- IMNM skeletal muscle biopsies. Macrophages, as major players in the innate immune system are present in all tissues of the body where they inherit tissue-specific functions (e.g. microglia in the central nervous system or osteoclasts in the bone). Correspondingly, a small number of macrophages reside in the endo- and perimysium of muscle fibers, adopting an indispensable role for muscle repair and regeneration under physiological and pathological conditions. Upon muscle damage like exercise-induced microlesions, pathogen invasion or experimentally induced sterile myofiber injury resident macrophages are responsible for the first, immediate response. Cytokines produced by resident macrophages as well as intracellular components and myokines released from damaged myofibers act as so-called damage-associated molecular patterns (DAMPs) and lead to the recruiting of blood monocytes. Subsequently, these differentiate into macrophages and take over different functions in the injured muscle. (143, 144) By release of a number of pro-inflammatory cytokines these macrophages at first induce an “inflamed state” of the muscle that is, however, essential for the complete functional regeneration of the muscle (145, 146). The reconstitution of the damaged muscle tissue includes phagocytosis and the disposal of impaired myofibers and cellular debris, repair and synthesis of components of the extracellular matrix by additional activation of fibroblasts and, also via secretion of cytokines and growth factors, the initiation of myofiber regeneration by myoblast proliferation and later differentiation into mature myotubes (147).

The number of macrophages present in the muscle after an injury has been shown to increase with time and depending on the type of injury (147), possibly indicating a longer course of disease in V+ patients skeletal muscle tissue displaying more leucocytes/macrophages. On the other hand, higher numbers of macrophages in V+ skeletal muscle biopsies could also be a phenomenon associated with the significantly higher amount of necrosis in this group, as it has been shown in cardiotoxin-induced myofiber damage: macrophages surround necrotic fibers after invasion and stay within the muscle until regeneration was completed (148). A direct myodestructive role of macrophages in IMNM is suggested by a recent study by Allenbach *et al.* (124). Hence, macrophage invasion in IMNM might be a reason for or a result of the variable number of necrotic fibers in V- and V+ patients with no specific relation to vacuole formation. Interestingly, in both of the analysed IMNM subgroups macrophages were present not only in the proximity of necrotic or regenerating fibers as for example in the study of Martinez *et al*. (148), but distributed between normal appearing myofibers.

A major role in the correct and finely balanced sequence of injury and inflammation followed by repair mechanisms and regeneration is achieved by the differential development of the infiltrating macrophages. Macrophages can be classified according to their activation modus into M1 polarized or M2 polarized macrophages. IFNγ and TNFα, cytokines released by T-helper cells Type 1 (Th1) are thought to stimulate macrophages towards an M1 phenotype. Thus, blood monocytes differentiating into M1 polarized macrophages are, in addition to resident macrophages, among the first immune cells at the site of muscle damage. They promote the initial pro-inflammatory state by expression of inducible nitric oxide synthase (iNOS) and secretion of TNFα, IL-6, IL-1β and GCSF. These cytokines have been shown to be major satellite cell proliferation stimuli while at the same time inhibiting terminal myoblast differentiation. After the first wave of inflammation and immune cell recruiting, this state must subside in order to allow completion of the regeneration processes. This is achieved by transition of M1 polarized macrophages into so-called M2 polarized macrophages that exhibit a rather anti-inflammatory phenotype. M2 macrophages secrete mainly IL-10 and thereby facilitate myoblast differentiation and myotube fusion as well as further tissue repair and neoangiogenesis. (144, 147)

These different sets of activated macrophages have been shown to be induced by distinct Th1- and Th2-derived cytokines *in vitro* but the exact mechanisms of phenotype transition are unknown, and *in vivo* circumstances deviate highly from *in vitro* conditions, so a determined separation of phenotypes seems questionable. Thus, it is now widely accepted that both kinds of macrophages

and additional subtypes exist within a spectrum of activation modes and do not exclude each other in presence. (149)

The present analysis revealed more than tenfold increased mRNA levels of Th1-released cytokines IFNγ and TNFα and of M1 secreted cytokines IL-6 and IL-1β in V+ patients´ skeletal muscle tissue when compared with non-diseased control patients. Likewise, mRNA levels of Th2/M2-related cytokines like CD206, IL-4 receptor and TGFβ were significantly increased in V+ patients compared with non-diseased control patients. These results demonstrate that M1-promoted pro-inflammatory effects and repair mechanisms as well as M2-induced attenuation of inflammation and completion of the regeneration processes take place at the same time in IMNM muscle. This supports the idea that a continuously present trigger for immune cell activation exists within the muscle, possibly hampering the completion of repair processes. Comparing V+ and V- IMNM patients, no significant differences in the expression levels of Th1/M1-related cytokine transcripts could be observed, which indicates that irrespective of the presence of vacuoles the same degree of pro-inflammatory environment within the muscle is present. Interestingly, this is not the case for any of the Th2/M2-related cytokine transcripts investigated. In contrast, significant differences could be observed between V- and V+ IMNM patients regarding the M2-associated molecules CD206 and IL-4 receptor, with mRNA all of these being expressed at significantly higher levels in V+ patients. Since M1-derived chemokines are upregulated to a similar extent in both groups, the significant higher expression of M2-related molecules in V+ compared to V- patients appears to be independent of the initial M1 presence and signifies a notable difference between the two groups. Increased activity of M2 macrophages in V+ skeletal muscle biopsies might reflect either a higher or prolonged anti-inflammatory state possibly due to insufficient suppression of the initial inflammation. Alternatively, a dysregulation in the orchestrated process of M1 and M2 activation and transition leading to a faulty M2 persistence might be the reason for higher levels of Th2/M2-related transcripts and result in chronic muscle damage. The up to 40-fold increased expression of *TGFB* in V+ IMNM muscle biopsies is another indicator of a constant cellular immune response that is significantly more pronounced in V+ patients. TGFβ is an immune-modulatory cytokine secreted by macrophages and other inflammatory cells, which, by influencing T cell differentiation, plays an important role in balancing pro- and anti-inflammatory reactions (150, 151). As TGFβ stimulates fibroblasts and has been associated with the development of fibrotic diseases in *in vivo* models (e.g. scleroderma, pulmonary fibrosis, hepatic fibrosis) (152, 153). It also causes fibrotic remodelling of injured skeletal muscle and inhibits proper muscle regeneration (153-155). In line with this, Mendias *et al*. (156) have demonstrated how TGFβ can mediate

muscle fibrosis, myofiber atrophy and reduction in contractile strength. Therefore, increased *TGFB* levels in IMNM patient muscle could be a reason for myofiber damage and possibly lead to vacuole formation. However, since fibrosis is not a histopathological sign of IMNM and the modulating role of TGFβ in context of inflammation is also eminent, I propose that increased *TGFB* levels are a "side effect" of the occurring immune response and immune cell invasion in IMNM muscle, and are an expression of the inflammatory environment within the muscle rather than a causing agent.

The presence of $CD8^+$ cytotoxic T cells has been described in IMNM and at times been implicated in the immune-mediated origin of myofiber damage (129), although others claim that the minimal number of T cells in contrast with high numbers of necrotic fibers disfavour the role of T cells in IMNM pathogenesis (157). In the present group of analysed IMNM patient biopsies, $CD8^+$ cytotoxic T cells were found in 93% of all skeletal muscle biopsies (which is in contrast to other findings with only 50% of the biopsies containing $CD8^+$ T cells (123)), although most patient biopsies contain only single or few $CD8^+$ T cells focally. Regarding localization, $CD8^+$ T cells were often found in proximity of necrotic or regenerating fibers, although this was not exclusively the case. The number of T cells was similar in both V- and V+ IMNM patients, demonstrating that vacuole formation is not related to T cell mediated cytotoxic effects. In line with this, sarcolemmal or sarcoplasmic MHC class I expression on non-necrotic myofibers was found in comparable numbers in both V- as well as V+ skeletal muscle biopsies, ranging from focal areas of MHC class I expressing myofibers to more than 60% of all fibers in one biopsy expressing MHC class I on the sarcolemma. MHC class I upregulation on myofibers is a common, but not a specific, phenomenon of idiopathic inflammatory myopathies that can be used diagnostically (158, 159). Pathological MHC class I upregulation in different tissues has been proposed as a potential starting point of autoimmune diseases. Likewise, it has been suggested and supported by murine *in vivo* studies, that an aberrant MHC class I expression on myofibers could pose the underlying pathology of inflammatory myopathies by triggering an MHC class I/T cell mediated immune response and thereby causing autoimmunity (160). An association of T cells with MHC class I-expressing myofibers and a consecutive T cell/perforin mediated cytotoxicity has been illustrated in Polymyositis (161). In PM, T cells show explicit invasion into the muscle fibers, whereas in IMNM T cells are distributed in the perimysium, hence making a direct T cell mediated myofiber damage seem unlikely. Given the consistency and not too scarce presence of $CD8^+$ T cells in the analysed IMNM skeletal muscle biopsies, the hypothesis of T cell originating chemokines (IFNγ) taking part in myofiber damage but not through direct MHC class I/T cell interaction can be favoured.

Myofiber damage in IMNM due to humoral processes has been brought forward by different investigators based on several observations. The presence of the IMNM-specific autoantibodies against SRP and HMGCR molecules, which in case of HMGCR positively correlate with CK levels and negatively with muscle strength, strongly supports a pathogenic role. Secondly, the upregulation of C5b-9 on normal appearing myofibers underlines this hypothesis by suggesting an antibody/complement mediated process. Additionally, a cytotoxic effect of anti-SRP^+ serum on myoblasts has been demonstrated and more recently, two studies revealed evidence for direct complement-mediated myofiber damage via IMNM-patient derived antibodies (124-126). B cells and plasma cells, although rare, have been observed in IMNM skeletal muscle. Furthermore, the beneficial effects of intravenous immunoglobulin, plasmapheresis and B cell depletion via Rituximab hint at humoral mechanisms playing a role in IMNM. I investigated whether plasma cell presence could be correlated with the presence of vacuoles, hence pointing at a specific vacuole formation mechanism. Small numbers of plasma cells were present in most of both analysed IMNM subgroups and no significant differences in the amount could be observed between V- and V+ patients, indicating that vacuole formation is not affiliated with a humoral/plasma cell-mediated process. It could be discerned, however, that two biopsies with high numbers of plasma cells (50 and 100 plasma cells/10 HPFs) were found in the V+ group, possibly reflecting a stronger inflammatory reaction in these patients with recruitment of more immune cells. The high number of plasma cells might also represent a generally greater involvement of humoral immunity in these patients. The analysis of the B cell chemoattractant CXCL13 supports a role of humoral immunity in IMNM pathology, as *CXCL13* mRNA levels were increased in both IMNM subgroups when compared with NDC; up to 200-fold higher in V+ and 20-fold higher in V- patients. This complements existing data showing *CXCL13* upregulation in IMNM patients, though Anti-synthetase syndrome patients were included in that study as well (129). High *CXCL13* transcript levels were for the most part reflected by high numbers of plasma cells in the biopsy, proving a functional presence of plasma cells *in situ*. Regarding complement deposition, positive staining for C5b-9 on non-necrotic fibers was observed in both subgroups, supporting existing data and possibly implying complement-mediated cytotoxicity. However, this mechanism does not seem to be the causing agent for vacuole formation in IMNM, since no significant difference in the pattern or degree of complement deposition between V- and V+ patients was present nor was C5b-9 reactivity specifically found on vacuole containing myofibers. As observed with infiltrating immune cells, more V+ patients displayed a high number of diffusely distributed myofibers with a strong MAC deposition on the sarcolemma, possibly reflecting a stronger immune response, more severe affection or an advanced course of disease. No specific association of either

infiltrating cells, complement or MHC class I deposition with vacuole-containing myofibers was found, suggesting that these immune mechanisms are not directly involved in vacuole formation. Nevertheless, it should be kept in mind that others have found cues for direct antibody-complement induced myofiber destruction (124-126). Notwithstanding, the presented data strongly suggests that vacuoles are not a distinct expression of that process but rather a sign of general affection.

In order to assess the origin of the vacuoles detected in skeletal muscle tissue of IMNM patients, different proteins physiologically found on or associated with the sarcolemma of muscle fibers were analysed. Sarcolemmal features in vacuoles can be a distinct characteristic and are even name-giving for a group of vacuolar myopathies (44). However, most vacuoles in IMNM showed no presence of the sarcolemmal proteins β-spectrin and no enzyme activity of acetylcholine esterase. In AVMs with AVSFs staining of vacuoles with these and other sarcolemmal proteins was a constant phenomenon and especially the reactivity of AchE led Sugie and colleagues to hypothesize that AVSFs are formed *de novo* and are not derived from the sarcolemma (44). The absence of sarcolemmal features in IMNM vacuoles therefore implies that the vacuoles are not derived from the sarcolemma nor are they enclosed membrane-surrounded cavities, and thus cannot be counted among AVM with AVSFs.

A multiplicity of myopathies with abnormal protein aggregation are known, including myofibrillar myopathies, distal myopathies and hereditary IBM (162). Desminopathies and sIBM are only two examples in which pathologic protein accumulation and vacuole formation are simultaneously present and are strongly asserted to depend on each other (162, 163). Therefore, I hypothesized that vacuole formation in IMNM is also related to protein aggregation. However, the analysis of common aggregate-prone proteins (FUS, TDP43, amyloid and phosphorylated tau) revealed no presence of these molecules in either vacuolar structures or myofibers in general, leading to the rejection of this hypothesis.

The degree of lysosomal-associated membrane protein Type 2 (LAMP2) immunostaining is increased in myofibers of both IMNM subgroups compared with non-diseased controls with no differences between the V- and V+ subgroups. This excludes vacuole formation as a consequence of autophagosome build-up due to a LAMP2 deficiency as in Danon disease. Increased LAMP2 immunopositivity is not specifically present in vacuolated fibers or found within vacuoles, as in sIBM and distal myopathy with rimmed vacuoles (DMRV), implying that vacuoles in IMNM also do not originate from the lysosomal compartment (164). In contrast to Vittonato *et al.* (34), in the present study LAMP2 staining was observed not only in necrotic but also in normal appearing

IMNM myofibers, a finding indicating a possible involvement of lysosome turnover in IMNM pathophysiology. That vacuole formation is directly related to an excess of lysosomes is unlikely, since no differences in LAMP2 expression in V- versus V+ patients was detected nor could a lining of vacuoles with LAMP2 be observed (data not shown).

Since the hypothesis that abnormal protein aggregates or lysosomal pathology are reason for vacuole formation in IMNM could be rejected, other possible mechanisms causing these intracellular defects were to be investigated. The observation of strong staining for LAMP2, though not associated with vacuoles, indicated the presence of lysosomes and implied that cellular protein degradation pathways resolving in the lysosomal compartment could be altered in IMNM. Thus, autophagy, the main intracellular pathway cumulating in lysosomal degradation and one that is involved in other myopathies, could be involved in IMNM pathophysiology and might lead to vacuole formation. The obtained findings strongly corroborated the hypothesis that autophagic processes are modified in IMNM, showing myofiber immuno-positivity for the autophagy proteins LC3 and p62 in the majority of IMNM patient biopsies, which is not present in healthy control muscle. The distribution of LC3, which is an essential component of the growing phagophore, and of p62, the adaptor protein between the autophagosome and its dedicated cargo, was found in a diffuse punctate pattern of variable intensity throughout the entire sarcoplasm. Physiologically, this expression of autophagosome-related proteins was not observed, leading to suspicion of a defect or alteration in the autophagy process in IMNM. But how to interpret these findings? The increased staining could be caused by an increased autophagic activity or the disruption of the process at some point. This would prohibit correct disassembly and recycling of autophagosomes and their components LC3 and p62; subsequently leading to their accumulation.

One can find abundant literature about the investigation, monitoring and pitfalls of autophagy in cell culture models (135, 165-167). However, under stationary conditions as was the case in the present study with tissue acquired from patients for diagnostic reasons, autophagy mechanisms are more difficult to analyse. Although many limitations remain, several studies aimed at validating an immunohistochemical staining protocol have shown that LC3-B and p62 IHC, as in the present study, can be used to monitor autophagy in frozen or formalin-fixed paraffin embedded (FFPE) tissue (53, 168, 169). Schläfli *et al.,* for example, could show that specific and reliable staining for LC3-B and p62 on FFPE tissue is possible and conclude that "*applying LC3B and p62 IHC on single tissue samples and tissue collections may be a valuable tool for determining the impact of autophagy on human diseases…"* (169). Taking this study into account, the presence of the

cytoplasmic p62-positive puncta in IMNM patient myofibers can be reliably interpreted as a sign of the involvement of autophagy.

In patients treated with drugs known to inhibit autophagy and cause myopathy (chloroquine, hydroxychloroquine or colchicine), p62 and LC3 staining on formalin fixed paraffin embedded (FFPE) muscle tissue showed a finely dotted pattern in some fibers, similar to the staining pattern observed in IMNM patients muscle biopsies of the present study (53). In the same study, the authors were able to show that p62 protein levels were increased and the detected LC3 staining in IHC corresponds to an autophagosome-specific LC3 increase in drug-treated patients (53). Accordingly, the discoveries on hand of variable punctate staining of p62 and LC3 in immunohistochemical studies of IMNM myofiber robustly represent the presence of autophagosomes. FFPE tissue of autophagy-deficient (Atg7 or Atg5 knockout) mice shows an accumulation of p62 positive puncta (170) and inhibiting autophagy via bafilomycin (hinders fusion of autophagosome with lysosome) leads to an increase of p62 accumulations compared to starvation (= autophagy-inducing) conditions in lung cancer cells (169). Equally, formation of LC3 puncta increased upon bafilomycin treatment (169). Thus, the present findings of punctate p62 and LC3 staining in IMNM skeletal muscle biopsies indicate a failure to complete the regular autophagy process, where the involved proteins that themselves are degraded via autophagy accumulate (86, 169, 170). This hypothesis of disturbed completion of autophagy is supported by the gene expression analysis showing no change in *p62* expression, as Komatsu *et al.* have shown that *p62* mRNA levels remain unchanged in tissue of Atg7-deficient mice (Atg7 is essential for autophagy in mice) while p62 puncta appear (170). Also, the gene expression analysis revealed no increase in mRNA levels of *BECLIN* and *ULK1*, both involved in the initiation of autophagosome formation in IMNM patients compared with healthy controls. These results, however, have to be interpreted with caution regarding *p62* mRNA expression as a marker for autophagy induction or inhibition, since it is involved in a number of cellular tasks besides its autophagy adaptor function and underlies a complex posttranslational modification (83, 171). Intriguingly, on the other hand, is the significant increase in *LC3* transcript levels in IMNM patients compared with NDC, which could indicate that an increased need for autophagosome formation exists. These results suggest that induction of autophagy is taking place regularly or slightly increased, indicated by significantly increased *LC3* levels but autophagosomes (solidly marked by LC3 IHC) and p62-bodies remain in the cytoplasm. Thus, selective cargo binding or further autophagosome processing or substrate recycling is hindered. Curiously, no ubiquitin aggregates were found in the present analysis, as other studies investigating the comportment of p62 and LC3 in autophagy

deficiency reliably show (170). Parallel to the presented data the group of Girolamo *at el.* also showed a significant expression of LC3 and p62 in IMNM when compared to DM and PM. They also observed a high proportion of ubiquitin$^+$ cells, a finding that in this study could not be reported. (172)

With respect to the presence of vacuoles, a similar degree of LC3 staining in the histopathological analysis of both V- and V+ IMNM patients was found, but a significantly higher number of myofibers expressing p62 was observed in V+ patients. Regarding the mRNA expression of *p62* and *LC3*, no significant differences between V- and V+ IMNM patients were identified.

Since both subgroups expressed the proteins in a non-physiological manner and no difference between transcript levels of autophagy-related genes was found between the subgroups, one can deduce that autophagy does indeed play a role in IMNM pathology, as also proposed by Girolamo *et al.,* but does not sufficiently explain vacuole formation. Moreover, autophagosome-resident proteins p62 and LC3 were not specifically found in or around vacuolar structures but distributed diffusely in normal appearing myofibers, also indicating that vacuoles are not derived from merging autophagosomes. The significant difference in the number of p62$^+$ myofibers between V- and V+ patients might mean that in V+ myofibers underlying pathophysiologic processes are more pronounced. This complements the obtained data about the general histopathological and immunologic features, indicating vacuole formation as an expression of a more severe affection of V+ IMNM patients without vacuoles holding a causal role in IMNM pathophysiology.

Since the hypothesis that autophagic processes directly lead to vacuole formation could not be confirmed, other major protein degrading pathways were explored to evaluate their role in IMNM pathogenesis and the development of vacuoles. Investigating ER stress related transcripts, it could be shown that the main ER stress response induced transcription factor *XBP1* and the ERAD protein *EDEM1*, which is also induced upon ER stress (173) were both expressed at significantly higher levels in V+ patients compared with healthy controls. However, no significantly increased mRNA levels of *GRP78*, encoding for the protein in charge of the UPR initiation (binds all UPR effector proteins in an inactive state) or the ER stress induced cell death mediating transcription factor *CHOP* were found in either IMNM subgroup when compared with non-diseased control patients. These results suggest that ER stress response mechanisms, represented by increased UPR induced transcription factors are needed and present in IMNM. However, the lack of *GRP78* and *CHOP* upregulation in the present IMNM subgroups, which in contrast is found in studies about ER stress in PM, DM, sIBM patients and transgenic mice overexpressing MHC class I (112, 136)

could signify that the activation of ER stress response pathways is relatively moderate in IMNM. The elevated levels of ER stress gene transcripts are especially interesting in IMNM because of the pathognomonic autoantibodies against SRP and HMGCR in IMNM, two structures both present on the ER. One can therefore suggest that autoantibodies binding to ER structures (SRP, HMGCR or unknown antigens in seronegative patients) cause ER stress (174). Overwhelming ER stress, in any case, most likely does not contribute to vacuole formation, as no significant differences in the mRNA levels of analysed UPR-related genes between V- and V+ IMNM patients were found.

The immunoproteasome seemed to be another intriguing player for IMNM pathophysiology and possibly vacuole formation, as positive immunofluorescence staining for immunoproteasome subunits β1i and β5i was shown in IMNM (103). Interestingly, while Ghannam and colleagues did not find a significant increase in *β1i* and *β5i* expression compared with healthy controls, the present investigation showed significantly higher mRNA levels of *β1i* and *β5i* in V+ IMNM patients, as well as significantly higher levels of *β5i* in V- patients compared with healthy control patients. The discrepancy of the results between the two studies could be explained by the small IMNM patient group in the study of Ghannam *et al.* (n=6 vs. n=45 in the present study). Between the V- and V+ subgroup, no statistically significant differences in the transcript levels of *β1i* and *β5i* were found, which allows the conclusion that vacuoles in IMNM can most probably not be traced back to changes in the immunoproteasome system. Nevertheless, the immunoproteasome is activated in IMNM, which has been indicated by immunofluorescence data of another study and has now been supported by the present analysis. The main function of the immunoproteasome, being activated in inflammatory conditions upon the influence of IFNγ and TNFα, is the decomposition of intracellular proteins/antigenic material for subsequent presentation of produced peptides via MHC class I molecules on the cell surface. Thus, the immunoproteasome is regularly expressed in professional antigen-presenting cells but can be induced in almost all tissues under inflammatory conditions (175), facilitating antigen presentation as a response to a possible infectious attack. In line with this, Ghannam *et al.* proposed an association between the immunoproteasome and MHC class I expression in IIMs, based on their observation of co-localization between immunoproteasome subunits and MHC class I^+ myofibers and myoblast culture experiments. Although the induction of the immunoproteasome in myoblasts and IIM muscle tissue is an interesting phenomenon and possibly related to pathological MHC class I expression on myofibers, a specific role in disease pathogenesis remains questionable. In contrast, an induction of the immunoproteasome in context of the prevailing inflammatory environment (high levels of

IFN and TNFα, which have been demonstrated to be strong inducers of the immunoproteasome (176, 177)) caused by macrophages and T cells seems more likely. It must be added that the increased levels of *β1i* and *β5i* found in the muscle tissue of IMNM patients could partly be caused by the infiltrating immune cells that constitutively express immunoproteasome subunits.

Summarizing the results up to this point, in virtually none of the analysed protein degradation pathways were significant differences present in the protein expression (as demonstrated by selected histopathological stains) or mRNA transcript levels of respective genes between V- and V+ IMNM patients. Moreover, vacuoles were not characterised by sarcolemmal features or related to abnormal intracellular protein aggregates. This leads to a rejection of the hypothesis that vacuole formation is a specific, disease related phenomenon that can be ascribed to a distinct intracellular degradation pathway, as is possible in other myopathies with vacuole formation. However, analysing the histopathological hallmarks of IMNM and the immune response in both subgroups, some significant differences were revealed. Although regeneration processes seem to be comparable in both subgroups, a higher amount of both necrosis and myophagocytosis in V+ skeletal muscle biopsies was present, which may point to a higher disease activity and severity in this group, manifesting itself in disintegration of myofibers. Supporting the hypothesis of vacuole formation as a collateral damage of more severe affection and higher disease activity in V+ patients is the present data showing a higher number of leucocytes in V+ skeletal muscle biopsies and significantly increased *TGFB* mRNA and markers of the M2/Th2-mediated immune response. Nevertheless, gene transcript level of the main markers of the M1/Th1-mediated immune response are highly increased in both subgroups and other immunological phenomena such as MHC class I expression and complement deposition are similarly high in both groups, which demonstrates their role in IMNM pathogenesis and indicates that severe inflammation exists prior to vacuole formation. Hence, it can be proposed that vacuole formation in IMNM is indeed a pathological feature (being present in almost 80% of IMNM skeletal muscle biopsies) but possibly represents a different disease stage or degree of severity. The correlation of vacuole formation with a more severe course of disease or longer disease duration would have to be confirmed by clinical data.

Nevertheless, the peculiar expression pattern of the autophagy proteins LC3 and p62 intrigued me to further investigate this phenomenon. In this respect, the comparison of IMNM with sIBM, which is the first and only IIM in which the p62 expression pattern has been thoroughly investigated and proposed as a useful diagnostic feature (70, 138), was particularly interesting. A comparison with sIBM seemed auspicious also because protein aggregates in sIBM are shown to co-localize with p62 and other autophagy-related proteins (70, 178), emphasizing the role of

autophagy in sIBM and deeming p62 as a sensible starting point for a comparative investigation. Since the present exploration generally showed no significant differences between the V- and V+ subgroups, and vacuoles probably representative of the disease spectrum, both subgroups were combined for comparison with sIBM.

Several studies, as well as the investigation on hand showed p62 in sIBM as prominent intracellular aggregates, displaying coarse, thick, round, "comma-shaped" or "squiggly" shapes up to 10µm (70, 137, 138). In striking contrast to that are the present findings of the distribution of p62 in IMNM myofibers. In IMNM, a diffuse distribution of p62 puncta throughout the entire sarcoplasm in 90% (n=54) of the analysed patients was found. All of them showed the same expression pattern, albeit the strength of p62 expression (meaning intensity of the staining) and the number of $p62^{+}$ myofibers was variable. Another noteworthy difference between IMNM and sIBM was that in IMNM p62 expression was not only found in smaller, irregular but also in rather normal appearing myofibers, whereas in sIBM p62 aggregates were mainly found in vacuolated fibers (70) or abnormally shaped fibers, although presence in normal appearing muscle fibers was also noticed (137).

P62 inherits several important functions within the cell that are mediated and can be well-explained via its different domains. P62s main cellular role, however, lies in its function as an adaptor protein for autophagic processes, which is reflected by three of its domains related to that purpose. The N-terminus of p62 contains a PB1 domain that facilitates its self-polymerization into helical structures, possibly building a scaffolding structure for autophagosome formation (88). The interaction of p62(-helices) with the growing phagophore is facilitated via its LC3-interacting region (LIR) domain that binds to LC3 via hydrophobic effects (179). Last but not least, in the C-terminus of the protein a ubiquitin-associated (UBA) domain is present, which connects p62 to mono- or polyubiquitinated proteins (179). Thus, as described above, p62 acts as a main connecting element between ubiquitin-labelled, degradation prone aggregates and the forming autophagosome, possibly even aiding in its correct assembly. For sIBM, it has been hypothesized that defective/insufficient binding of p62 with its cargo attached to LC3, impedes its transportation to and subsequent degradation by the autophagosome, leading to the accumulation of p62 as well as its cargo, displayed as large intracytoplasmic chunks (137). The pathophysiology of sIBM is considered multifactorial and complex, but a central pathophysiological aspect commonly agreed on is that accumulation of misfolded proteins (namely APP, TDP43 and αSynuclein) in so-called "inclusions" contributes to myodegeneration and co-localization with autophagy-related proteins is often seen (70, 180-182). In IMNM a completely different expression pattern of p62 is present

and no deposits of common involved misfolded proteins are found, implying that autophagy and p62 processing are affected in a distinctly different way. Additionally, I did not find any ubiquitin positive deposits in IMNM. We can therefore conclude that a defect in the autophagy pathway must lie upstream of p62/ubiquitin binding or must be independent of that reaction.

Interestingly, some authors report that p62 can deliver some substrates to selective autophagy without the Ub-recognition motif (183). Also, posttranslational modifications control the ability of p62 ability to either bind ubiquitin or to self-polymerize, thus self-polymerization of p62 is a possible explanation for the $p62^{+}Ub^{-}$ puncta in IMNM (184).

Consequently, it is possible that aggregates in sIBM comprise large p62-Ub^{+} conglomerates that are formed as a futile control mechanism upon the accumulating protein aggregates (185), whereas the fine puncta in IMNM might be small p62 oligomers that form without the binding of ubiquitin via self-polymerization. It has been shown in several studies using cell culture as well as murine models that impairment of the UPS, but also inhibition or absence of the autophagosomal pathway result in the accumulation of ubiquitin-positive aggregates (170, 186). A complete impairment of either the UPS or autophagy would therefore most likely lead to the accumulation of Ub^{+} aggregates, which I did not find in IMNM myofibers. The presence of the many very small p62 positive puncta and the absence of ubiquitin reactivity in IMNM skeletal muscle biopsies indicates that p62 puncta do not form because of decompensated protein degradation systems. The cause for the observed distribution of p62 in IMNM patient muscle possibly lies further upstream before the formation of large aggregates at the beginning of its function in conveying single misfolded proteins towards the autophagic machinery. The question was therefore: Which p62 related pathways are important in skeletal muscle tissue and could be the reason for this peculiar p62 expression pattern? The co-chaperone BAG3 was interesting in this context.

BAG3 is part of a protein family of co-chaperones that closely interact with the mammalian Hsc70/Hsp70 chaperones (187). BAG3, a 75kDa protein, comprises several different amino acid motifs, two of which are essential for its function as a co-chaperone: the BAG-domain that binds ATP-dependent to the HSC/HSP70 chaperone and the IPV region that can bind the small heat shock proteins HSPB8, HSPB6 und HSPB5 (αB-crystalline) und HSPB1 (188). During recent decades, BAG3 has been shown to play an emerging role in different pathophysiological contexts as reviewed by Stürner and Behl (189, 190). As commented above, BAG3 also contributes to muscle disease, exemplified by severe myofibrillar and dilated cardiomyopathies caused by spontaneous genetic mutations (189), making it an interesting candidate for the present study. In a

process termed BAG3-mediated selective autophagy, the chaperone complex of BAG3, HSP70 and HSPB8 feed ubiquitinated, misfolded proteins into the autophagic system via recruiting of p62. In cell culture models, BAG3 and its associated chaperones have been shown to relocate ubiquitin-labelled substrates to degradation by autophagy, if the proteasome is inhibited (191). During this process the cargo is sequestered in small agglomerates that appear as cytoplasmic puncta positive for BAG3, HSP70, p62 and ubiquitin (191), resembling our results with the staining pattern found in the IHC serial sections of IMNM patient myofibers and double immunofluorescence studies (174).

In muscle tissue, BAG3 has been shown to obtain an additional, myofiber specific function: The maintenance of myofiber protein homeostasis by degradation of "used" Z-disc associated proteins in order to sustain normal muscle function (93, 95). This specific function of BAG3 in degrading myofiber protein has been termed chaperone-assisted selective autophagy (CASA). Strikingly, in our study staining for CASA-essential proteins BAG3, HSP70 and αB-Crystallin (HSPB5) revealed their expression in IMNM skeletal muscle fibers, which is not present in healthy controls (174). Similar to p62, diffuse distribution of BAG3, HSP70 and αB-Crystallin (HSPB5) within the entire sarcoplasm was observed, although for BAG3 only subsarcolemmal staining was often found. Serial section staining of a skeletal muscle biopsy of an IMNM patient demonstrated that the same fibers showed expression of p62, HSP70, αB-Crystallin and BAG3, indicating the presence of CASA/BAG3-mediated selective autophagy. Nonetheless, different fibers in one biopsy could be positive for either of the proteins, which could be owed to the fact that the CASA pathway does not take place synchronically in all fibers and was thus captured at different stages, where, for example, the association of HSP70 and BAG3 has already occurred but p62 has not yet bound. Immune fluorescence analysis showed that p62 and HSP70 strongly co-localized in the same punctate structures within the sarcoplasm and the co-localization of p62 and BAG3, though weaker, was also found. (174) This staining pattern in double immune fluorescence staining and of the IHC serial sections also resembles the results of the cell culture study of Minoia *et al.* showing the BAG3-mediated delivery of formerly "proteasome-clients" to the autophagosome. Sher and her colleagues introduced the model of "BAG-instructed proteasomal to autophagosomal switch and sorting" (BIPASS) via modulation of the BAG1/BAG3-ratio if the proteasome is inhibited or overloaded (191). Since no ubiquitin aggregates ("pathognomonic" for proteasome dysfunction) were found in myofibers of IMNM patients in this present investigation, one can assume that CASA/BAG3-mediated selective autophagy in IMNM is not activated due to extreme proteasome overload. Nevertheless, as upregulation of ER stress related as well as

immunoproteasome gene transcripts indicate, myofibers in IMNM are exposed to increased protein folding/turnover demands, which could lead to a preventive and/or compensatory initiation of a shift from proteasome-dominant to an autophagy-dominant handling of protein quality control. Gene transcripts of the involved chaperones *BAG3*, *HSPA8* and *HSPB8* are not altered in IMNM, which indicates that CASA is not transcriptionally upregulated. Yet, immunoreactivity for these proteins is found in the sarcoplasm, indicating that CASA is taking place but compensation mechanisms for arising protein processing are exhausted.

In sIBM, we could show that *BAG3* transcript levels are significantly decreased compared to IMNM (174), which has not been described in the literature before. Since in sIBM degenerative protein aggregation is postulated as one disease mechanism, one could speculate that low levels of BAG3 in that case reflect an insufficient proteasome to autophagy switch and could be part of the pathological processes that lead to protein junk build-up. Nakano *et al.* have proposed compromised selective autophagy in sIBM (137); an observation that might be complemented by the present findings of decreased *BAG3* mRNA levels, which might be related to a possible failing or insufficient autophagy in sIBM. For IMNM this could mean intact protein quality control systems that, upon increasing proteotoxic stress (like overboarding MHC class I production) induce BAG3-mediated selective autophagy to alleviate the UPS and increased degradation over the autophagic-lysosomal pathway. It is possible that this degradation pathway at one point exceeds in its turnover capabilities as well, which leads to the build-up of p62 due to slower self-degradation via autophagy.

Another possible factor explaining the diagnostically relevant differing p62 pattern between IMNM and sIBM might be a distinct involvement of CASA: a decreased function on the gene expression level in sIBM and an increased need for CASA in IMNM that cannot be met, leading to a processing error of p62 and Ubiquitin-independent polymerization and therefore the failure of completing the process. Interestingly, in addition to the coarse, sIBM-typical $p62^{+}$ aggregates, Nakano *et al*. observed the formation of smaller, Ub^{-} $p62^{+}$ puncta and a p62-independent, diffuse LC3 staining, similar to the present results. According to their group, this phenomenon might develop due to other cell stresses independent of autophagy. (137) This remains a possible explanation for p62 deposits in IMNM as well, though the clear co-localization with CASA proteins leaves a CASA-related reason more likely.

Connection between inflammation, immune response and CASA

Autophagy is induced under a number of different factors (192, 193), among which ER stress has been investigated as an inducer of autophagy, which was reviewed by Yang *et al*. (165). In different human tissue, the provocation of ER stress and the successive initiation of the UPR via oxidative stress or chemicals (*i.e.* Tunicamycin, Brefeldin A, Thapsigargin) leads to autophagy activation (194). The present study showed a significant transcriptional upregulation of essential ER stress response genes in the muscle tissue of IMNM patients (174). On the background of the other cited studies, this allows the assumption that ER stress in myofibers of IMNM patients could lead to the induction of autophagy, represented by increased *LC3* mRNA as well as by $LC3^+$ and $p62^+$ staining pattern of myofibers. Comparing ER stress related mechanisms in both diseases, Vattemi *et al*. have shown that in sIBM essential effector molecules of the UPR are expressed in the sarcoplasm of myofibers. Additionally, these UPR effector molecules co-precipitate with AβPP and are associated with AβPP in immunofluorescence studies; thus, Vattemi *et al*. hypothesize that they might be involved in futile AβPP folding/degrading. (136) The present results showing significantly increased mRNA transcript levels of the UPR effector genes *XBP1* and *EDEM1* in sIBM compared with NDC support the findings of Vattemi and his group of an activated UPR. Equally, *XBP1* and *EDEM1* levels are increased up to 2-4-fold in IMNM compared with NDC, indicating that here, too, the UPR is active (174). Relating this to the other results on hand, it seems highly likely that the processes leading to the activation of the UPR differ between IMNM and sIBM. As commented above and in our publication (174), a disease specific and probably pathophysiological important aspect in IMNM is the presence of autoantibodies (anti-SRP, anti-HMGCR) (121), that bind to ER-resident antigens and could, by disturbing orderly protein folding, cause ER stress. In sIBM on the other hand, studies indicate that the UPR is activated as a result of misfolded proteins (i.e. AβPP, phosphor-tau, α-synuclein) (182), whereas in IMNM ER stress is the intracellular starting point of a pathologic cascade, leading to the initiation of CASA. Immunohistochemistry on serial sections, as well as double immunofluorescence studies, support the hypothesis of operating CASA in IMNM. Gene transcript levels of the involved chaperones *BAG3*, *HSPA8* and *HSPB8* are not altered, but immunoreactivity for these proteins is found in the sarcoplasm, indicating that normal CASA function is overwhelmed. This overstrain, as a result, leads to decompensation of the autophagy machinery, where components stay in the cytoplasm without being processed and self-polymerization of p62 occurs. The role of BAG3 in IMNM seems to lie rather in its function as a part of the protein quality control systems upon increased proteotoxic stress than in direct

mediation of myofiber damage as in the BAG3-mutant myopathies. Strikingly, our results also suggest a connection between pathologic MHC class I presentation on myofibers and altered CASA, indicated by co-localization of sarcoplasmic p62 and sarcolemmal MHC class I (Figure 22). As Kettern *et al.* have proposed, chaperone-mediated protein homeostasis mechanisms play a role in antigen presentation via MHC class I in professional antigen presenting cells (195). Transferring this to the present study could mean that the overburdened CASA mechanisms affect and possibly fuel MHC class I expression, and as a result "mark" myofibers for the immune system.

As a synopsis of the histopathological and molecular findings in IMNM patients' skeletal muscle, the following model can be proposed (modified from Fischer *et al*. (174)):

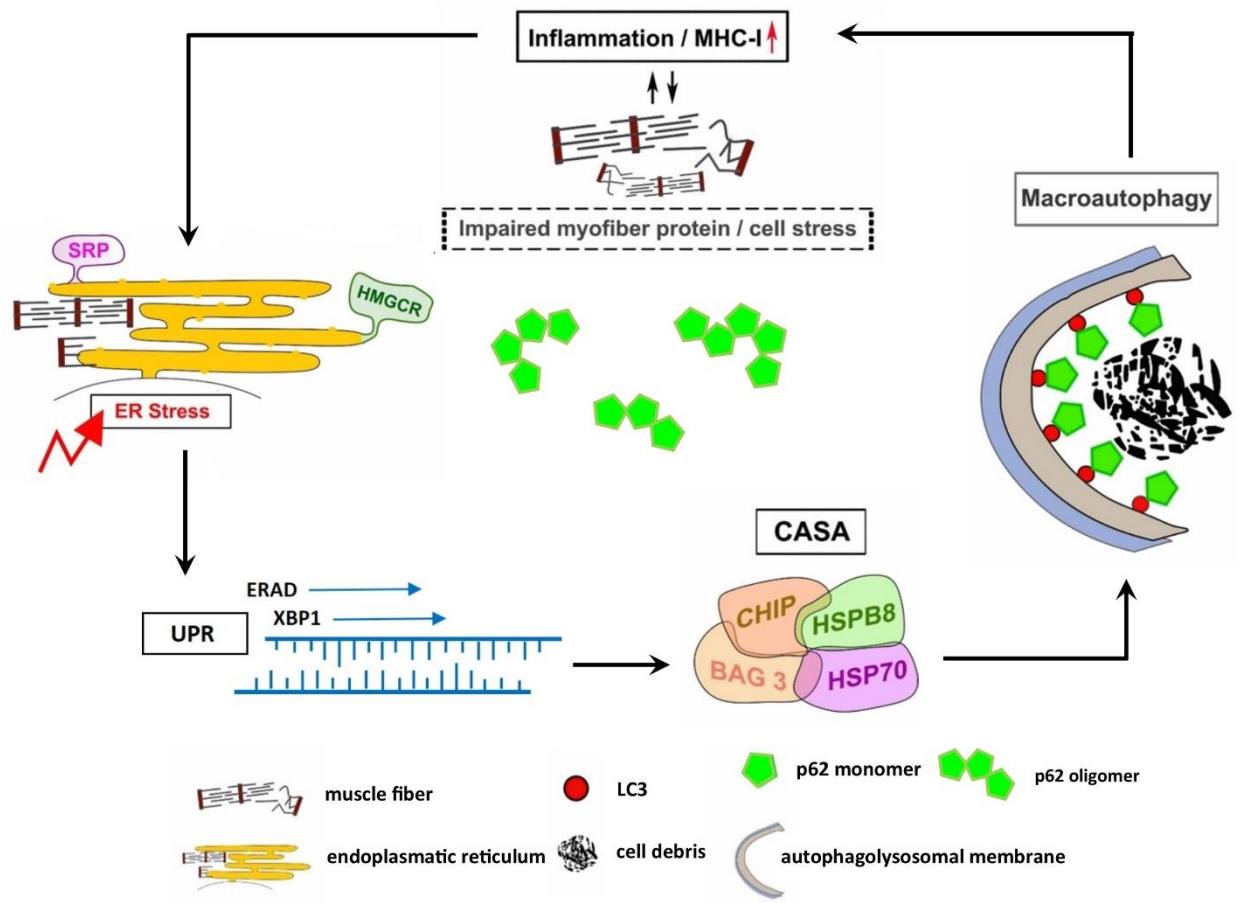

Figure 23 Proposed pathomechanism in IMNM

An inflammatory environment within the muscle with increased processing of putative antigens and MHC class I production poses enormous requirements for the protein folding machinery of the cell, leading to ER stress. Autoantibodies against the ER-resident molecules SRP, HMGCR and possibly other, not yet identified antigens in seronegative patients impede normal ER function and additionally cause ER stress. As a result, (insufficient) ER stress response mechanisms like the UPR are activated. In order to contain the increasing proteotoxic stress or within the framework of a proteasome-to-autophagy switch, CASA is initiated and starts autophagic degradation of misfolded proteins. Due to persistent ER stress as well as immunologic/inflammatory stress within the myofiber environment, autophagy processes are overwhelmed and regulatory mechanisms decompensate, leading to a vicious circle with MHC class I presentation, more inflammation and immunologic "attack" and more cell stress; eventually cumulating in myofiber necrosis.

6. Conclusion and outlook

All in all, the present exploration revealed that vacuoles, although a common feature in IMNM, are not a specific phenomenon but probably an expression of a longer course of disease or sign for stronger disease activity. Further clinical studies could show whether IMNM patients harbouring vacuoles in myofibers upon diagnosis of the disease profit from earlier or intensified immunosuppressant therapy. For the first time, it has been shown that the autophagy protein p62 is present in a specific pattern in IMNM skeletal muscle biopsies, which could be used for diagnostic means. This finding was shortly thereafter confirmed by Girolamo *et al.* (172). Additionally, this p62 pattern led to the discovery of BAG3-mediated selective autophagy as an important mechanism in IMNM that is closely linked to immunological events (174).

Further studies need to be conducted in order to understand the exact relation between the immune response in the muscle and BAG3-mediated selective autophagy in IMNM. In this regard, investigating the mechanisms of 1) antibody/complement-reaction leading to ER stress and 2) the interconnection of ER stress and CASA in myoblast cultures would further elucidate the pathological processes in IMNM patients´ skeletal muscle. By illuminating the role of CASA/BAG3-mediated selective autophagy in IMNM, new therapeutic approaches via autophagy-modulating drugs could be unlocked that might be especially promising for immunosuppressant resistant IMNM patients. Concerning the different antibodies in IMNM patients, investigating the differential association of CASA with different serotypes could bring insight to the general understanding of IMNM as a still heterogeneous disease entity (196). Furthermore, special focus is needed on seronegative IMNM patients since they show a significantly higher risk for development of cancer within three years before and after a myopathy diagnosis (197). Also in this context BAG3 pathology might be of great interest, since its involvement in different kinds of malignancies has been shown (190). Taken together, shedding light on CASA and BAG3 pathology in IMNM unlocks many promising implications in disease understanding and the approach to new therapeutic options for affected patients.

References

1. De Bleecker JL, De Paepe B, Aronica E, de Visser M, Amato A, Benveniste O, De Bleecker J, de Boer O, Dimachkie M, Gherardi R, Goebel HH, Hilton-Jones D, Holton J, Lundberg IE, Mammen A, Mastaglia F, Nishino I, Rushing E, Schroder HD, Selcen D, Stenzel W. 205th ENMC International Workshop: Pathology diagnosis of idiopathic inflammatory myopathies part II 28-30 March 2014, Naarden, The Netherlands. Neuromuscular disorders : NMD. 2015;25(3):268-72.
2. Keitel W, Wolff HP. [Originators and eponyms of dermatomyositis : Ernst Leberecht Wagner (1821-1888) and Heinrich Unverricht (1853-1912)]. Zeitschrift fur Rheumatologie. 2016;75(4):429-34.
3. Levine TD. History of dermatomyositis. Archives of neurology. 2003;60(5):780-2.
4. Bohan A, Peter JB. Polymyositis and dermatomyositis (first of two parts). The New England journal of medicine. 1975;292(7):344-7.
5. Bohan A, Peter JB. Polymyositis and dermatomyositis (second of two parts). The New England journal of medicine. 1975;292(8):403-7.
6. Caspary EA, Gubbay SS, Stern GM. CIRCULATING ANTIBODIES IN POLYMYOSITIS AND OTHER MUSCLE-WASTING DISORDERS. Lancet (London, England). 1964;2(7366):941.
7. Stern GM, Rose AL, Jacobs K. Circulating antibodies in polymyositis. Journal of the neurological sciences. 1967;5(1):181-3.
8. Fine RM. Autoantibodies in dermatomyositis and polymyositis. International journal of dermatology. 1985;24(7):433-4.
9. Nishikai M, Homma M. Anti-myoglobin antibody in polymyositis. Lancet (London, England). 1972;2(7788):1205-6.
10. Venables PJ, Mumford PA, Maini RN. Antibodies to nuclear antigens in polymyositis: relationship to autoimmune 'overlap syndromes' and carcinoma. Annals of the rheumatic diseases. 1981;40(3):217-23.
11. Rosa MD, Hendrick JP, Jr., Lerner MR, Steitz JA, Reichlin M. A mammalian tRNAHis-containing antigen is recognized by the polymyositis-specific antibody anti-Jo-1. Nucleic acids research. 1983;11(3):853-70.
12. Yoshida S, Akizuki M, Mimori T, Yamagata H, Inada S, Homma M. The precipitating antibody to an acidic nuclear protein antigen, the Jo-1, in connective tissue diseases. A marker for a subset of polymyositis with interstitial pulmonary fibrosis. Arthritis and rheumatism. 1983;26(5):604-11.
13. Targoff IN, Reichlin M. The association between Mi-2 antibodies and dermatomyositis. Arthritis and rheumatism. 1985;28(7):796-803.
14. Jonsson J. Symptomatology and diagnosis in connective tissue disease. Antibodies to extractable ribonucleoprotein in 123 patients reacting with cell nuclei in the immunofluorescence test. Scandinavian journal of rheumatology. 1976;5(3):177-83.
15. Lerner MR, Steitz JA. Antibodies to small nuclear RNAs complexed with proteins are produced by patients with systemic lupus erythematosus. Proceedings of the National Academy of Sciences of the United States of America. 1979;76(11):5495-9.
16. Reddy R, Tan EM, Henning D, Nohga K, Busch H. Detection of a nucleolar 7-2 ribonucleoprotein and a cytoplasmic 8-2 ribonucleoprotein with autoantibodies from patients with scleroderma. The Journal of biological chemistry. 1983;258(3):1383-6.
17. Fritzler MJ, Ali R, Tan EM. Antibodies from patients with mixed connective tissue disease react with heterogeneous nuclear ribonucleoprotein or ribonucleic acid (hnRNP/RNA) of the nuclear matrix. Journal of immunology (Baltimore, Md : 1950). 1984;132(3):1216-22.

18. Reeves WH, Nigam SK, Blobel G. Human autoantibodies reactive with the signal-recognition particle. Proceedings of the National Academy of Sciences of the United States of America. 1986;83(24):9507-11.
19. Mathews MB, Reichlin M, Hughes GR, Bernstein RM. Anti-threonyl-tRNA synthetase, a second myositis-related autoantibody. The Journal of experimental medicine. 1984;160(2):420-34.
20. Bunn CC, Bernstein RM, Mathews MB. Autoantibodies against alanyl-tRNA synthetase and tRNAAla coexist and are associated with myositis. The Journal of experimental medicine. 1986;163(5):1281-91.
21. Mathews MB, Bernstein RM. Myositis autoantibody inhibits histidyl-tRNA synthetase: a model for autoimmunity. Nature. 1983;304(5922):177-9.
22. Reichlin M, Maddison PJ, Targoff I, Bunch T, Arnett F, Sharp G, Treadwell E, Tan EM. Antibodies to a nuclear/nucleolar antigen in patients with polymyositis overlap syndromes. Journal of clinical immunology. 1984;4(1):40-4.
23. Treadwell EL, Alspaugh MA, Wolfe JF, Sharp GC. Clinical relevance of PM-1 antibody and physiochemical characterization of PM-1 antigen. The Journal of rheumatology. 1984;11(5):658-62.
24. Love LA, Leff RL, Fraser DD, Targoff IN, Dalakas M, Plotz PH, Miller FW. A new approach to the classification of idiopathic inflammatory myopathy: myositis-specific autoantibodies define useful homogeneous patient groups. Medicine. 1991;70(6):360-74.
25. Miller T, Al-Lozi M, Lopate G, Pestronk A. Myopathy with antibodies to the signal recognition particle: clinical and pathological features. J Neurol Neurosurg Psychiatry. 2002;73(4):420-8.
26. Hoogendijk JE, Amato AA, Lecky BR, Choy EH, Lundberg IE, Rose MR, Vencovsky J, de Visser M, Hughes RA. 119th ENMC international workshop: trial design in adult idiopathic inflammatory myopathies, with the exception of inclusion body myositis, 10-12 October 2003, Naarden, The Netherlands. Neuromuscular disorders : NMD. 14. England2004. p. 337-45.
27. Allenbach Y, Mammen AL, Benveniste O, Stenzel W. 224th ENMC International Workshop:: Clinico-sero-pathological classification of immune-mediated necrotizing myopathies Zandvoort, The Netherlands, 14-16 October 2016. Neuromuscular disorders : NMD. 2018;28(1):87-99.
28. Basharat P, Christopher-Stine L. Immune-Mediated Necrotizing Myopathy: Update on Diagnosis and Management. Current rheumatology reports. 2015;17(12):72.
29. Lim J, Rietveld A, De Bleecker JL, Badrising UA, Saris CGJ, van der Kooi AJ, de Visser M. Seronegative patients form a distinctive subgroup of immune-mediated necrotizing myopathy. Neurology(R) neuroimmunology & neuroinflammation. 2019;6(1):e513.
30. Mammen A. Autoimmune muscle disease. Handbook of clinical neurology. 2016;133:467-84.
31. Pinal-Fernandez I, Parks C, Werner JL, Albayda J, Paik J, Danoff SK, Casciola-Rosen L, Christopher-Stine L, Mammen AL. Longitudinal Course of Disease in a Large Cohort of Myositis Patients With Autoantibodies Recognizing the Signal Recognition Particle. Arthritis care & research. 2017;69(2):263-70.
32. Allenbach Y, Drouot L, Rigolet A, Charuel JL, Jouen F, Romero NB, Maisonobe T, Dubourg O, Behin A, Laforet P, Stojkovic T, Eymard B, Costedoat-Chalumeau N, Campana-Salort E, Tournadre A, Musset L, Bader-Meunier B, Kone-Paut I, Sibilia J, Servais L, Fain O, Larroche C, Diot E, Terrier B, De Paz R, Dossier A, Menard D, Morati C, Roux M, Ferrer X, Martinet J, Besnard S, Bellance R, Cacoub P, Arnaud L, Grosbois B, Herson S, Boyer O, Benveniste O. Anti-HMGCR autoantibodies in European patients with autoimmune necrotizing myopathies: inconstant exposure to statin. Medicine (Baltimore). 2014;93(3):150-7.
33. Werner JL, Christopher-Stine L, Ghazarian SR, Pak KS, Kus JE, Daya NR, Lloyd TE, Mammen AL. Antibody levels correlate with creatine kinase levels and strength in anti-3-hydroxy-3-

methylglutaryl-coenzyme A reductase-associated autoimmune myopathy. Arthritis and rheumatism. 2012;64(12):4087-93.
34. Vittonatto E, Boschi S, L CH-P, Ponzalino V, Bortolani S, Brusa C, Rainero I, Ricci F, Vercelli L, Mongini T. Differential diagnosis of vacuolar muscle biopsies: use of p62, LC3 and LAMP2 immunohistochemistry. Acta Myol. 2017;36(4):191-8.
35. Nishino I. Autophagic vacuolar myopathy. Seminars in pediatric neurology. 2006;13(2):90-5.
36. Hirschhorn R, Reuser AJJ. Glycogen storage disease Type II: acid α-glucosidase (acid maltase) deficiency. 2001. In: The Online Metabolic and Molecular Bases of Inherited Disease New York [Internet]. New York: McGraw-Hill; [3389–420].
37. Raben N, Plotz P, Byrne BJ. Acid alpha-glucosidase deficiency (glycogenosis type II, Pompe disease). Current molecular medicine. 2002;2(2):145-66.
38. Reuser AJ, Koster JF, Hoogeveen A, Galjaard H. Biochemical, immunological, and cell genetic studies in glycogenosis type II. Am J Hum Genet. 1978;30(2):132-43.
39. Malicdan MC, Nishino I. Autophagy in lysosomal myopathies. Brain pathology (Zurich, Switzerland). 2012;22(1):82-8.
40. Hirschhorn R, Reuser AJJ. Glycogen storage disease Type II: acid α-glucosidase (acid maltase) deficiency. 2001. In: The Online M*etabolic* and M*olecular Bases* of I*nherited Disease* [Internet]. New York: The McGraw-Hill Companies; [3389–420].
41. Lejeune N, Thines-Sempoux D, Hers HG. Tissue fractionation studies. 16. Intracellular distribution and properties of alpha-glucosidases in rat liver. Biochem J. 1963;86:16-21.
42. Nishino I, Fu J, Tanji K, Yamada T, Shimojo S, Koori T, Mora M, Riggs JE, Oh SJ, Koga Y, Sue CM, Yamamoto A, Murakami N, Shanske S, Byrne E, Bonilla E, Nonaka I, DiMauro S, Hirano M. Primary LAMP-2 deficiency causes X-linked vacuolar cardiomyopathy and myopathy (Danon disease). Nature. 2000;406(6798):906-10.
43. Nascimbeni AC, Fanin M, Angelini C, Sandri M. Autophagy dysregulation in Danon disease. Cell death & disease. 2017;8(1):e2565.
44. Sugie K, Noguchi S, Kozuka Y, Arikawa-Hirasawa E, Tanaka M, Yan C, Saftig P, von Figura K, Hirano M, Ueno S, Nonaka I, Nishino I. Autophagic vacuoles with sarcolemmal features delineate Danon disease and related myopathies. Journal of neuropathology and experimental neurology. 2005;64(6):513-22.
45. Ramachandran N, Munteanu I, Wang P, Ruggieri A, Rilstone JJ, Israelian N, Naranian T, Paroutis P, Guo R, Ren ZP, Nishino I, Chabrol B, Pellissier JF, Minetti C, Udd B, Fardeau M, Tailor CS, Mahuran DJ, Kissel JT, Kalimo H, Levy N, Manolson MF, Ackerley CA, Minassian BA. VMA21 deficiency prevents vacuolar ATPase assembly and causes autophagic vacuolar myopathy. Acta neuropathologica. 2013;125(3):439-57.
46. VMA21 VMA21, vacuolar ATPase assembly factor [Homo sapiens (human)] - Gene - NCBI [Internet]. 2017. Available from: https://www.ncbi.nlm.nih.gov/pubmed/.
47. Finbow ME, Harrison MA. The vacuolar H+-ATPase: a universal proton pump of eukaryotes. Biochem J. 1997;324(Pt 3):697-712.
48. Dowling JJ, Moore SA, Kalimo H, Minassian BA. X-linked myopathy with excessive autophagy: a failure of self-eating. Acta neuropathologica. 2015;129(3):383-90.
49. Pasnoor M, Barohn RJ, Dimachkie MM. Toxic Myopathies. Neurol Clin. 2014;32(3):647-viii.
50. Posada C, Garcia-Cruz A, Garcia-Doval I, Millan BS, Teijeira S. Chloroquine-induced myopathy. Lupus. 20. England2011. p. 773-4.
51. Abdel-Hamid H, Oddis CV, Lacomis D. Severe hydroxychloroquine myopathy. Muscle & nerve. 2008;38(3):1206-10.

52. Lee HS, Daniels BH, Salas E, Bollen AW, Debnath J, Margeta M. Clinical utility of LC3 and p62 immunohistochemistry in diagnosis of drug-induced autophagic vacuolar myopathies: a case-control study. PloS one. 2012;7(4):e36221.
53. Lee HS, Daniels BH, Salas E, Bollen AW, Debnath J, Margeta M. Clinical Utility of LC3 and p62 Immunohistochemistry in Diagnosis of Drug-Induced Autophagic Vacuolar Myopathies: A Case-Control Study. PloS one. 72012.
54. Mastaglia FL, Papadimitriou JM, Dawkins RL, Beveridge B. Vacuolar myopathy associated with chloroquine, lupus erythematosus and thymoma. Report of a case with unusual mitochondrial changes and lipid accumulation in muscle. Journal of the neurological sciences. 1977;34(3):315-28.
55. Riggs JE, Schochet SS, Jr., Gutmann L, Crosby TW, DiBartolomeo AG. Chronic human colchicine neuropathy and myopathy. Archives of neurology. 1986;43(5):521-3.
56. Younger DS, Mayer SA, Weimer LH, Alderson LM, Seplowitz AH, Lovelace RE. Colchicine-induced myopathy and neuropathy. Neurology. 1991;41(6):943.
57. De Deyn PP, Ceuterick C, Saxena V, Crols R, Chappel R, Martin JJ. Chronic colchicine-induced myopathy and neuropathy. Acta neurologica Belgica. 1995;95(1):29-32.
58. Wilbur K, Makowsky M. Colchicine myotoxicity: case reports and literature review. Pharmacotherapy. 2004;24(12):1784-92.
59. Sayarlioglu M, Sayarlioglu H, Ozen S, Erkoc R, Gul A. Colchicine-induced myopathy in a teenager with familial Mediterranean fever. The Annals of pharmacotherapy. 2003;37(12):1821-4.
60. Kuncl RW, Duncan G, Watson D, Alderson K, Rogawski MA, Peper M. Colchicine myopathy and neuropathy. The New England journal of medicine. 1987;316(25):1562-8.
61. Ching JK, Ju JS, Pittman SK, Margeta M, Weihl CC. Increased autophagy accelerates colchicine-induced muscle toxicity. Autophagy. 2013;9(12):2115-25.
62. Pulipaka U, Lacomis D, Omalu B. Amiodarone-induced neuromyopathy: three cases and a review of the literature. Journal of clinical neuromuscular disease. 2002;3(3):97-105.
63. Heinz Lüllmann KM, Lutz Hein. Pharmakologie und Toxikologie : Arzneimittelwirkungen verstehen - Medikamente gezielt einsetzen ; ein Lehrbuch für Studierende der Medizin, der Pharmazie und der Biowissenschaften, eine Informationsquelle für Ärzte, Apotheker und Gesundheitspolitiker ; 130 Tabellen. 17 ed. Georg Thieme Verlag2010.
64. Lullmann H, Lullmann-Rauch R, Wassermann O. Drug-induced phospholipidoses. II. Tissue distribution of the amphiphilic drug chlorphentermine. CRC critical reviews in toxicology. 1975;4(2):185-218.
65. Rose MR. 188th ENMC International Workshop: Inclusion Body Myositis, 2-4 December 2011, Naarden, The Netherlands. Neuromuscular disorders : NMD. 2013;23(12):1044-55.
66. Schmidt J, Barthel K, Wrede A, Salajegheh M, Bahr M, Dalakas MC. Interrelation of inflammation and APP in sIBM: IL-1 beta induces accumulation of beta-amyloid in skeletal muscle. Brain : a journal of neurology. 2008;131(Pt 5):1228-40.
67. Greenberg SA. Comment on 'Interrelation of inflammation and APP in sIBM: IL-1beta induces accumulation of beta-amyloid in skeletal muscle'. Brain : a journal of neurology. 132. England2009. p. e106; author reply e7.
68. Haq SA, Tournadre A. Idiopathic inflammatory myopathies: from immunopathogenesis to new therapeutic targets. International journal of rheumatic diseases. 2015;18(8):818-25.
69. Benveniste O, Stenzel W, Hilton-Jones D, Sandri M, Boyer O, van Engelen BGM. Amyloid deposits and inflammatory infiltrates in sporadic inclusion body myositis: the inflammatory egg comes before the degenerative chicken. Acta neuropathologica. 1292015. p. 611-24.
70. Nogalska A, Terracciano C, D'Agostino C, King Engel W, Askanas V. p62/SQSTM1 is overexpressed and prominently accumulated in inclusions of sporadic inclusion-body myositis

muscle fibers, and can help differentiating it from polymyositis and dermatomyositis. Acta neuropathologica. 2009;118(3):407-13.
71. Badrising UA, Schreuder GM, Giphart MJ, Geleijns K, Verschuuren JJ, Wintzen AR, Maat-Schieman ML, van Doorn P, van Engelen BG, Faber CG, Hoogendijk JE, de Jager AE, Koehler PJ, de Visser M, van Duinen SG. Associations with autoimmune disorders and HLA class I and II antigens in inclusion body myositis. Neurology. 2004;63(12):2396-8.
72. Rojana-udomsart A, Mitrpant C, James I, Witt C, Needham M, Day T, Kiers L, Corbett A, Martinez P, Wilton SD, Mastaglia FL. Analysis of HLA-DRB3 alleles and supertypical genotypes in the MHC Class II region in sporadic inclusion body myositis. Journal of neuroimmunology. 2013;254(1-2):174-7.
73. Lampe JB, Gossrau G, Kempe A, Fussel M, Schwurack K, Schroder R, Krause S, Kohnen R, Walter MC, Reichmann H, Lochmuller H. Analysis of HLA class I and II alleles in sporadic inclusion-body myositis. Journal of neurology. 2003;250(11):1313-7.
74. Price P, Santoso L, Mastaglia F, Garlepp M, Kok CC, Allcock R, Laing N. Two major histocompatibility complex haplotypes influence susceptibility to sporadic inclusion body myositis: critical evaluation of an association with HLA-DR3. Tissue antigens. 2004;64(5):575-80.
75. Koffman BM, Sivakumar K, Simonis T, Stroncek D, Dalakas MC. HLA allele distribution distinguishes sporadic inclusion body myositis from hereditary inclusion body myopathies. Journal of neuroimmunology. 1998;84(2):139-42.
76. Rothwell S, Lilleker JB, Lamb JA. Genetics in inclusion body myositis. Current opinion in rheumatology. 2017.
77. Greenberg SA, Pinkus JL, Kong SW, Baecher-Allan C, Amato AA, Dorfman DM. Highly differentiated cytotoxic T cells in inclusion body myositis. Brain : a journal of neurology. 2019;142(9):2590-604.
78. Knauss S, Preusse C, Allenbach Y, Leonard-Louis S, Touat M, Fischer N, Radbruch H, Mothes R, Matyash V, Bohmerle W, Endres M, Goebel HH, Benveniste O, Stenzel W. PD1 pathway in immune-mediated myopathies: Pathogenesis of dysfunctional T cells revisited. Neurology(R) neuroimmunology & neuroinflammation. 2019;6(3):e558.
79. Bento CF, Renna M, Ghislat G, Puri C, Ashkenazi A, Vicinanza M, Menzies FM, Rubinsztein DC. Mammalian Autophagy: How Does It Work? Annual review of biochemistry. 2016;85:685-713.
80. Tooze SA, Jefferies HB, Kalie E, Longatti A, McAlpine FE, McKnight NC, Orsi A, Polson HE, Razi M, Robinson DJ, Webber JL. Trafficking and signaling in mammalian autophagy. IUBMB life. 2010;62(7):503-8.
81. Kesidou E, Lagoudaki R, Touloumi O, Poulatsidou KN, Simeonidou C. Autophagy and neurodegenerative disorders. Neural regeneration research. 2013;8(24):2275-83.
82. Levine B, Klionsky DJ. Development by self-digestion: molecular mechanisms and biological functions of autophagy. Developmental cell. 2004;6(4):463-77.
83. Klionsky DJ, Abdelmohsen K, Abe A, Abedin MJ, Abeliovich H, Acevedo Arozena A, Adachi H, Adams CM, Adams PD, Adeli K, Adhihetty PJ, Adler SG, Agam G, Agarwal R, Aghi MK, Agnello M, Agostinis P, Aguilar PV, Aguirre-Ghiso J, Airoldi EM, Ait-Si-Ali S, Akematsu T, Akporiaye ET, Al-Rubeai M, Albaiceta GM, Albanese C, Albani D, Albert ML, Aldudo J, Algül H, Alirezaei M, Alloza I, Almasan A, Almonte-Beceril M, Alnemri ES, Alonso C, Altan-Bonnet N, Altieri DC, Alvarez S, Alvarez-Erviti L, Alves S, Amadoro G, Amano A, Amantini C, Ambrosio S, Amelio I, Amer AO, Amessou M, Amon A, An Z, Anania FA, Andersen SU, Andley UP, Andreadi CK, Andrieu-Abadie N, Anel A, Ann DK, Anoopkumar-Dukie S, Antonioli M, Aoki H, Apostolova N, Aquila S, Aquilano K, Araki K, Arama E, Aranda A, Araya J, Arcaro A, Arias E, Arimoto H, Ariosa AR, Armstrong JL, Arnould T, Arsov I, Asanuma K, Askanas V, Asselin E, Atarashi R, Atherton SS, Atkin JD, Attardi LD, Auberger P, Auburger G, Aurelian L, Autelli R, Avagliano L,

Avantaggiati ML, Avrahami L, Awale S, Azad N, Bachetti T, Backer JM, Bae DH, Bae JS, Bae ON, Bae SH, Baehrecke EH, Baek SH, Baghdiguian S, Bagniewska-Zadworna A, Bai H, Bai J, Bai XY, Bailly Y, Balaji KN, Balduini W, Ballabio A, Balzan R, Banerjee R, Bánhegyi G, Bao H, Barbeau B, Barrachina MD, Barreiro E, Bartel B, Bartolomé A, Bassham DC, Bassi MT, Bast RC, Basu A, Batista MT, Batoko H, Battino M, Bauckman K, Baumgarner BL, Bayer KU, Beale R, Beaulieu JF, Beck GR, Becker C, Beckham JD, Bédard PA, Bednarski PJ, Begley TJ, Behl C, Behrends C, Behrens GM, Behrns KE, Bejarano E, Belaid A, Belleudi F, Bénard G, Berchem G, Bergamaschi D, Bergami M, Berkhout B, Berliocchi L, Bernard A, Bernard M, Bernassola F, Bertolotti A, Bess AS, Besteiro S, Bettuzzi S, Bhalla S, Bhattacharyya S, Bhutia SK, Biagosch C, Bianchi MW, Biard-Piechaczyk M, Billes V, Bincoletto C, Bingol B, Bird SW, Bitoun M, Bjedov I, Blackstone C, Blanc L, Blanco GA, Blomhoff HK, Boada-Romero E, Böckler S, Boes M, Boesze-Battaglia K, Boise LH, Bolino A, Boman A, Bonaldo P, Bordi M, Bosch J, Botana LM, Botti J, Bou G, Bouché M, Bouchecareilh M, Boucher MJ, Boulton ME, Bouret SG, Boya P, Boyer-Guittaut M, Bozhkov PV, Brady N, Braga VM, Brancolini C, Braus GH, Bravo-San Pedro JM, Brennan LA, Bresnick EH, Brest P, Bridges D, Bringer MA, Brini M, Brito GC, Brodin B, Brookes PS, Brown EJ, Brown K, Broxmeyer HE, Bruhat A, Brum PC, Brumell JH, Brunetti-Pierri N, Bryson-Richardson RJ, Buch S, Buchan AM, Budak H, Bulavin DV, Bultman SJ, Bultynck G, Bumbasirevic V, Burelle Y, Burke RE, Burmeister M, Bütikofer P, Caberlotto L, Cadwell K, Cahova M, Cai D, Cai J, Cai Q, Calatayud S, Camougrand N, Campanella M, Campbell GR, Campbell M, Campello S, Candau R, Caniggia I, Cantoni L, Cao L, Caplan AB, Caraglia M, Cardinali C, Cardoso SM, Carew JS, Carleton LA, Carlin CR, Carloni S, Carlsson SR, Carmona-Gutierrez D, Carneiro LA, Carnevali O, Carra S, Carrier A, Carroll B, Casas C, Casas J, Cassinelli G, Castets P, Castro-Obregon S, Cavallini G, Ceccherini I, Cecconi F, Cederbaum AI, Ceña V, Cenci S, Cerella C, Cervia D, Cetrullo S, Chaachouay H, Chae HJ, Chagin AS, Chai CY, Chakrabarti G, Chamilos G, Chan EY, Chan MT, Chandra D, Chandra P, Chang CP, Chang RC, Chang TY, Chatham JC, Chatterjee S, Chauhan S, Che Y, Cheetham ME, Cheluvappa R, Chen CJ, Chen G, Chen GC, Chen H, Chen JW, Chen JK, Chen M, Chen P, Chen Q, Chen SD, Chen S, Chen SS, Chen W, Chen WJ, Chen WQ, Chen X, Chen YH, Chen YG, Chen Y, Chen YJ, Chen YQ, Chen Z, Cheng A, Cheng CH, Cheng H, Cheong H, Cherry S, Chesney J, Cheung CH, Chevet E, Chi HC, Chi SG, Chiacchiera F, Chiang HL, Chiarelli R, Chiariello M, Chieppa M, Chin LS, Chiong M, Chiu GN, Cho DH, Cho SG, Cho WC, Cho YY, Cho YS, Choi AM, Choi EJ, Choi EK, Choi J, Choi ME, Choi SI, Chou TF, Chouaib S, Choubey D, Choubey V, Chow KC, Chowdhury K, Chu CT, Chuang TH, Chun T, Chung H, Chung T, Chung YL, Chwae YJ, Cianfanelli V, Ciarcia R, Ciechomska IA, Ciriolo MR, Cirone M, Claerhout S, Clague MJ, Clària J, Clarke PG, Clarke R, Clementi E, Cleyrat C, Cnop M, Coccia EM, Cocco T, Codogno P, Coers J, Cohen EE, Colecchia D, Coletto L, Coll NS, Colucci-Guyon E, Comincini S, Condello M, Cook KL, Coombs GH, Cooper CD, Cooper JM, Coppens I, Corasaniti MT, Corazzari M, Corbalan R, Corcelle-Termeau E, Cordero MD, Corral-Ramos C, Corti O, Cossarizza A, Costelli P, Costes S, Cotman SL, Coto-Montes A, Cottet S, Couve E, Covey LR, Cowart LA, Cox JS, Coxon FP, Coyne CB, Cragg MS, Craven RJ, Crepaldi T, Crespo JL, Criollo A, Crippa V, Cruz MT, Cuervo AM, Cuezva JM, Cui T, Cutillas PR, Czaja MJ, Czyzyk-Krzeska MF, Dagda RK, Dahmen U, Dai C, Dai W, Dai Y, Dalby KN, Dalla Valle L, Dalmasso G, D'Amelio M, Damme M, Darfeuille-Michaud A, Dargemont C, Darley-Usmar VM, Dasarathy S, Dasgupta B, Dash S, Dass CR, Davey HM, Davids LM, Dávila D, Davis RJ, Dawson TM, Dawson VL, Daza P, de Belleroche J, de Figueiredo P, de Figueiredo RC, de la Fuente J, De Martino L, De Matteis A, De Meyer GR, De Milito A, De Santi M, de Souza W, De Tata V, De Zio D, Debnath J, Dechant R, Decuypere JP, Deegan S, Dehay B, Del Bello B, Del Re DP, Delage-Mourroux R, Delbridge LM, Deldicque L, Delorme-Axford E, Deng Y, Dengjel J, Denizot M, Dent P, Der CJ, Deretic V, Derrien B, Deutsch E, Devarenne TP, Devenish RJ, Di

Bartolomeo S, Di Daniele N, Di Domenico F, Di Nardo A, Di Paola S, Di Pietro A, Di Renzo L, DiAntonio A, Díaz-Araya G, Díaz-Laviada I, Diaz-Meco MT, Diaz-Nido J, Dickey CA, Dickson RC, Diederich M, Digard P, Dikic I, Dinesh-Kumar SP, Ding C, Ding WX, Ding Z, Dini L, Distler JH, Diwan A, Djavaheri-Mergny M, Dmytruk K, Dobson RC, Doetsch V, Dokladny K, Dokudovskaya S, Donadelli M, Dong XC, Dong X, Dong Z, Donohue TM, Doran KS, D'Orazi G, Dorn GW, Dosenko V, Dridi S, Drucker L, Du J, Du LL, Du L, du Toit A, Dua P, Duan L, Duann P, Dubey VK, Duchen MR, Duchosal MA, Duez H, Dugail I, Dumit VI, Duncan MC, Dunlop EA, Dunn WA, Dupont N, Dupuis L, Durán RV, Durcan TM, Duvezin-Caubet S, Duvvuri U, Eapen V, Ebrahimi-Fakhari D, Echard A, Eckhart L, Edelstein CL, Edinger AL, Eichinger L, Eisenberg T, Eisenberg-Lerner A, Eissa NT, El-Deiry WS, El-Khoury V, Elazar Z, Eldar-Finkelman H, Elliott CJ, Emanuele E, Emmenegger U, Engedal N, Engelbrecht AM, Engelender S, Enserink JM, Erdmann R, Erenpreisa J, Eri R, Eriksen JL, Erman A, Escalante R, Eskelinen EL, Espert L, Esteban-Martínez L, Evans TJ, Fabri M, Fabrias G, Fabrizi C, Facchiano A, Færgeman NJ, Faggioni A, Fairlie WD, Fan C, Fan D, Fan J, Fang S, Fanto M, Fanzani A, Farkas T, Faure M, Favier FB, Fearnhead H, Federici M, Fei E, Felizardo TC, Feng H, Feng Y, Ferguson TA, Fernández Á, Fernandez-Barrena MG, Fernandez-Checa JC, Fernández-López A, Fernandez-Zapico ME, Feron O, Ferraro E, Ferreira-Halder CV, Fesus L, Feuer R, Fiesel FC, Filippi-Chiela EC, Filomeni G, Fimia GM, Fingert JH, Finkbeiner S, Finkel T, Fiorito F, Fisher PB, Flajolet M, Flamigni F, Florey O, Florio S, Floto RA, Folini M, Follo C, Fon EA, Fornai F, Fortunato F, Fraldi A, Franco R, Francois A, François A, Frankel LB, Fraser ID, Frey N, Freyssenet DG, Frezza C, Friedman SL, Frigo DE, Fu D, Fuentes JM, Fueyo J, Fujitani Y, Fujiwara Y, Fujiya M, Fukuda M, Fulda S, Fusco C, Gabryel B, Gaestel M, Gailly P, Gajewska M, Galadari S, Galili G, Galindo I, Galindo MF, Galliciotti G, Galluzzi L, Galy V, Gammoh N, Gandy S, Ganesan AK, Ganesan S, Ganley IG, Gannagé M, Gao FB, Gao F, Gao JX, García Nannig L, García Véscovi E, Garcia-Macía M, Garcia-Ruiz C, Garg AD, Garg PK, Gargini R, Gassen NC, Gatica D, Gatti E, Gavard J, Gavathiotis E, Ge L, Ge P, Ge S, Gean PW, Gelmetti V, Genazzani AA, Geng J, Genschik P, Gerner L, Gestwicki JE, Gewirtz DA, Ghavami S, Ghigo E, Ghosh D, Giammarioli AM, Giampieri F, Giampietri C, Giatromanolaki A, Gibbings DJ, Gibellini L, Gibson SB, Ginet V, Giordano A, Giorgini F, Giovannetti E, Girardin SE, Gispert S, Giuliano S, Gladson CL, Glavic A, Gleave M, Godefroy N, Gogal RM, Gokulan K, Goldman GH, Goletti D, Goligorsky MS, Gomes AV, Gomes LC, Gomez H, Gomez-Manzano C, Gómez-Sánchez R, Gonçalves DA, Goncu E, Gong Q, Gongora C, Gonzalez CB, Gonzalez-Alegre P, Gonzalez-Cabo P, González-Polo RA, Goping IS, Gorbea C, Gorbunov NV, Goring DR, Gorman AM, Gorski SM, Goruppi S, Goto-Yamada S, Gotor C, Gottlieb RA, Gozes I, Gozuacik D, Graba Y, Graef M, Granato GE, Grant GD, Grant S, Gravina GL, Green DR, Greenhough A, Greenwood MT, Grimaldi B, Gros F, Grose C, Groulx JF, Gruber F, Grumati P, Grune T, Guan JL, Guan KL, Guerra B, Guillen C, Gulshan K, Gunst J, Guo C, Guo L, Guo M, Guo W, Guo XG, Gust AA, Gustafsson Å, Gutierrez E, Gutierrez MG, Gwak HS, Haas A, Haber JE, Hadano S, Hagedorn M, Hahn DR, Halayko AJ, Hamacher-Brady A, Hamada K, Hamai A, Hamann A, Hamasaki M, Hamer I, Hamid Q, Hammond EM, Han F, Han W, Handa JT, Hanover JA, Hansen M, Harada M, Harhaji-Trajkovic L, Harper JW, Harrath AH, Harris AL, Harris J, Hasler U, Hasselblatt P, Hasui K, Hawley RG, Hawley TS, He C, He CY, He F, He G, He RR, He XH, He YW, He YY, Heath JK, Hébert MJ, Heinzen RA, Helgason GV, Hensel M, Henske EP, Her C, Herman PK, Hernández A, Hernandez C, Hernández-Tiedra S, Hetz C, Hiesinger PR, Higaki K, Hilfiker S, Hill BG, Hill JA, Hill WD, Hino K, Hofius D, Hofman P, Höglinger GU, Höhfeld J, Holz MK, Hong Y, Hood DA, Hoozemans JJ, Hoppe T, Hsu C, Hsu CY, Hsu LC, Hu D, Hu G, Hu HM, Hu H, Hu MC, Hu YC, Hu ZW, Hua F, Hua Y, Huang C, Huang HL, Huang KH, Huang KY, Huang S, Huang WP, Huang YR, Huang Y, Huber TB, Huebbe P, Huh WK, Hulmi JJ, Hur GM, Hurley JH, Husak Z, Hussain SN, Hussain S, Hwang JJ, Hwang S, Hwang TI,

Ichihara A, Imai Y, Imbriano C, Inomata M, Into T, Iovane V, Iovanna JL, Iozzo RV, Ip NY, Irazoqui JE, Iribarren P, Isaka Y, Isakovic AJ, Ischiropoulos H, Isenberg JS, Ishaq M, Ishida H, Ishii I, Ishmael JE, Isidoro C, Isobe K, Isono E, Issazadeh-Navikas S, Itahana K, Itakura E, Ivanov AI, Iyer AK, Izquierdo JM, Izumi Y, Izzo V, Jäättelä M, Jaber N, Jackson DJ, Jackson WT, Jacob TG, Jacques TS, Jagannath C, Jain A, Jana NR, Jang BK, Jani A, Janji B, Jannig PR, Jansson PJ, Jean S, Jendrach M, Jeon JH, Jessen N, Jeung EB, Jia K, Jia L, Jiang H, Jiang L, Jiang T, Jiang X, Jiang Y, Jiménez A, Jin C, Jin H, Jin L, Jin M, Jin S, Jinwal UK, Jo EK, Johansen T, Johnson DE, Johnson GV, Johnson JD, Jonasch E, Jones C, Joosten LA, Jordan J, Joseph AM, Joseph B, Joubert AM, Ju D, Ju J, Juan HF, Juenemann K, Juhász G, Jung HS, Jung JU, Jung YK, Jungbluth H, Justice MJ, Jutten B, Kaakoush NO, Kaarniranta K, Kaasik A, Kabuta T, Kaeffer B, Kågedal K, Kahana A, Kajimura S, Kakhlon O, Kalia M, Kalvakolanu DV, Kamada Y, Kambas K, Kaminskyy VO, Kampinga HH, Kandouz M, Kang C, Kang R, Kang TC, Kanki T, Kanneganti TD, Kanno H, Kanthasamy AG, Kantorow M, Kaparakis-Liaskos M, Kapuy O, Karantza V, Karim MR, Karmakar P, Kaser A, Kaushik S, Kawula T, Kaynar AM, Ke PY, Ke ZJ, Kehrl JH, Keller KE, Kemper JK, Kenworthy AK, Kepp O, Kern A, Kesari S, Kessel D, Ketteler R, Kettelhut IoC, Khambu B, Khan MM, Khandelwal VK, Khare S, Kiang JG, Kiger AA, Kihara A, Kim AL, Kim CH, Kim DR, Kim DH, Kim EK, Kim HY, Kim HR, Kim JS, Kim JH, Kim JC, Kim KW, Kim MD, Kim MM, Kim PK, Kim SW, Kim SY, Kim YS, Kim Y, Kimchi A, Kimmelman AC, Kimura T, King JS, Kirkegaard K, Kirkin V, Kirshenbaum LA, Kishi S, Kitajima Y, Kitamoto K, Kitaoka Y, Kitazato K, Kley RA, Klimecki WT, Klinkenberg M, Klucken J, Knævelsrud H, Knecht E, Knuppertz L, Ko JL, Kobayashi S, Koch JC, Koechlin-Ramonatxo C, Koenig U, Koh YH, Köhler K, Kohlwein SD, Koike M, Komatsu M, Kominami E, Kong D, Kong HJ, Konstantakou EG, Kopp BT, Korcsmaros T, Korhonen L, Korolchuk VI, Koshkina NV, Kou Y, Koukourakis MI, Koumenis C, Kovács AL, Kovács T, Kovacs WJ, Koya D, Kraft C, Krainc D, Kramer H, Kravic-Stevovic T, Krek W, Kretz-Remy C, Krick R, Krishnamurthy M, Kriston-Vizi J, Kroemer G, Kruer MC, Kruger R, Ktistakis NT, Kuchitsu K, Kuhn C, Kumar AP, Kumar A, Kumar D, Kumar R, Kumar S, Kundu M, Kung HJ, Kuno A, Kuo SH, Kuret J, Kurz T, Kwok T, Kwon TK, Kwon YT, Kyrmizi I, La Spada AR, Lafont F, Lahm T, Lakkaraju A, Lam T, Lamark T, Lancel S, Landowski TH, Lane DJ, Lane JD, Lanzi C, Lapaquette P, Lapierre LR, Laporte J, Laukkarinen J, Laurie GW, Lavandero S, Lavie L, LaVoie MJ, Law BY, Law HK, Law KB, Layfield R, Lazo PA, Le Cam L, Le Roch KG, Le Stunff H, Leardkamolkarn V, Lecuit M, Lee BH, Lee CH, Lee EF, Lee GM, Lee HJ, Lee H, Lee JK, Lee J, Lee JH, Lee M, Lee MS, Lee PJ, Lee SW, Lee SJ, Lee SY, Lee SH, Lee SS, Lee S, Lee YR, Lee YJ, Lee YH, Leeuwenburgh C, Lefort S, Legouis R, Lei J, Lei QY, Leib DA, Leibowitz G, Lekli I, Lemaire SD, Lemasters JJ, Lemberg MK, Lemoine A, Leng S, Lenz G, Lenzi P, Lerman LO, Lettieri Barbato D, Leu JI, Leung HY, Levine B, Lewis PA, Lezoualc'h F, Li C, Li F, Li FJ, Li J, Li K, Li L, Li M, Li Q, Li R, Li S, Li W, Li X, Li Y, Lian J, Liang C, Liang Q, Liao Y, Liberal J, Liberski PP, Lie P, Lieberman AP, Lim HJ, Lim KL, Lim K, Lima RT, Lin CS, Lin CF, Lin F, Lin FC, Lin K, Lin KH, Lin PH, Lin T, Lin WW, Lin YS, Lin Y, Linden R, Lindholm D, Lindqvist LM, Lingor P, Linkermann A, Liotta LA, Lipinski MM, Lira VA, Lisanti MP, Liton PB, Liu B, Liu C, Liu CF, Liu F, Liu HJ, Liu J, Liu JJ, Liu JL, Liu K, Liu L, Liu Q, Liu RY, Liu S, Liu W, Liu XD, Liu X, Liu XH, Liu Y, Liu Z, Liuzzi JP, Lizard G, Ljujic M, Lodhi IJ, Logue SE, Lokeshwar BL, Long YC, Lonial S, Loos B, López-Otín C, López-Vicario C, Lorente M, Lorenzi PL, Lõrincz P, Los M, Lotze MT, Lovat PE, Lu B, Lu J, Lu Q, Lu SM, Lu S, Lu Y, Luciano F, Luckhart S, Lucocq JM, Ludovico P, Lugea A, Lukacs NW, Lum JJ, Lund AH, Luo H, Luo J, Luo S, Luparello C, Lyons T, Ma J, Ma Y, Ma Z, Machado J, Machado-Santelli GM, Macian F, MacIntosh GC, MacKeigan JP, Macleod KF, MacMicking JD, MacMillan-Crow LA, Madeo F, Madesh M, Madrigal-Matute J, Maeda A, Maeda T, Maegawa G, Maellaro E, Maes H, Magariños M, Maiese K, Maiti TK, Maiuri L, Maiuri MC, Maki CG, Malli R, Malorni W, Maloyan A, Mami-

Chouaib F, Man N, Mancias JD, Mandelkow EM, Mandell MA, Manfredi AA, Manié SN, Manzoni C, Mao K, Mao Z, Mao ZW, Marambaud P, Marconi AM, Marelja Z, Marfe G, Margeta M, Margittai E, Mari M, Mariani FV, Marin C, Marinelli S, Mariño G, Markovic I, Marquez R, Martelli AM, Martens S, Martin KR, Martin SJ, Martin S, Martin-Acebes MA, Martín-Sanz P, Martinand-Mari C, Martinet W, Martinez J, Martinez-Lopez N, Martinez-Outschoorn U, Martínez-Velázquez M, Martinez-Vicente M, Martins WK, Mashima H, Mastrianni JA, Matarese G, Matarrese P, Mateo R, Matoba S, Matsumoto N, Matsushita T, Matsuura A, Matsuzawa T, Mattson MP, Matus S, Maugeri N, Mauvezin C, Mayer A, Maysinger D, Mazzolini GD, McBrayer MK, McCall K, McCormick C, McInerney GM, McIver SC, McKenna S, McMahon JJ, McNeish IA, Mechta-Grigoriou F, Medema JP, Medina DL, Megyeri K, Mehrpour M, Mehta JL, Mei Y, Meier UC, Meijer AJ, Meléndez A, Melino G, Melino S, de Melo EJ, Mena MA, Meneghini MD, Menendez JA, Menezes R, Meng L, Meng LH, Meng S, Menghini R, Menko AS, Menna-Barreto RF, Menon MB, Meraz-Ríos MA, Merla G, Merlini L, Merlot AM, Meryk A, Meschini S, Meyer JN, Mi MT, Miao CY, Micale L, Michaeli S, Michiels C, Migliaccio AR, Mihailidou AS, Mijaljica D, Mikoshiba K, Milan E, Miller-Fleming L, Mills GB, Mills IG, Minakaki G, Minassian BA, Ming XF, Minibayeva F, Minina EA, Mintern JD, Minucci S, Miranda-Vizuete A, Mitchell CH, Miyamoto S, Miyazawa K, Mizushima N, Mnich K, Mograbi B, Mohseni S, Moita LF, Molinari M, Møller AB, Mollereau B, Mollinedo F, Mongillo M, Monick MM, Montagnaro S, Montell C, Moore DJ, Moore MN, Mora-Rodriguez R, Moreira PI, Morel E, Morelli MB, Moreno S, Morgan MJ, Moris A, Moriyasu Y, Morrison JL, Morrison LA, Morselli E, Moscat J, Moseley PL, Mostowy S, Motori E, Mottet D, Mottram JC, Moussa CE, Mpakou VE, Mukhtar H, Mulcahy Levy JM, Muller S, Muñoz-Moreno R, Muñoz-Pinedo C, Münz C, Murphy ME, Murray JT, Murthy A, Mysorekar IU, Nabi IR, Nabissi M, Nader GA, Nagahara Y, Nagai Y, Nagata K, Nagelkerke A, Nagy P, Naidu SR, Nair S, Nakano H, Nakatogawa H, Nanjundan M, Napolitano G, Naqvi NI, Nardacci R, Narendra DP, Narita M, Nascimbeni AC, Natarajan R, Navegantes LC, Nawrocki ST, Nazarko TY, Nazarko VY, Neill T, Neri LM, Netea MG, Netea-Maier RT, Neves BM, Ney PA, Nezis IP, Nguyen HT, Nguyen HP, Nicot AS, Nilsen H, Nilsson P, Nishimura M, Nishino I, Niso-Santano M, Niu H, Nixon RA, Njar VC, Noda T, Noegel AA, Nolte EM, Norberg E, Norga KK, Noureini SK, Notomi S, Notterpek L, Nowikovsky K, Nukina N, Nürnberger T, O'Donnell VB, O'Donovan T, O'Dwyer PJ, Oehme I, Oeste CL, Ogawa M, Ogretmen B, Ogura Y, Oh YJ, Ohmuraya M, Ohshima T, Ojha R, Okamoto K, Okazaki T, Oliver FJ, Ollinger K, Olsson S, Orban DP, Ordonez P, Orhon I, Orosz L, O'Rourke EJ, Orozco H, Ortega AL, Ortona E, Osellame LD, Oshima J, Oshima S, Osiewacz HD, Otomo T, Otsu K, Ou JH, Outeiro TF, Ouyang DY, Ouyang H, Overholtzer M, Ozbun MA, Ozdinler PH, Ozpolat B, Pacelli C, Paganetti P, Page G, Pages G, Pagnini U, Pajak B, Pak SC, Pakos-Zebrucka K, Pakpour N, Palková Z, Palladino F, Pallauf K, Pallet N, Palmieri M, Paludan SR, Palumbo C, Palumbo S, Pampliega O, Pan H, Pan W, Panaretakis T, Pandey A, Pantazopoulou A, Papackova Z, Papademetrio DL, Papassideri I, Papini A, Parajuli N, Pardo J, Parekh VV, Parenti G, Park JI, Park J, Park OK, Parker R, Parlato R, Parys JB, Parzych KR, Pasquet JM, Pasquier B, Pasumarthi KB, Patschan D, Patterson C, Pattingre S, Pattison S, Pause A, Pavenstädt H, Pavone F, Pedrozo Z, Peña FJ, Peñalva MA, Pende M, Peng J, Penna F, Penninger JM, Pensalfini A, Pepe S, Pereira GJ, Pereira PC, Pérez-de la Cruz V, Pérez-Pérez ME, Pérez-Rodríguez D, Pérez-Sala D, Perier C, Perl A, Perlmutter DH, Perrotta I, Pervaiz S, Pesonen M, Pessin JE, Peters GJ, Petersen M, Petrache I, Petrof BJ, Petrovski G, Phang JM, Piacentini M, Pierdominici M, Pierre P, Pierrefite-Carle V, Pietrocola F, Pimentel-Muiños FX, Pinar M, Pineda B, Pinkas-Kramarski R, Pinti M, Pinton P, Piperdi B, Piret JM, Platanias LC, Platta HW, Plowey ED, Pöggeler S, Poirot M, Polčic P, Poletti A, Poon AH, Popelka H, Popova B, Poprawa I, Poulose SM, Poulton J, Powers SK, Powers T, Pozuelo-Rubio M, Prak K, Prange R, Prescott M, Priault M, Prince S, Proia RL, Proikas-Cezanne T, Prokisch H, Promponas VJ, Przyklenk K, Puertollano R,

Pugazhenthi S, Puglielli L, Pujol A, Puyal J, Pyeon D, Qi X, Qian WB, Qin ZH, Qiu Y, Qu Z, Quadrilatero J, Quinn F, Raben N, Rabinowich H, Radogna F, Ragusa MJ, Rahmani M, Raina K, Ramanadham S, Ramesh R, Rami A, Randall-Demllo S, Randow F, Rao H, Rao VA, Rasmussen BB, Rasse TM, Ratovitski EA, Rautou PE, Ray SK, Razani B, Reed BH, Reggiori F, Rehm M, Reichert AS, Rein T, Reiner DJ, Reits E, Ren J, Ren X, Renna M, Reusch JE, Revuelta JL, Reyes L, Rezaie AR, Richards RI, Richardson DR, Richetta C, Riehle MA, Rihn BH, Rikihisa Y, Riley BE, Rimbach G, Rippo MR, Ritis K, Rizzi F, Rizzo E, Roach PJ, Robbins J, Roberge M, Roca G, Roccheri MC, Rocha S, Rodrigues CM, Rodríguez CI, de Cordoba SR, Rodriguez-Muela N, Roelofs J, Rogov VV, Rohn TT, Rohrer B, Romanelli D, Romani L, Romano PS, Roncero MI, Rosa JL, Rosello A, Rosen KV, Rosenstiel P, Rost-Roszkowska M, Roth KA, Roué G, Rouis M, Rouschop KM, Ruan DT, Ruano D, Rubinsztein DC, Rucker EB, Rudich A, Rudolf E, Rudolf R, Ruegg MA, Ruiz-Roldan C, Ruparelia AA, Rusmini P, Russ DW, Russo GL, Russo G, Russo R, Rusten TE, Ryabovol V, Ryan KM, Ryter SW, Sabatini DM, Sacher M, Sachse C, Sack MN, Sadoshima J, Saftig P, Sagi-Eisenberg R, Sahni S, Saikumar P, Saito T, Saitoh T, Sakakura K, Sakoh-Nakatogawa M, Sakuraba Y, Salazar-Roa M, Salomoni P, Saluja AK, Salvaterra PM, Salvioli R, Samali A, Sanchez AM, Sánchez-Alcázar JA, Sanchez-Prieto R, Sandri M, Sanjuan MA, Santaguida S, Santambrogio L, Santoni G, Dos Santos CN, Saran S, Sardiello M, Sargent G, Sarkar P, Sarkar S, Sarrias MR, Sarwal MM, Sasakawa C, Sasaki M, Sass M, Sato K, Sato M, Satriano J, Savaraj N, Saveljeva S, Schaefer L, Schaible UE, Scharl M, Schatzl HM, Schekman R, Scheper W, Schiavi A, Schipper HM, Schmeisser H, Schmidt J, Schmitz I, Schneider BE, Schneider EM, Schneider JL, Schon EA, Schönenberger MJ, Schönthal AH, Schorderet DF, Schröder B, Schuck S, Schulze RJ, Schwarten M, Schwarz TL, Sciarretta S, Scotto K, Scovassi AI, Screaton RA, Screen M, Seca H, Sedej S, Segatori L, Segev N, Seglen PO, Seguí-Simarro JM, Segura-Aguilar J, Seki E, Sell C, Seiliez I, Semenkovich CF, Semenza GL, Sen U, Serra AL, Serrano-Puebla A, Sesaki H, Setoguchi T, Settembre C, Shacka JJ, Shajahan-Haq AN, Shapiro IM, Sharma S, She H, Shen CK, Shen CC, Shen HM, Shen S, Shen W, Sheng R, Sheng X, Sheng ZH, Shepherd TG, Shi J, Shi Q, Shi Y, Shibutani S, Shibuya K, Shidoji Y, Shieh JJ, Shih CM, Shimada Y, Shimizu S, Shin DW, Shinohara ML, Shintani M, Shintani T, Shioi T, Shirabe K, Shiri-Sverdlov R, Shirihai O, Shore GC, Shu CW, Shukla D, Sibirny AA, Sica V, Sigurdson CJ, Sigurdsson EM, Sijwali PS, Sikorska B, Silveira WA, Silvente-Poirot S, Silverman GA, Simak J, Simmet T, Simon AK, Simon HU, Simone C, Simons M, Simonsen A, Singh R, Singh SV, Singh SK, Sinha D, Sinha S, Sinicrope FA, Sirko A, Sirohi K, Sishi BJ, Sittler A, Siu PM, Sivridis E, Skwarska A, Slack R, Slaninová I, Slavov N, Smaili SS, Smalley KS, Smith DR, Soenen SJ, Soleimanpour SA, Solhaug A, Somasundaram K, Son JH, Sonawane A, Song C, Song F, Song HK, Song JX, Song W, Soo KY, Sood AK, Soong TW, Soontornniyomkij V, Sorice M, Sotgia F, Soto-Pantoja DR, Sotthibundhu A, Sousa MJ, Spaink HP, Span PN, Spang A, Sparks JD, Speck PG, Spector SA, Spies CD, Springer W, Clair DS, Stacchiotti A, Staels B, Stang MT, Starczynowski DT, Starokadomskyy P, Steegborn C, Steele JW, Stefanis L, Steffan J, Stellrecht CM, Stenmark H, Stepkowski TM, Stern ST, Stevens C, Stockwell BR, Stoka V, Storchova Z, Stork B, Stratoulias V, Stravopodis DJ, Strnad P, Strohecker AM, Ström AL, Stromhaug P, Stulik J, Su YX, Su Z, Subauste CS, Subramaniam S, Sue CM, Suh SW, Sui X, Sukseree S, Sulzer D, Sun FL, Sun J, Sun SY, Sun Y, Sundaramoorthy V, Sung J, Suzuki H, Suzuki K, Suzuki N, Suzuki T, Suzuki YJ, Swanson MS, Swanton C, Swärd K, Swarup G, Sweeney ST, Sylvester PW, Szatmari Z, Szegezdi E, Szlosarek PW, Taegtmeyer H, Tafani M, Taillebourg E, Tait SW, Takacs-Vellai K, Takahashi Y, Takáts S, Takemura G, Takigawa N, Talbot NJ, Tamagno E, Tamburini J, Tan CP, Tan L, Tan ML, Tan M, Tan YJ, Tanaka K, Tanaka M, Tang D, Tang G, Tanida I, Tanji K, Tannous BA, Tapia JA, Tasset-Cuevas I, Tatar M, Tavassoly I, Tavernarakis N, Taylor A, Taylor GS, Taylor GA, Taylor JP, Taylor MJ, Tchetina EV, Tee AR, Teixeira-Clerc F, Telang S, Tencomnao T, Teng BB,

Teng RJ, Terro F, Tettamanti G, Theiss AL, Theron AE, Thomas KJ, Thomé MP, Thomes PG, Thorburn A, Thorner J, Thum T, Thumm M, Thurston TL, Tian L, Till A, Ting JP, Titorenko VI, Toker L, Toldo S, Tooze SA, Topisirovic I, Torgersen ML, Torosantucci L, Torriglia A, Torrisi MR, Tournier C, Towns R, Trajkovic V, Travassos LH, Triola G, Tripathi DN, Trisciuoglio D, Troncoso R, Trougakos IP, Truttmann AC, Tsai KJ, Tschan MP, Tseng YH, Tsukuba T, Tsung A, Tsvetkov AS, Tu S, Tuan HY, Tucci M, Tumbarello DA, Turk B, Turk V, Turner RF, Tveita AA, Tyagi SC, Ubukata M, Uchiyama Y, Udelnow A, Ueno T, Umekawa M, Umemiya-Shirafuji R, Underwood BR, Ungermann C, Ureshino RP, Ushioda R, Uversky VN, Uzcátegui NL, Vaccari T, Vaccaro MI, Váchová L, Vakifahmetoglu-Norberg H, Valdor R, Valente EM, Vallette F, Valverde AM, Van den Berghe G, Van Den Bosch L, van den Brink GR, van der Goot FG, van der Klei IJ, van der Laan LJ, van Doorn WG, van Egmond M, van Golen KL, Van Kaer L, van Lookeren Campagne M, Vandenabeele P, Vandenberghe W, Vanhorebeek I, Varela-Nieto I, Vasconcelos MH, Vasko R, Vavvas DG, Vega-Naredo I, Velasco G, Velentzas AD, Velentzas PD, Vellai T, Vellenga E, Vendelbo MH, Venkatachalam K, Ventura N, Ventura S, Veras PS, Verdier M, Vertessy BG, Viale A, Vidal M, Vieira HL, Vierstra RD, Vigneswaran N, Vij N, Vila M, Villar M, Villar VH, Villarroya J, Vindis C, Viola G, Viscomi MT, Vitale G, Vogl DT, Voitsekhovskaja OV, von Haefen C, von Schwarzenberg K, Voth DE, Vouret-Craviari V, Vuori K, Vyas JM, Waeber C, Walker CL, Walker MJ, Walter J, Wan L, Wan X, Wang B, Wang C, Wang CY, Wang D, Wang F, Wang G, Wang HJ, Wang H, Wang HG, Wang HD, Wang J, Wang M, Wang MQ, Wang PY, Wang P, Wang RC, Wang S, Wang TF, Wang X, Wang XJ, Wang XW, Wang Y, Wang YJ, Wang YT, Wang ZN, Wappner P, Ward C, Ward DM, Warnes G, Watada H, Watanabe Y, Watase K, Weaver TE, Weekes CD, Wei J, Weide T, Weihl CC, Weindl G, Weis SN, Wen L, Wen X, Wen Y, Westermann B, Weyand CM, White AR, White E, Whitton JL, Whitworth AJ, Wiels J, Wild F, Wildenberg ME, Wileman T, Wilkinson DS, Wilkinson S, Willbold D, Williams C, Williams K, Williamson PR, Winklhofer KF, Witkin SS, Wohlgemuth SE, Wollert T, Wolvetang EJ, Wong E, Wong GW, Wong RW, Wong VK, Woodcock EA, Wright KL, Wu C, Wu D, Wu GS, Wu J, Wu M, Wu S, Wu WK, Wu Y, Wu Z, Xavier CP, Xavier RJ, Xia GX, Xia T, Xia W, Xia Y, Xiao H, Xiao J, Xiao S, Xiao W, Xie CM, Xie Z, Xilouri M, Xiong Y, Xu C, Xu F, Xu H, Xu J, Xu L, Xu X, Xu Y, Xu ZX, Xu Z, Xue Y, Yamada T, Yamamoto A, Yamanaka K, Yamashina S, Yamashiro S, Yan B, Yan X, Yan Z, Yanagi Y, Yang DS, Yang JM, Yang L, Yang M, Yang PM, Yang P, Yang Q, Yang W, Yang WY, Yang X, Yang Y, Yang Z, Yao MC, Yao PJ, Yao X, Yao Z, Yasui LS, Ye M, Yedvobnick B, Yeganeh B, Yeh ES, Yeyati PL, Yi F, Yi L, Yin XM, Yip CK, Yoo YM, Yoo YH, Yoon SY, Yoshida K, Yoshimori T, Young KH, Yu H, Yu JJ, Yu JT, Yu J, Yu L, Yu WH, Yu XF, Yu Z, Yuan J, Yuan ZM, Yue BY, Yue J, Yue Z, Zacks DN, Zacksenhaus E, Zaffaroni N, Zaglia T, Zakeri Z, Zecchini V, Zeng J, Zeng M, Zeng Q, Zervos AS, Zhang DD, Zhang F, Zhang G, Zhang GC, Zhang H, Zhang J, Zhang JP, Zhang L, Zhang MY, Zhang X, Zhang XD, Zhang Y, Zhao M, Zhao WL, Zhao X, Zhao YG, Zhao Y, Zhao YX, Zhao Z, Zhao ZJ, Zheng D, Zheng XL, Zheng X, Zhivotovsky B, Zhong Q, Zhou GZ, Zhou G, Zhou H, Zhou SF, Zhou XJ, Zhu H, Zhu WG, Zhu W, Zhu XF, Zhu Y, Zhuang SM, Zhuang X, Ziparo E, Zois CE, Zoladek T, Zong WX, Zorzano A, Zughaier SM. Guidelines for the use and interpretation of assays for monitoring autophagy (3rd edition). Autophagy. 2016;12(1):1-222.

84. Itakura E, Mizushima N. Characterization of autophagosome formation site by a hierarchical analysis of mammalian Atg proteins. Autophagy. 2010;6(6):764-76.

85. Nakatogawa H, Ichimura Y, Ohsumi Y. Atg8, a ubiquitin-like protein required for autophagosome formation, mediates membrane tethering and hemifusion. Cell. 2007;130(1):165-78.

86. Kabeya Y, Mizushima N, Ueno T, Yamamoto A, Kirisako T, Noda T, Kominami E, Ohsumi Y, Yoshimori T. LC3, a mammalian homologue of yeast Apg8p, is localized in autophagosome membranes after processing. The EMBO journal. 2000;19(21):5720-8.

87. Schreiber A, Peter M. Substrate recognition in selective autophagy and the ubiquitin-proteasome system. Biochimica et biophysica acta. 2014;1843(1):163-81.
88. Ciuffa R, Lamark T, Tarafder AK, Guesdon A, Rybina S, Hagen WJ, Johansen T, Sachse C. The selective autophagy receptor p62 forms a flexible filamentous helical scaffold. Cell reports. 2015;11(5):748-58.
89. Tanida I, Ueno T, Kominami E. LC3 and Autophagy. Methods in molecular biology (Clifton, NJ). 2008;445:77-88.
90. Bjorkoy G, Lamark T, Brech A, Outzen H, Perander M, Overvatn A, Stenmark H, Johansen T. p62/SQSTM1 forms protein aggregates degraded by autophagy and has a protective effect on huntingtin-induced cell death. The Journal of cell biology. 2005;171(4):603-14.
91. Li WW, Li J, Bao JK. Microautophagy: lesser-known self-eating. Cellular and molecular life sciences : CMLS. 2012;69(7):1125-36.
92. Cuervo AM, Wong E. Chaperone-mediated autophagy: roles in disease and aging. Cell research. 2014;24(1):92-104.
93. Arndt V, Dick N, Tawo R, Dreiseidler M, Wenzel D, Hesse M, Furst DO, Saftig P, Saint R, Fleischmann BK, Hoch M, Hohfeld J. Chaperone-assisted selective autophagy is essential for muscle maintenance. Current biology : CB. 2010;20(2):143-8.
94. Arndt V, Rogon C, Hohfeld J. To be, or not to be--molecular chaperones in protein degradation. Cellular and molecular life sciences : CMLS. 2007;64(19-20):2525-41.
95. Ulbricht A, Gehlert S, Leciejewski B, Schiffer T, Bloch W, Höhfeld J. Induction and adaptation of chaperone-assisted selective autophagy CASA in response to resistance exercise in human skeletal muscle. Autophagy. 2015;11(3):538-46.
96. Homma S, Iwasaki M, Shelton GD, Engvall E, Reed JC, Takayama S. BAG3 deficiency results in fulminant myopathy and early lethality. The American journal of pathology. 2006;169(3):761-73.
97. Selcen D, Muntoni F, Burton BK, Pegoraro E, Sewry C, Bite AV, Engel AG. Mutation in BAG3 causes severe dominant childhood muscular dystrophy. Annals of neurology. 2009;65(1):83-9.
98. Schwartz AL, Ciechanover A. The ubiquitin-proteasome pathway and pathogenesis of human diseases. Annual review of medicine. 1999;50:57-74.
99. Rechsteiner M, Hoffman L, Dubiel W. The multicatalytic and 26 S proteases. The Journal of biological chemistry. 1993;268(9):6065-8.
100. Lam YA, Lawson TG, Velayutham M, Zweier JL, Pickart CM. A proteasomal ATPase subunit recognizes the polyubiquitin degradation signal. Nature. 2002;416(6882):763-7.
101. Sijts EJ, Kloetzel PM. The role of the proteasome in the generation of MHC class I ligands and immune responses. Cell Mol Life Sci. 2011;68(9):1491-502.
102. Nathan JA, Spinnenhirn V, Schmidtke G, Basler M, Groettrup M, Goldberg AL. Immuno- and constitutive proteasomes do not differ in their abilities to degrade ubiquitinated proteins. Cell. 2013;152(5):1184-94.
103. Ghannam K, Martinez-Gamboa L, Spengler L, Krause S, Smiljanovic B, Bonin M, Bhattarai S, Grutzkau A, Burmester GR, Haupl T, Feist E. Upregulation of immunoproteasome subunits in myositis indicates active inflammation with involvement of antigen presenting cells, CD8 T-cells and IFNGamma. PloS one. 2014;9(8):e104048.
104. Zhang K, Kaufman RJ. From endoplasmic-reticulum stress to the inflammatory response. Nature. 2008;454(7203):455-62.
105. Schroder M, Kaufman RJ. The mammalian unfolded protein response. Annual review of biochemistry. 2005;74:739-89.
106. Harding HP, Novoa I, Zhang Y, Zeng H, Wek R, Schapira M, Ron D. Regulated translation initiation controls stress-induced gene expression in mammalian cells. Molecular cell. 2000;6(5):1099-108.

107. Hetz C. The unfolded protein response: controlling cell fate decisions under ER stress and beyond. Nature reviews Molecular cell biology. 2012;13(2):89-102.
108. Bertolotti A, Zhang Y, Hendershot LM, Harding HP, Ron D. Dynamic interaction of BiP and ER stress transducers in the unfolded-protein response. Nature cell biology. 2000;2(6):326-32.
109. Haze K, Yoshida H, Yanagi H, Yura T, Mori K. Mammalian transcription factor ATF6 is synthesized as a transmembrane protein and activated by proteolysis in response to endoplasmic reticulum stress. Molecular biology of the cell. 1999;10(11):3787-99.
110. Roth J, Zuber C. Quality control of glycoprotein folding and ERAD: the role of N-glycan handling, EDEM1 and OS-9. Histochemistry and cell biology. 2017;147(2):269-84.
111. Olivari S, Cali T, Salo KE, Paganetti P, Ruddock LW, Molinari M. EDEM1 regulates ER-associated degradation by accelerating de-mannosylation of folding-defective polypeptides and by inhibiting their covalent aggregation. Biochemical and biophysical research communications. 2006;349(4):1278-84.
112. Nagaraju K, Casciola-Rosen L, Lundberg I, Rawat R, Cutting S, Thapliyal R, Chang J, Dwivedi S, Mitsak M, Chen YW, Plotz P, Rosen A, Hoffman E, Raben N. Activation of the endoplasmic reticulum stress response in autoimmune myositis: potential role in muscle fiber damage and dysfunction. Arthritis and rheumatism. 2005;52(6):1824-35.
113. Delaunay A, Bromberg KD, Hayashi Y, Mirabella M, Burch D, Kirkwood B, Serra C, Malicdan MC, Mizisin AP, Morosetti R, Broccolini A, Guo LT, Jones SN, Lira SA, Puri PL, Shelton GD, Ronai Z. The ER-bound RING finger protein 5 (RNF5/RMA1) causes degenerative myopathy in transgenic mice and is deregulated in inclusion body myositis. PloS one. 2008;3(2):e1609.
114. Korolchuk VI, Menzies FM, Rubinsztein DC. Mechanisms of cross-talk between the ubiquitin-proteasome and autophagy-lysosome systems. FEBS letters. 2010;584(7):1393-8.
115. Korolchuk VI, Mansilla A, Menzies FM, Rubinsztein DC. Autophagy inhibition compromises degradation of ubiquitin-proteasome pathway substrates. Molecular cell. 2009;33(4):517-27.
116. Hoyer-Hansen M, Jaattela M. Connecting endoplasmic reticulum stress to autophagy by unfolded protein response and calcium. Cell death and differentiation. 2007;14(9):1576-82.
117. Kouroku Y, Fujita E, Tanida I, Ueno T, Isoai A, Kumagai H, Ogawa S, Kaufman RJ, Kominami E, Momoi T. ER stress (PERK/eIF2alpha phosphorylation) mediates the polyglutamine-induced LC3 conversion, an essential step for autophagy formation. Cell death and differentiation. 2007;14(2):230-9.
118. Hirsch C, Gauss R, Horn SC, Neuber O, Sommer T. The ubiquitylation machinery of the endoplasmic reticulum. Nature. 2009;458(7237):453-60.
119. Hengstman GJD, ter Laak HJ, Egberts W, Lundberg IE, Moutsopoulos HM, Vencovsky J, Doria A, Mosca M, van Venrooij WJ, van Engelen BGM. Anti-signal recognition particle autoantibodies: marker of a necrotising myopathy. Annals of the rheumatic diseases. 652006. p. 1635-8.
120. Allenbach Y, Drouot L, Rigolet A, Charuel JL, Jouen F, Romero NB, Maisonobe T, Dubourg O, Behin A, Laforet P, Stojkovic T, Eymard B, Costedoat-Chalumeau N, Campana-Salort E, Tournadre A, Musset L, Bader-Meunier B, Kone-Paut I, Sibilia J, Servais L, Fain O, Larroche C, Diot E, Terrier B, De Paz R, Dossier A, Menard D, Morati C, Roux M, Ferrer X, Martinet J, Besnard S, Bellance R, Cacoub P, Arnaud L, Grosbois B, Herson S, Boyer O, Benveniste O. Anti-HMGCR Autoantibodies in European Patients With Autoimmune Necrotizing Myopathies: Inconstant Exposure to Statin. Medicine. 932014.
121. Arouche-Delaperche L, Allenbach Y, Amelin D, Preusse C, Mouly V, Mauhin W, Tchoupou GD, Drouot L, Boyer O, Stenzel W, Butler-Browne G, Benveniste O. Pathogenic role of anti-signal recognition protein and anti-3-Hydroxy-3-methylglutaryl-CoA reductase antibodies in necrotizing myopathies: Myofiber atrophy and impairment of muscle regeneration in necrotizing autoimmune myopathies. Annals of neurology. 2017;81(4):538-48.

122. Werner JL, Christopher-Stine L, Ghazarian SR, Pak KS, Kus JE, Daya NR, Lloyd TE, Mammen AL. Antibody Levels Correlate with Creatine Kinase Levels and Strength in Anti-HMG-CoA Reductase-Associated Autoimmune Myopathy. Arthritis and rheumatism. 2012;64(12):4087-93.
123. Bergua C, Chiavelli H, Simon JP, Boyer O, Jouen F, Stenzel W, Martinet J. Immune-mediated necrotizing myopathy. Zeitschrift fur Rheumatologie. 2016;75(2):151-6.
124. Allenbach Y, Arouche-Delaperche L, Preusse C, Radbruch H, Butler-Browne G, Champtiaux N, Mariampillai K, Rigolet A, Hufnagl P, Zerbe N, Amelin D, Maisonobe T, Louis-Leonard S, Duyckaerts C, Eymard B, Goebel HH, Bergua C, Drouot L, Boyer O, Benveniste O, Stenzel W. Necrosis in anti-SRP(+) and anti-HMGCR(+)myopathies: Role of autoantibodies and complement. Neurology. 2018;90(6):e507-e17.
125. Rojana-udomsart A, Mitrpant C, Bundell C, Price L, Luo YB, Fabian V, Wilton SD, Hollingsworth P, Mastaglia FL. Complement-mediated muscle cell lysis: a possible mechanism of myonecrosis in anti-SRP associated necrotizing myopathy (ASANM). Journal of neuroimmunology. 2013;264(1-2):65-70.
126. Bergua C, Chiavelli H, Allenbach Y, Arouche-Delaperche L, Arnoult C, Bourdenet G, Jean L, Zoubairi R, Guerout N, Mahler M, Benveniste O, Drouot L, Boyer O. In vivo pathogenicity of IgG from patients with anti-SRP or anti-HMGCR autoantibodies in immune-mediated necrotising myopathy. Annals of the rheumatic diseases. 2019;78(1):131-9.
127. Mammen AL. Statin-Associated Autoimmune Myopathy. The New England journal of medicine. 2016;374(7):664-9.
128. Askanas V, Engel WK. Inclusion-body myositis: a myodegenerative conformational disorder associated with Abeta, protein misfolding, and proteasome inhibition. Neurology. 2006;66(2 Suppl 1):S39-48.
129. Preusse C, Goebel HH, Held J, Wengert O, Scheibe F, Irlbacher K, Koch A, Heppner FL, Stenzel W. Immune-mediated necrotizing myopathy is characterized by a specific Th1-M1 polarized immune profile. The American journal of pathology. 2012;181(6):2161-71.
130. Needham M, Fabian V, Knezevic W, Panegyres P, Zilko P, Mastaglia FL. Progressive myopathy with up-regulation of MHC-I associated with statin therapy. Neuromuscular disorders : NMD. 2007;17(2):194-200.
131. CXCL13 C-X-C motif chemokine ligand 13 [Homo sapiens (human)] - Gene - NCBI [Internet]. 2017 [cited 2017 Sep 02]. Available from: https://www.ncbi.nlm.nih.gov/pubmed/.
132. Saez de Guinoa J, Barrio L, Mellado M, Carrasco YR. CXCL13/CXCR5 signaling enhances BCR-triggered B-cell activation by shaping cell dynamics. Blood. 2011;118(6):1560-9.
133. Mackenzie IR, Rademakers R. The role of TDP-43 in amyotrophic lateral sclerosis and frontotemporal dementia. Curr Opin Neurol. 2008;21(6):693-700.
134. Weihl CC, Temiz P, Miller SE, Watts G, Smith C, Forman M, Hanson PI, Kimonis V, Pestronk A. TDP-43 accumulation in inclusion body myopathy muscle suggests a common pathogenic mechanism with frontotemporal dementia. J Neurol Neurosurg Psychiatry. 2008;79(10):1186-9.
135. Barth S, Glick D, Macleod KF. Autophagy: assays and artifacts. The Journal of pathology. 2010;221(2):117-24.
136. Vattemi G, Engel WK, McFerrin J, Askanas V. Endoplasmic reticulum stress and unfolded protein response in inclusion body myositis muscle. The American journal of pathology. 2004;164(1):1-7.
137. Nakano S, Oki M, Kusaka H. The role of p62/SQSTM1 in sporadic inclusion body myositis. Neuromuscular disorders : NMD. 2017;27(4):363-9.
138. Brady S, Squier W, Sewry C, Hanna M, Hilton-Jones D, Holton JL. A retrospective cohort study identifying the principal pathological features useful in the diagnosis of inclusion body myositis. BMJ open. 2014;4(4):e004552.

139. Amalfitano A, Bengur AR, Morse RP, Majure JM, Case LE, Veerling DL, Mackey J, Kishnani P, Smith W, McVie-Wylie A, Sullivan JA, Hoganson GE, Phillips JA, 3rd, Schaefer GB, Charrow J, Ware RE, Bossen EH, Chen YT. Recombinant human acid alpha-glucosidase enzyme therapy for infantile glycogen storage disease type II: results of a phase I/II clinical trial. Genetics in medicine : official journal of the American College of Medical Genetics. 2001;3(2):132-8.
140. Kishnani PS, Corzo D, Nicolino M, Byrne B, Mandel H, Hwu WL, Leslie N, Levine J, Spencer C, McDonald M, Li J, Dumontier J, Halberthal M, Chien YH, Hopkin R, Vijayaraghavan S, Gruskin D, Bartholomew D, van der Ploeg A, Clancy JP, Parini R, Morin G, Beck M, De la Gastine GS, Jokic M, Thurberg B, Richards S, Bali D, Davison M, Worden MA, Chen YT, Wraith JE. Recombinant human acid [alpha]-glucosidase: major clinical benefits in infantile-onset Pompe disease. Neurology. 2007;68(2):99-109.
141. Gene Therapy for Male Patients With Danon Disease Using RP-A501; AAV9.LAMP2B [Internet]. 2019 Mar 20 [cited 2020 Mar 18]. Available from: https://clinicaltrials.gov/ct2/show/NCT03882437.
142. D'Souza R S, Levandowski C, Slavov D, Graw SL, Allen LA, Adler E, Mestroni L, Taylor MR. Danon disease: clinical features, evaluation, and management. Circulation Heart failure. 2014;7(5):843-9.
143. Brigitte M, Schilte C, Plonquet A, Baba-Amer Y, Henri A, Charlier C, Tajbakhsh S, Albert M, Gherardi RK, Chretien F. Muscle resident macrophages control the immune cell reaction in a mouse model of notexin-induced myoinjury. Arthritis and rheumatism. 2010;62(1):268-79.
144. Kharraz Y, Guerra J, Mann CJ, Serrano AL, Muñoz-Cánoves P. Macrophage Plasticity and the Role of Inflammation in Skeletal Muscle Repair. Mediators Inflamm. 2013;2013.
145. Sun D, Martinez CO, Ochoa O, Ruiz-Willhite L, Bonilla JR, Centonze VE, Waite LL, Michalek JE, McManus LM, Shireman PK. Bone marrow-derived cell regulation of skeletal muscle regeneration. FASEB J. 232009. p. 382-95.
146. Pillon NJ, Bilan PJ, Fink LN, Klip A. Cross-talk between skeletal muscle and immune cells: muscle-derived mediators and metabolic implications. American journal of physiology Endocrinology and metabolism. 2013;304(5):E453-65.
147. Saclier M, Cuvellier S, Magnan M, Mounier R, Chazaud B. Monocyte/macrophage interactions with myogenic precursor cells during skeletal muscle regeneration. The FEBS journal. 2013;280(17):4118-30.
148. Martinez CO, McHale MJ, Wells JT, Ochoa O, Michalek JE, McManus LM, Shireman PK. Regulation of skeletal muscle regeneration by CCR2-activating chemokines is directly related to macrophage recruitment. Am J Physiol Regul Integr Comp Physiol. 2992010. p. R832-42.
149. Murray PJ. Macrophage Polarization. Annu Rev Physiol. 2017;79:541-66.
150. Travis MA, Sheppard D. TGF-beta activation and function in immunity. Annu Rev Immunol. 2014;32:51-82.
151. Sanjabi S, Zenewicz LA, Kamanaka M, Flavell RA. Anti-inflammatory and pro-inflammatory roles of TGF-beta, IL-10, and IL-22 in immunity and autoimmunity. Curr Opin Pharmacol. 2009;9(4):447-53.
152. Biernacka A, Dobaczewski M, Frangogiannis NG. TGF-β signaling in fibrosis. Growth Factors. 2011;29(5):196-202.
153. Roberts AB, Sporn MB, Assoian RK, Smith JM, Roche NS, Wakefield LM, Heine UI, Liotta LA, Falanga V, Kehrl JH. Transforming growth factor type beta: rapid induction of fibrosis and angiogenesis in vivo and stimulation of collagen formation in vitro. Proceedings of the National Academy of Sciences of the United States of America. 1986;83(12):4167-71.
154. Li Y, Foster W, Deasy BM, Chan Y, Prisk V, Tang Y, Cummins J, Huard J. Transforming growth factor-beta1 induces the differentiation of myogenic cells into fibrotic cells in injured skeletal

muscle: a key event in muscle fibrogenesis. The American journal of pathology. 2004;164(3):1007-19.
155. Delaney K, Kasprzycka P, Ciemerych MA, Zimowska M. The role of TGF-beta1 during skeletal muscle regeneration. Cell Biol Int. 2017;41(7):706-15.
156. Mendias CL, Gumucio JP, Davis ME, Bromley CW, Davis CS, Brooks SV. Transforming growth factor-beta induces skeletal muscle atrophy and fibrosis through the induction of atrogin-1 and scleraxis. Muscle & nerve. 2012;45(1):55-9.
157. Chung T, Christopher-Stine L, Paik JJ, Corse A, Mammen AL. The composition of cellular infiltrates in anti-HMG-CoA reductase-associated myopathy. Muscle & nerve. 2015;52(2):189-95.
158. van der Pas J, Hengstman GJ, ter Laak HJ, Borm GF, van Engelen BG. Diagnostic value of MHC class I staining in idiopathic inflammatory myopathies. J Neurol Neurosurg Psychiatry. 2004;75(1):136-9.
159. Salaroli R, Baldin E, Papa V, Rinaldi R, Tarantino L, De Giorgi LB, Fusconi M, Malavolta N, Meliconi R, D'Alessandro R, Cenacchi G. Validity of internal expression of the major histocompatibility complex class I in the diagnosis of inflammatory myopathies. Journal of clinical pathology. 2012;65(1):14-9.
160. Nagaraju K, Raben N, Loeffler L, Parker T, Rochon PJ, Lee E, Danning C, Wada R, Thompson C, Bahtiyar G, Craft J, Hooft Van Huijsduijnen R, Plotz P. Conditional up-regulation of MHC class I in skeletal muscle leads to self-sustaining autoimmune myositis and myositis-specific autoantibodies. Proceedings of the National Academy of Sciences of the United States of America. 2000;97(16):9209-14.
161. Goebels N, Michaelis D, Engelhardt M, Huber S, Bender A, Pongratz D, Johnson MA, Wekerle H, Tschopp J, Jenne D, Hohlfeld R. Differential expression of perforin in muscle-infiltrating T cells in polymyositis and dermatomyositis. J Clin Invest. 1996;97(12):2905-10.
162. Goebel HH, Blaschek A. Protein aggregation in congenital myopathies. Seminars in pediatric neurology. 2011;18(4):272-6.
163. Weihl CC, Iyadurai S, Baloh RH, Pittman SK, Schmidt RE, Lopate G, Pestronk A, Harms MB. Autophagic vacuolar pathology in desminopathies. Neuromuscular disorders : NMD. 2015;25(3):199-206.
164. Tsuruta Y, Furuta A, Furuta K, Yamada T, Kira J, Iwaki T. Expression of the lysosome-associated membrane proteins in myopathies with rimmed vacuoles. Acta neuropathologica. 2001;101(6):579-84.
165. Yang YP, Hu LF, Zheng HF, Mao CJ, Hu WD, Xiong KP, Wang F, Liu CF. Application and interpretation of current autophagy inhibitors and activators. Acta Pharmacol Sin. 2013;34(5):625-35.
166. Bjorkoy G, Lamark T, Pankiv S, Overvatn A, Brech A, Johansen T. Monitoring autophagic degradation of p62/SQSTM1. Methods in enzymology. 2009;452:181-97.
167. Yoshii SR, Mizushima N. Monitoring and Measuring Autophagy. Int J Mol Sci. 2017;18(9).
168. Rosenfeldt MT, Nixon C, Liu E, Mah LY, Ryan KM. Analysis of macroautophagy by immunohistochemistry. Autophagy. 2012;8(6):963-9.
169. Schläfli AM, Berezowska S, Adams O, Langer R, Tschan MP. Reliable LC3 and p62 autophagy marker detection in formalin fixed paraffin embedded human tissue by immunohistochemistry. European journal of histochemistry : EJH. 2015;59(2):2481.
170. Komatsu M, Waguri S, Koike M, Sou YS, Ueno T, Hara T, Mizushima N, Iwata J, Ezaki J, Murata S, Hamazaki J, Nishito Y, Iemura S, Natsume T, Yanagawa T, Uwayama J, Warabi E, Yoshida H, Ishii T, Kobayashi A, Yamamoto M, Yue Z, Uchiyama Y, Kominami E, Tanaka K. Homeostatic levels of p62 control cytoplasmic inclusion body formation in autophagy-deficient mice. Cell. 2007;131(6):1149-63.

171. Gómez-Sánchez R, Yakhine-Diop SM, Rodríguez-Arribas M, Bravo-San Pedro JM, Martínez-Chacón G, Uribe-Carretero E, Pinheiro de Castro DC, Pizarro-Estrella E, Fuentes JM, González-Polo RA. mRNA and protein dataset of autophagy markers (LC3 and p62) in several cell lines. Data Brief. 2016;7:641-7.
172. Girolamo F, Lia A, Annese T, Giannini M, Amati A, D'Abbicco D, Tampoia M, Virgintino D, Ribatti D, Serlenga L, Iannone F, Trojano M. Autophagy markers LC3 and p62 accumulate in immune-mediated necrotizing myopathy. Muscle & nerve. 2019;60(3):315-27.
173. Yoshida H. ER stress and diseases. The FEBS journal. 2007;274(3):630-58.
174. Fischer N, Preusse C, Radke J, Pehl D, Allenbach Y, Schneider U, Feist E, von Casteleyn V, Hahn K, Ruck T, Meuth SG, Goebel HH, Graf R, Mammen A, Benveniste O, Stenzel W. Sequestosome-1 (p62) expression reveals chaperone-assisted selective autophagy in immune-mediated necrotizing myopathies. Brain pathology (Zurich, Switzerland). 2019.
175. Kniepert A, Groettrup M. The unique functions of tissue-specific proteasomes. Trends in biochemical sciences. 2014;39(1):17-24.
176. Aki M, Shimbara N, Takashina M, Akiyama K, Kagawa S, Tamura T, Tanahashi N, Yoshimura T, Tanaka K, Ichihara A. Interferon-gamma induces different subunit organizations and functional diversity of proteasomes. Journal of biochemistry. 1994/02/01 ed1994. p. 257-69.
177. Basler M, Mundt S, Bitzer A, Schmidt C, Groettrup M. The immunoproteasome: a novel drug target for autoimmune diseases. Clinical and experimental rheumatology. 2015;33(4 Suppl 92):S74-9.
178. Cappelletti C, Galbardi B, Kapetis D, Vattemi G, Guglielmi V, Tonin P, Salerno F, Morandi L, Tomelleri G, Mantegazza R, Bernasconi P. Autophagy, inflammation and innate immunity in inflammatory myopathies. PloS one. 2014;9(11):e111490.
179. Johansen T, Lamark T. Selective autophagy mediated by autophagic adapter proteins. Autophagy. 2011;7(3):279-96.
180. D'Agostino C, Nogalska A, Cacciottolo M, Engel WK, Askanas V. Abnormalities of NBR1, a novel autophagy-associated protein, in muscle fibers of sporadic inclusion-body myositis. Acta neuropathologica. 2011;122(5):627-36.
181. Vattemi G, Nogalska A, King Engel W, D'Agostino C, Checler F, Askanas V. Amyloid-beta42 is preferentially accumulated in muscle fibers of patients with sporadic inclusion-body myositis. Acta neuropathologica. 2009;117(5):569-74.
182. Keller CW, Schmidt J, Lünemann JD. Immune and myodegenerative pathomechanisms in inclusion body myositis. Annals of clinical and translational neurology. 2017;4(6):422-45.
183. Gal J, Strom AL, Kwinter DM, Kilty R, Zhang J, Shi P, Fu W, Wooten MW, Zhu H. Sequestosome 1/p62 links familial ALS mutant SOD1 to LC3 via an ubiquitin-independent mechanism. Journal of neurochemistry. 2009;111(4):1062-73.
184. Lamark T, Svenning S, Johansen T. Regulation of selective autophagy: the p62/SQSTM1 paradigm. Essays Biochem. 2017;61(6):609-24.
185. Jabari D, Vedanarayanan VV, Barohn RJ, Dimachkie MM. Update on Inclusion Body Myositis. Current rheumatology reports. 2018;20(8):52.
186. Komatsu M, Waguri S, Ueno T, Iwata J, Murata S, Tanida I, Ezaki J, Mizushima N, Ohsumi Y, Uchiyama Y, Kominami E, Tanaka K, Chiba T. Impairment of starvation-induced and constitutive autophagy in Atg7-deficient mice. The Journal of cell biology. 2005;169(3):425-34.
187. Takayama S, Xie Z, Reed JC. An evolutionarily conserved family of Hsp70/Hsc70 molecular chaperone regulators. The Journal of biological chemistry. 1999;274(2):781-6.
188. Rauch JN, Tse E, Freilich R, Mok SA, Makley LN, Southworth DR, Gestwicki JE. BAG3 Is a Modular, Scaffolding Protein that physically Links Heat Shock Protein 70 (Hsp70) to the Small Heat Shock Proteins. Journal of molecular biology. 2017;429(1):128-41.

189. Stürner E, Behl C. The Role of the Multifunctional BAG3 Protein in Cellular Protein Quality Control and in Disease. Front Mol Neurosci. 2017;10:177.
190. Behl C. Breaking BAG: The Co-Chaperone BAG3 in Health and Disease. Trends Pharmacol Sci. 2016;37(8):672-88.
191. Minoia M, Boncoraglio A, Vinet J, Morelli FF, Brunsting JF, Poletti A, Krom S, Reits E, Kampinga HH, Carra S. BAG3 induces the sequestration of proteasomal clients into cytoplasmic puncta: Implications for a proteasome-to-autophagy switch. Autophagy. 102014. p. 1603-21.
192. Dunn WA. Autophagy and related mechanisms of lysosome-mediated protein degradation. Trends Cell Biol. 1994;4(4):139-43.
193. Gordon PB, Kovacs AL, Seglen PO. Temperature dependence of protein degradation, autophagic sequestration and mitochondrial sugar uptake in rat hepatocytes. Biochimica et biophysica acta. 1987;929(2):128-33.
194. Ogata M, Hino S, Saito A, Morikawa K, Kondo S, Kanemoto S, Murakami T, Taniguchi M, Tanii I, Yoshinaga K, Shiosaka S, Hammarback JA, Urano F, Imaizumi K. Autophagy is activated for cell survival after endoplasmic reticulum stress. Mol Cell Biol. 2006;26(24):9220-31.
195. Kettern N, Rogon C, Limmer A, Schild H, Höhfeld J. The Hsc/Hsp70 co-chaperone network controls antigen aggregation and presentation during maturation of professional antigen presenting cells. PloS one. 2011;6(1):e16398.
196. Allenbach Y, Benveniste O. Peculiar clinicopathological features of immune-mediated necrotizing myopathies. Current opinion in rheumatology. 2018;30(6):655-63.
197. Allenbach Y, Keraen J, Bouvier AM, Jooste V, Champtiaux N, Hervier B, Schoindre Y, Rigolet A, Gilardin L, Musset L, Charuel JL, Boyer O, Jouen F, Drouot L, Martinet J, Stojkovic T, Eymard B, Laforet P, Behin A, Salort-Campana E, Fain O, Meyer A, Schleinitz N, Mariampillai K, Grados A, Benveniste O. High risk of cancer in autoimmune necrotizing myopathies: usefulness of myositis specific antibody. Brain : a journal of neurology. 2016;139(Pt 8):2131-5.

Statutory Declaration

"I, Norina Fischer, by personally signing this document in lieu of an oath, hereby affirm that I prepared the submitted dissertation on the topic „Investigating vacuolar features reveals distinct autophagy pathway as a key feature in the pathophysiology of Immune-mediated necrotizing myopathy" – „Die Untersuchung vakuolärer Strukturen enthüllt spezifischen Autophagie-Mechanismus als Teil der Pathophysiologie der Immunvermittelten nekrotisierenden Myopathie" independently and without the support of third parties, and that I used no other sources and aids than those stated.

All parts which are based on the publications or presentations of other authors, either in letter or in spirit, are specified as such in accordance with the citing guidelines. The sections on methodology (in particular regarding practical work, laboratory regulations, statistical processing) and results (in particular regarding figures, charts and tables) are exclusively my responsibility.

Furthermore, I declare that I have correctly marked all of the data, the analyses, and the conclusions generated from data obtained in collaboration with other persons, and that I have correctly marked my own contribution and the contributions of other persons (cf. declaration of contribution). I have correctly marked all texts or parts of texts that were generated in collaboration with other persons.

My contributions to any publications to this dissertation correspond to those stated in the below joint declaration made together with the supervisor. All publications created within the scope of the dissertation comply with the guidelines of the ICMJE (International Committee of Medical Journal Editors; www.icmje.org) on authorship. In addition, I declare that I shall comply with the regulations of Charité – Universitätsmedizin Berlin on ensuring good scientific practice.

I declare that I have not yet submitted this dissertation in identical or similar form to another Faculty.

The significance of this statutory declaration and the consequences of a false statutory declaration under criminal law (Sections 156, 161 of the German Criminal Code) are known to me."

Date Signature

Declaration of contribution

Norina Fischer contributed the following to publication listed below:

Fischer N, Preuße C, Radke J, Pehl D, Allenbach Y, Schneider U, Feist E, von Casteleyn V, Hahn K, Ruck T, Meuth SG, Goebel HH, Graf R, Mammen A, Benveniste O, Stenzel W.; *Sequestosome-1 (p62) expression reveals chaperone-assisted selective autophagy in immune-mediated necrotizing myopathies.*, Brain Pathology, March 2020. Doi: 10.1111/bpa.12772. Epub 2019 Aug 27.

After adequate training I performed the histopathological work-up on the patients´ muscle tissue (tissue cutting, preparation for standard staining procedures by the diagnostic laboratory, realization of immunofluorescence stainings). After appropriate instruction and thorough training, I independently performed the analysis of the obtained histological stainings. Furthermore, I conducted the biomolecular examination of the tissue, including RNA isolation, testing of RNA concentration, transcription of RNA to complementary DNA and execution of the quantitative PCR. The responsibility for the analysis of the obtained qPCR data was also mine. I independently conducted the statistical analysis under instructions by Dr. Preuße and consultations with the Institute of Biometry and Clinical Epidemiology of the Charité. Figures 1 and 5 were generated from my own statistical analysis, as well as the graphs in Figures 3 and 4. Additionally, the immunofluorescence images of Figure 3 originated from my examination. Also, I developed the layout for the diagram in Figure 6.

_____

Signature, date and stamp of first supervising university professor

_____

Signature of doctoral candidate

CURRICULUM VITAE

For reasons of data protection, my curriculum vitae will not be published in the electronical version of my work.

List of publications

Fischer N, Preuße C, Radke J, Pehl D, Allenbach Y, Schneider U, Feist E, von Casteleyn V, Hahn K, Ruck T, Meuth SG, Goebel HH, Graf R, Mammen A, Benveniste O, Stenzel W. Sequestosome-1 (p62) expression reveals chaperone-assisted selective autophagy in immune-mediated necrotizing myopathies. Brain Pathol. 2019 Aug 3. doi: 10.1111/bpa.12772.

Knauss S, Preusse C, Allenbach Y, Leonard-Louis S, Touat M, **Fischer N**, Radbruch H, Mothes R, Matyash V, Böhmerle W, Endres M, Goebel HH, Benveniste O, Stenzel W. PD1 pathway in immune-mediated myopathies: Pathogenesis of dysfunctional T cells revisited. Neurol Neuroimmunol Neuroinflamm. 2019 Apr 10;6(3):e558. doi: 10.1212/NXI.000000000000 055.

Danksagung

In erster Linie danke ich Werner Stenzel und Corinna Preuße für ihre großartige, unermüdliche und herzliche Unterstützung und Zusammenarbeit über eine lange Zeit, die weit über inhaltliche und formelle Aspekte hinausging.

Weiterhin danke ich allen anderen Mitarbeiter*innen aus dem Aschheim-Zondek-Haus und dem Institut für Neuropathologie, insbesondere Petra Matylewski und Alexandra Förster für ihre Hilfe und geduldige Antworten auf viele Fragen.

Besonders danken möchte ich außerdem meinen Eltern und meiner Schwester Ninja, die mich schon ein Leben lang durch Hoch- und Tiefzeiten begleitet haben.